Molecular and biochemical studies of the *Craterostigma plantagineum* cell wall during dehydration and rehydration

Dissertation

zur
Erlangung des Doktorgrades (Dr. rer. nat.)
der
Mathematisch-Naturwissenschaftlichen Fakultät
der
Rheinischen Friedrich-Wilhelms-Universität Bonn

vorgelegt von
Niklas Udo Jung

aus
Adenau, Deutschland

Bonn, 2019

Angefertigt mit Genehmigung der Mathematisch-Naturwissenschaftlichen Fakultät der Rheinischen Friedrich-Wilhelms-Universität Bonn.

1. Gutachter: Frau Prof. Dr. Dorothea Bartels

Institut für Molekulare Physiologie und Biotechnologie der Pflanzen

Kirschallee 1

53115 Bonn, Germany

2. Gutachter: Herr Prof. Dr. John Paul Knox

Centre for Plant Sciences, Faculty of Biological Sciences

University of Leeds

Leeds LS2 9JT, UK

Tag der mündlichen Prüfung: 11.02.2020

Erscheinungsjahr: 2020

I. ABBREVIATIONS

At:	*Arabidopsis thaliana*
CDTA:	1,2-cyclohexanediaminetetraacetic acid
CL:	cardiolipin
Cp:	*Craterostigma plantagineum*
D:	desiccated
GA:	galacturonic acid
GLP:	germin-like protein
GRP:	glycine-rich protein
HG:	homogalacturonan
Lb:	*Lindernia brevidens*
Ls:	*Lindernia subracemosa*
mAb:	monoclonal antibody
PA:	phosphatidic acid
PD:	partially dehydrated
PE:	phosphatidyl-ethanolamine
PC:	phosphatidylcholine
PIP2:	phosphatidylinositol-(4,5)-bisphosphate
PME:	pectinmethylesterase
PMEI:	pectinmethylesterase inhibitor
R 1:	rehydrated 24 h
R 2:	rehydrated 48 h
RWC:	relative water content
RG-I:	rhamnogalacturonan-I
RG-II:	rhamnogalacturonan-II
U:	untreated
WAK:	wall-associated protein kinase

II. FIGURES AND TABLES

List of figures and tables page

III. TABLE OF CONTENTS

1. SUMMARY

Craterostigma plantagineum belongs to the desiccation tolerant angiosperm plants. Upon dehydration leaves fold and the cells shrink which is reversed during rehydration. To understand this process changes in cell wall pectin composition, and the role of the apoplastic glycine-rich protein1 (CpGRP1) were analysed. Cellular microstructural changes in hydrated, desiccated and rehydrated leaf sections were analysed using scanning electron microscopy. These studies visualised the folding and unfolding of cell walls upon dehydration and rehydration. Pectin composition in different cell wall fractions was analysed with monoclonal antibodies against homogalacturonan, rhamnogalacturonan-I, rhamnogalacturonan-II and hemicellulose epitopes. The data demonstrate changes in pectin composition during dehydration/rehydration which is suggested to affect cell wall properties. Homogalacturonan was less methylesterified upon desiccation and changes were also demonstrated in the detection of rhamno-galacturonan-I, rhamnogalacturonan-II and hemicelluloses. CpGRP1 seems to have a central role in cellular adaptations to water deficit, as it interacts with pectin through a cluster of arginine residues, and de-methylesterified pectin presents more binding sites for the protein-pectin interaction than pectin from hydrated leaves. CpGRP1 can also bind phosphatidic acid and cardiolipin. The binding of CpGRP1 to pectin appears to be dependent on the pectin methylesterification status and it has a higher affinity to pectin than its binding partner CpWAK1. It is hypothesised that changes in pectin composition are sensed by the CpGRP1-CpWAK1 complex thus leading to the activation of dehydration-related responses and leaf folding (Figure 1). Phosphatidic acid might participate in the modulation of CpGRP1 activity.

To investigate the process of pectin de-methylesterification upon desiccation transcriptome data for pectinmethylesterases and pectinmethylesterase inhibitor proteins were analysed. One enzyme was selected as an interesting candidate because it was the only pectinmethylesterase which was upregulated upon desiccation. This pectinmethylesterase had similarities to the pectinmethylesterase31 from *Arabidopsis thaliana* (AtPME31). The transcript was highly abundant in the vegetative tissue of *C. plantagineum* upon desiccation, but in *A. thaliana* the transcript is highly abundant in dry seeds. This pectinmethylesterase might be an interesting candidate to understand cell wall remodelling processes in *C. plantagineum*.

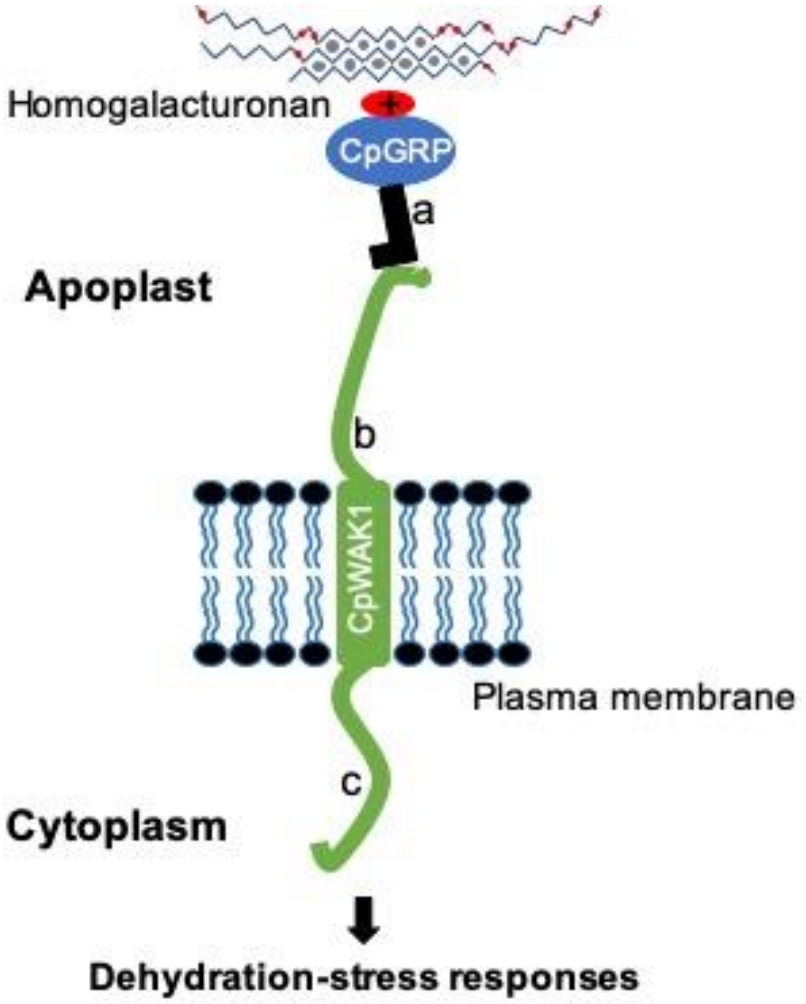

Figure 1 The CpGRP1-CpWAK1-pectin complex links the apoplast to the cytoplasm and is a candidate for sensing cell wall changes upon desiccation. The positively charged amino acid cluster of CpGRP1 **(+)** interacts with de-methylesterified homogalacturonan stretches. The cysteine-rich domain of CpGRP1 **(a)** interacts with the extracellular domain of CpWAK1 **(b)**, a plasma membrane spanning protein with an intracellular kinase domain **(c)** that might be involved in triggering dehydration-stress responses (modified from Maron, 2019).

2. INTRODUCTION

2.1 The importance of water for plant survival and desiccation tolerance

Most land plants are not able to survive prolonged periods of water shortage and even a mild water deficit can lead to irreversible damage and plant death (Zhang and Bartels, 2018). Water accounts for 80-95% of the biomass of leaves and roots in non-woody plants and plays a crucial role in the maintenance of cell turgor, transport of solutes and nutrients and it mediates hydrophobic and hydrophilic interactions essential for macromolecular structures (Hirt and Shinozaki, 2004). The continuous water transport from the roots to the leaf surface is driven by the water potential, which describes water-flow from a higher to a lower potential. The constant availability of water is crucial for plant survival.

As sessile organisms, plants can encounter dehydration. Plants have different strategies to reduce water loss and adapt to low water availability (Verslues and Juenger, 2011). The three different strategies can be described as drought `avoidance´, `resistance´ and `tolerance´ (Levitt, 1980). Most land plants produce specialised structures like seeds, pollen and spores which are able to survive periods of low water. Annual plants hardly face desiccation because they finish their life cycle in a period when water is available and growth conditions are favourable. These plants avoid desiccation. Resistant plants developed strategies to reduce water flux through the plant or to increase the uptake of water. An increased water uptake rate can be achieved by the development of specialised root structures. Reduced water loss is achieved by stomatal closure, smaller leaves or the reduction of transpiration by specialised leaf structures including waxes, hairs or embedded stomata. The CAM metabolism is a biochemical adaptation in which CO_2 is accumulated during the night, when the stomata are open. During the day the stomata are often closed and the plant metabolises the CO_2 in the Calvin cycle (Winter, 2019).

Desiccation tolerance is defined as the ability of an organism to dry to equilibrium with the dry air and to resume normal metabolic activity after rehydration (Bewley, 1979; Alpert, 2005; Wood, 2005; Alpert, 2006; Wood and Jenks, 2007). Desiccation tolerant plants can lose more than 90% of their relative water content (RWC), but still resume their metabolic activity when water is again available (Rascio and La Rocca, 2005).

Desiccation tolerance is an ancient trait and phylogenetic analyses gave evidence that initial land colonisation was only possible through the evolution of vegetative desiccation tolerance. The loss of desiccation tolerance in vegetative organs could be due to an increase in complexity and the development of a water transport system. The ability to tolerate desiccation is common in lower plants as well as in seeds and pollen of angiosperm plants, but only a small group of angiosperm plants can tolerate desiccation of their vegetative tissues. This group of plants is termed resurrection plants (Gaff, 1971). In resurrection plants seed specific adaptations to desiccation have been re-established in their vegetative tissue (Farrant and Moore, 2011; VanBuren *et al*., 2017). Desiccation tolerance did independently evolve (or re-evolve) in *Selaginella*, ferns and in some angiosperms (Oliver *et al*., 2000). Out of 250,000 vascular plant species about 330 are desiccation tolerant and more than 90% of them are found on inselbergs (Porembski and Barthlott, 2000). Desiccation tolerance in vascular plants occurs in 13 families and is present in monocotyledons and dicotyledons. In dicot plants desiccation tolerance exists in the families of Gesneriaceae, Myrothamnaceae and Linderniaceae (Porembski and Barthlott, 2000).

2.2. The Linderniaceae family

Resurrection plants can be found in tropical and subtropical regions, particularly in regions with variable water availability like rock outcrops. (Fischer, 1992). Desiccation tolerance in dicots has been reported in the order of Gunnerales and Lamiales (Porembski, 2011). Desiccation tolerant plants of the *Craterostigma* and the *Lindernia* genus were originally classified in the family of Scrophulariaceae within the order of Lamiales but according to a new classification the genera belong to the Linderniaceae family (Figure 2) (Rahmanzadeh *et al*., 2005). The separate linage of Linderniaceae has been confirmed by studies of Albach *et al*.

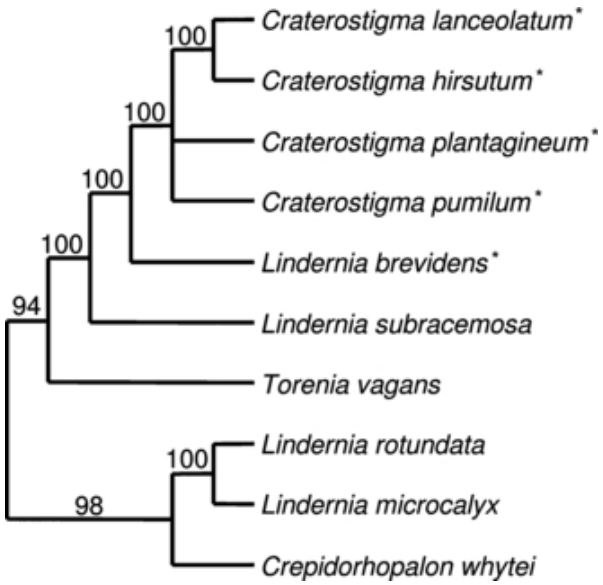

Figure 2 Phylogenetic tree of selected Linderniaceae family members. Desiccation tolerant species are indicated with an asterisk. Bootstrap values are indicated above the branches (from Phillips *et al*., 2008).

(2005), Oxelman *et al*. (2005) and Schäferhoff *et al*. (2010). Fischer *et al*. (2013) provided the first detailed phylogenetic analysis.

Overall the Linderniaceae family includes 13 genera with 195 species and recently two new genera and species from inselbergs in brazil had been described (Almeida *et al*., 2019). Asian representatives are found in rain forests and African representatives occur in seasonally filled rock pools, heavy metal soils and inselbergs (Rahmanzadeh *et al*., 2005). All representatives within the *Craterostigma* genus are desiccation tolerant, but within the *Lindernia* genus only a few species from rock outcrops are desiccation tolerant and the majority of *Lindernia* spp. are desiccation sensitive (Fischer, 1995; Seine *et al*., 1995).

2.3 Resurrection plants and adaptations to survive desiccation

Desiccation tolerance is a complex trait and involves many genes which are differentially expressed in response to dehydration. The two resurrection plants *Craterostigma plantagineum* (Cp) and *Lindernia brevidens* (Lb) and a closely related desiccation sensitive species, *Lindernia subracemosa* (Ls), belong to the family of Linderniaceae and have been extensively studied to identify mechanisms that are exclusively active in desiccation tolerant plants (Phillips *et al*., 2008; Giarola *et al*., 2017). Recently, the genome sequences of *L. brevidens* and *L. subracemosa* have become available and are a useful tool to study differentially activated pathways (VanBuren *et al*., 2018).

The use of *C. plantagineum* as an experimental system has the advantage that molecular analysis can be performed using both differentiated plant tissues and undifferentiated callus. This approach allows to compare the gene expression in two systems which are genetically identical (Bartels, 2005). Another advantage in using *C. plantagineum* as a model system for desiccation tolerance involves the phytohormone abscisic acid (ABA): *C. plantagineum* callus can be switched from a desiccation sensitive state to a desiccation tolerant state by a treatment with exogenous ABA (Bartels *et al*., 1990). Another observation which demonstrates the essential role of ABA in the acquisition of desiccation tolerance is the fact that ABA levels increase in leaves during dehydration and many dehydration-induced genes are also induced through ABA (Bartels, 2005). Other components and mechanisms which contribute to desiccation tolerance include the synthesis of protective proteins (e.g. late

embryogenesis abundant proteins (LEAs)), specific carbohydrates, morphological adaptations, changes in membrane lipids, regulatory promoter elements controlling the expression of helpful genes and changes in cell wall pectin composition (Vicré *et al*., 1999, 2004; Phillips *et al*., 2008; Dekkers *et al*., 2015; Gasulla *et al*., 2016; Zhang and Bartels, 2016; Giarola *et al*., 2017, 2018). The interaction and hierarchy of the different protective mechanisms contributing to desiccation tolerance is not deciphered so far (Giarola *et al*., 2017). An interplay of different adaptations finally leads to the protection and conservation of essential cellular components and enables resurrection plants to withstand desiccation.

C. plantagineum and *L. brevidens* belong to the group of homoiochlorophyllous resurrection plants, which retain their chlorophyll and keep their photosynthetic apparatus intact during dehydration. Thus, they have to defend against free radicals such as reactive oxygen species (ROS). In homoiochlorophyllous resurrection plants the formation of ROS is prevented by the downregulation of photosynthesis and leaf folding. General strategies to avoid ROS production like the downregulation of electron transfer reactions are active (Collet *et al*., 2003; Gechev *et al*., 2013; Ma *et al*., 2015; Zia *et al*., 2016; Yobi *et al*., 2017). Detoxification of ROS in resurrection plants is achieved by activating conserved pathways including superoxide dismutase, ascorbate peroxidase and glutathione reductase, which are upregulated or constitutively expressed (Dinakar *et al*., 2013; Challabathula *et al*., 2016; Yobi *et al*., 2017). Other defence mechanisms against ROS have evolved and are more species-specific: Examples for this are the accumulation of pigments in leaves of different resurrection plants in response to desiccation like zeaxanthin in *C. plantagineum* and *Myrothamnus flabellifolia* (Alamillo and Bartels, 2001; Kranner *et al*., 2002) or anthocyanins in *Xerophyta viscosa* and *L. brevidens* (Sherwin and Farrant, 1998; Dinakar *et al*., 2013). The pigments are proposed to dissipate excessive light radiation (Dinakar *et al*., 2013). In *X. viscosa* the stress-inducible enzyme 1-cysteine peroxiredoxin was identified (Mowla *et al*., 2002) and in *C. plantagineum* an ABA- and dehydration-inducible aldehyde dehydrogenase is up-regulated during desiccation which oxidises aldehydes in a NAD-dependent manner (Kirch *et al*., 2001). Some abundantly accumulated sugars may also function as ROS scavenging molecules. Zhang and Bartels (2016) found an accumulation of octulose which has superior ROS-scavenging abilities compared to other sugars in *C. plantagineum*.

2.4 Plant cell wall structure

The plant cell wall is the outermost structure of a plant cell and the first structure to encounter external changes. The behaviour of the cell wall upon different stresses is a key factor to understand the initiation of protective mechanisms. Desiccation leads to vacuole shrinkage and the cell contents are drawn inwards, which results in more tension between the plasmalemma and the cell wall (Levitt, 1980). For plant survival the protection of the plasmalemma is essential (Iljin, 1957). The important building blocks of plant cell walls are cellulose and callose, pectin and hemicelluloses. Pectin is the most abundant cell wall component and accounts for up to 50% (w/w) of the cell wall in *Arabidopsis thaliana* (Zablackis *et al*., 1995). Both, cellulose and callose are linear homopolysaccharides. Cellulose is composed of β-(1,4)-linked glucose residues, whereas callose is composed of β-(1,3)-linked glucose residues. Cellulose microfibrils are rigid structures and therefore build up the mechanical scaffold of the cell wall which becomes interconnected by hemicelluloses and pectin (Nishiyama, 2009; Wang *et al*., 2012). Callose synthesis is induced in response to different stresses and it functions as a local cell wall stabiliser (Nielsen *et al*., 2012; De Storme and Geelen, 2014). Pectin is a heterogenous compound and it is composed of homogalacturonan (HG), rhamnogalacturonan-I (RG-I), rhamnogalacturonan-II (RG-II) and xylogalacturonan (Figure 3). The ratio between these main pectin components is variable. Homogalacturonan is typically the most abundant compound and accounts for about 65% (w/w) of pectin. Rhamnogalacturonan-I accounts for 20-35% (w/w).

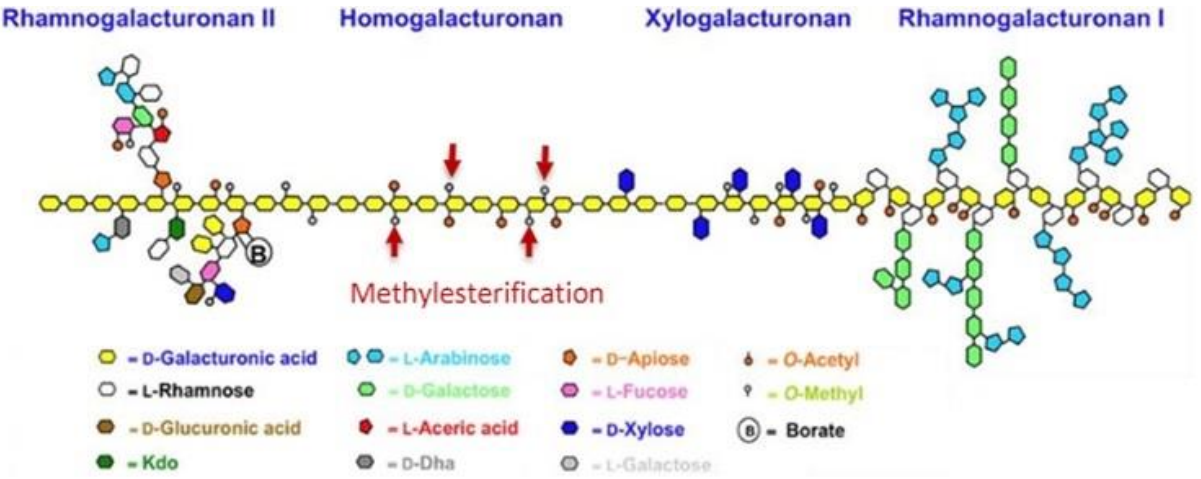

Figure 3 Composition of pectin. Pectin is composed of homogalacturonan, rhamnogalacturonan-II, rhamnogalacturonan-I and xylogalacturonan. Homogalacturonan and rhamnogalacturonan-I are the most abundant parts of pectin. The different sugars are indicated in the legend (modified from Harholt *et al*., 2010).

Rhamnogalacturonan-II and xylogalacturonan are minor components (Mohnen, 2008). Alpha (1,4)-linked D-galacturonic acid is the building block of homogalacturonan, where it is organised to linear chains. It is also the backbone of rhamnogalacturonan-II and, together with rhamnose, the backbone of rhamnogalacturonan-I. In rhamnogalacturonan-I and rhamnogalacturonan-II the backbone-forming sugars are substituted with a range of different sugar residues, which makes the rhamnogalacturonan-I and -II more complex and diverse compared to the homogalacturonan. The biosynthesis of pectin has been reviewed recently (Harholt *et al*., 2010, Lampugnani *et al*., 2018) and will not be described further.

Xyloglucan and xylan are the most abundant hemicelluloses in dicot cell walls and crosslink cellulose fibrils (Park and Cosgrove, 2015; Simmons *et al*., 2016). Xyloglucan has a β-(1,4)-linked glucose backbone with side chains which contain xylose, galactose (possibly acetylated), fucose and arabinose. Xylan is made of β-(1,4)-linked xylose residues with side chains of α-arabinofuranose and α-galacturonic acid. Modifications such as transglucosylation, acetylation or methylesterification and cross-linking of the different cell wall components play a major role in modifying the mechanical properties of plant cell walls (O'Neill *et al*., 2001; Ryden *et al*., 2003; Caffall and Mohnen, 2009; Caffall *et al*., 2009; Park and Cosgrove, 2015). In some species xyloglucan is also deposited during seed development. In this case xyloglucan is not linked to cellulose but water soluble and can rapidly be degraded upon germination to provide energy for the seedling (Edwards *et al*., 1985; dos Santos *et al*., 2004).

2.4.1 Cell wall remodelling in response to dehydration in resurrection plants

Resurrection plants require structural cell wall adaptations upon drying to reduce mechanical stress. An observation in some resurrection plants is the extensive folding of the cell wall upon dehydration and reversion of folding is fast after rehydration (Phillips *et al*., 2008). Controlled cell wall folding prevents tearing of the plasmalemma from the cell wall which is necessary for cell integrity (Farrant and Sherwin, 1996; Thomson and Platt 1997; Farrant, 2000; Vicré *et al*., 1999, 2004). Previous studies showed dehydration-induced changes in cell wall architecture, cell wall composition and variations of hemicellulose polysaccharides and pectin-associated arabinans in resurrection plants (Vicré *et al*., 1999, 2004; Moore *et al*., 2006, 2008). It has been proposed that high levels of pectic-arabinans, arabinogalactan-proteins and

arabinoxylans ensure the required cell wall plasticity upon dehydration for the resurrection plant *M*. *flabellifolia* (Moore *et al*., 2013). Changes in the homogalacturonan fractions were analysed with a set of monoclonal antibodies in *Craterostigma wilmsii* (Vicré *et al*., 1999). This demonstrated higher levels of de-methylesterified homogalacturonan upon desiccation which is reversed after rehydration. The role of homogalacturonan in desiccation tolerance is supported by findings that accumulation of homogalacturonan is correlated with desiccation resistance in the green *Zygnema sp.* algae (Herburger *et al*., 2019). Homogalacturonan is known to be synthesised in the methylesterified form only and then de-methylesterified in the cell wall, therefore these findings suggest *de novo* synthesis of homogalacturonan during the recovery process (Zhang and Staehelin, 1992; Staehelin and Moore, 1995; Sterling *et al*., 2001).

A higher proportion of de-methylesterified homogalacturonan upon desiccation, together with higher calcium levels (Vicré *et. al*., 1999) leads to the formation of the so-called `egg-box´ structures (Grant *et al*., 1973; Jarvis, 1984; Moore *et al*., 1986; Lloyd, 1991) which are proposed to strengthen the cell wall (Vicré *et al*., 1999). A higher proportion of de-methylesterified stretches of homogalacturonan provides more binding sites for pectin binding proteins that might be important to sense the cell wall hydration status (Spadoni *et al*., 2006; Giarola *et al*., 2016). Demonstrated changes in the hemicellulose xyloglucan did also point to a strengthened cell wall upon desiccation in the resurrection plant *C. wilmsii.* (Vicré *et al*., 1999). More xyloglucan points to more interconnected cellulose fibrils which also contributes to cell wall rigidity (Moore *et al*., 1986; Fry, 1989; Park and Cosgrove, 2015). The ability of Ca^{2+} to crosslink homogalacturonan and borate to crosslink rhamnogalacturonan-II (Kobayashi *et al*., 1996) is also a major factor to provide cell wall strength.

2.4.2 Cell wall modifying proteins

The complexity of the cell wall translates equally to a high number of different cell wall modifying proteins. These proteins are important in modulating the properties of the cell wall. They play crucial roles in plant development and in response to biotic and abiotic stresses (Sasidharan *et al*., 2011, Tenhaken, 2015). In this paragraph the most important cell wall modifying proteins will be briefly described.

Expansins are acid-induced cell wall proteins which disrupt non-covalent cellulose-hemicellulose interactions without lytic activity. The action of expansins translates in irreversible cell wall extensibility and cell wall relaxation (McQueen-Mason and Cosgrove, 1995). According to phylogenetic analyses expansins can be separated into two major groups, namely α-expansins and β-expansins (Cosgrove, 2015). Jones and McQueen-Mason, (2004) studied the expression of α-expansins in *C. plantagineum* leaves and proposed an expansin-induced cell wall extension in the early stages of dehydration and rehydration as the *CplExp1* transcript was more abundant in both stages. However, it can be questioned if expansins are active upon dehydration as the apoplast tends to alkalise and expansins are acid-activated (Geilfus, 2017).

The plant endo-β-1,4-glucanases (EGases) are proteins that hydrolyse β-1,4 glucan bonds (Sasidharan *et al*., 2011). Most EGases are secreted proteins but some were also found to be membrane bound and involved in cellulose synthesis (Nicol *et al*., 1998; Molhoj *et al*., 2002). Xyloglucan and cellulose have been proposed as potential substrates for EGases which is why they could have cell wall loosening activity (Ohmiya *et al*., 2000). However, they cannot induce cell wall loosening in isolated wall specimens like expansins (Cosgrove, 1999) but might be able to enhance the activity of other cell wall modifying enzymes and act as a secondary cell wall loosening agent (Sasidharan *et al*., 2011). The fungal Cel12A endoglucanase cleaves both cellulose and xyloglucan. Cosgrove (2016) compared the mode of action of Cel12A to α-expansins. Both proteins induce irreversible cell wall extension (creep) but other than α-expansin Cel12A shows hydrolytic activity and increases plasticity and elasticity. The lag time for creep induction for α-expansins is within seconds but for Cel12A its 6 min to >60 min (Yuan *et al*., 2001; Park and Cosgrove, 2012). A similar analysis for a plant endoglucanase has not been performed so far.

The group of xyloglucan endotransglucosylases/hydrolases (XHTs) is another major group of cell wall remodelling enzymes. They act on the hemicellulose-cellulose network which is the major tension bearing structure in the cell wall. XHTs can cleave the load-bearing xyloglucan links and therefore have the potential to increase the extensibility of the cell wall and positively regulate cellular expansion (Fry *et al*., 1992; Rose *et al*., 2002). Members of the XTH gene family can have irreversible xyloglucan hydrolysis (XEH) activity and/or reversible xyloglucan transglucosylation activity (XET) making them candidates to also act on cell wall re-assembling. The abilities of cutting

and re-joining xyloglucan chains shows the importance of XTHs in cell wall remodelling and regulation of the cellular expansion process (Rose *et al*., 2002). Oligosaccharides generated by endohydrolysis are released in the cell wall and further enzymatically degraded by glycosidases. The monosaccharides are transported into the cytosol by plasma membrane-localised transporters, where they are used to recycle nucleotide sugars in the salvage pathway (Pauly and Keegstra, 2016). The XTH gene HrhDR25 from the resurrection plant *Haberlea rhodopensis* was upregulated in early dehydration and rehydration and therefore mimicking the expression pattern of the expansin CplExp1 from *C. plantagineum*. In *A. thaliana* the overexpression of CaXTH3 from hot pepper was correlated with an increase in dehydration and salt stress tolerance (Cho *et al*., 2006; Choi *et al*., 2011; Georgieva *et al*., 2012). These results and the ability of

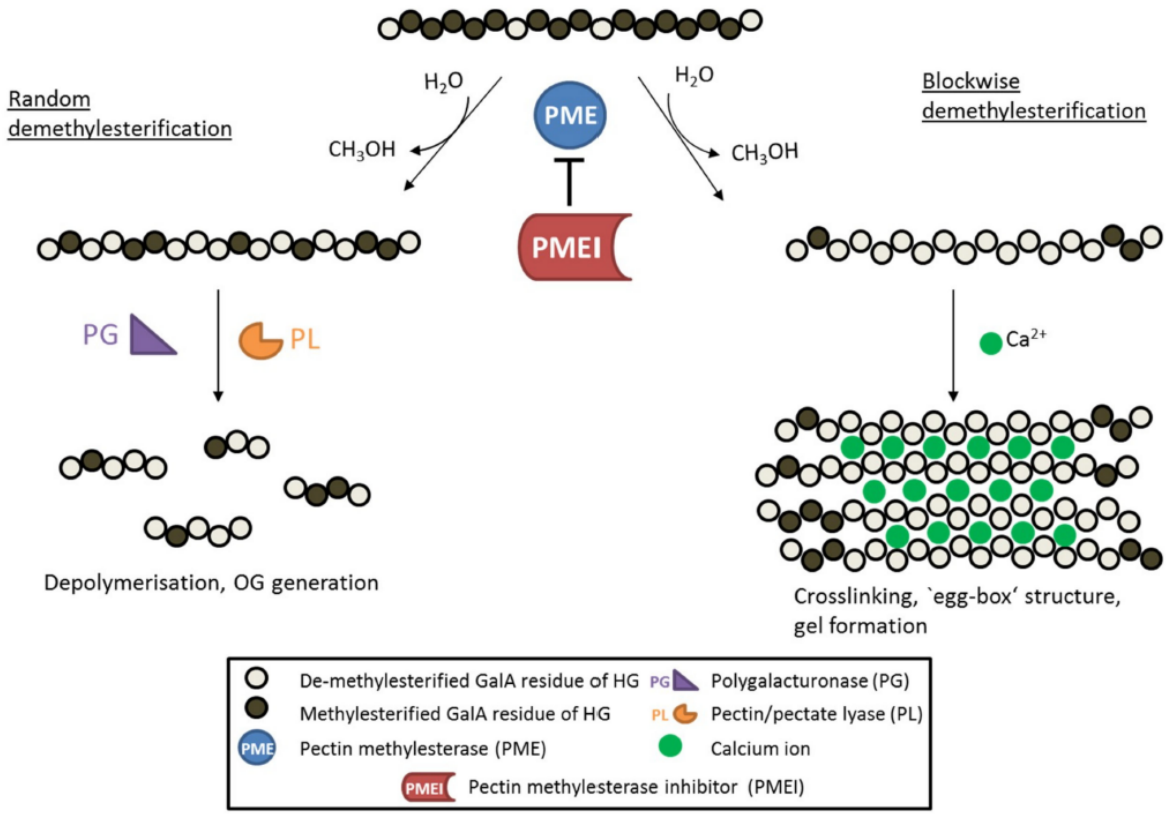

Figure 4 Scheme showing the two modes of action of pectin de-methylesterification. Homogalacturonan is transported to the apoplast in a highly methylesterified form. Pectinmethylesterases (PME) can de-methylesterify homogalacturonan in a blockwise pattern. The negatively charged homogalacturonan backbone can crosslink with calcium ions. This leads to the formation of the `egg-box´ structures and to a stiffer cell wall. On the other hand, random de-methylesterification leads to low-methylesterified homogalacturonan which is depolymerised by polygalacturonases and pectin lyases. This leads to the formation of oligogalacturonides and cell wall loosening. PME activity is inhibited by proteinaceouse inhibitors (PMEI) (from Wormit and Usadel, 2018).

XTHs to have different, possibly opposite activities, makes them an important research topic to explain cell wall remodelling processes upon dehydration.

Pectin is first synthesised inside the cell in a highly methylesterified form and then transported to the apoplast (Harholt *et al*., 2010, Lampugnani *et al*., 2018). The status of homogalacturonan methylesterification plays important roles in various developmental processes and in cell wall stress adaptations (Pelloux *et al*., 2007; Wu *et al*. 2018).

In *A. thaliana* the degree of pectin methylesterification is controlled by the action of pectinmethylesterases (PMEs), pectinmethylesterase inhibitors (PMEIs), subtilisin-type Ser proteases (SBTs) and at least one E3 ubiquitin ligase (Levesque-Tremblay *et al*., 2015). Pectinmethylesterases act on the methylesterified chains of D-galacturonic acid and catalyse the de-methylesterification reaction. The pattern of de-methylesterification is crucial whether the action of a PME leads to cell wall loosening or stiffening (Levesque-Tremblay *et al*., 2015). Blockwise de-methylesterification leads to blocks of free carboxyl groups which can be crosslinked through Ca^{2+} (Figure 4). This leads to the formation of `egg-boxes´ which are important for cell wall stability, and blockwise stretches of de-methylesterified homogalacturonan provide binding sites for pectin binding proteins which are important for signalling processes (Micheli, 2001; Spadoni *et al*., 2006; Harholt *et al*., 2010). Random de-methylesterification produces protons which can activate pH-dependent cell wall modifying enzymes. These enzymes (e.g. polygalacturonases) can then act on pectin thus promoting cell wall loosening. It is thought that cell wall properties such as the extent of homogalacturonan methylesterification and the pH determine the specificity of the PME activity (Micheli, 2001).

2.5 Glycine-rich proteins

Glycine-rich proteins (GRPs) have a high glycine content with glycine residues arranged in $(Gly)_n$-X repeats. In addition, a cysteine-rich region, an oleosin domain, RNA-recognition motifs, a cold-shock domain or zinc-finger motifs are found in GRPs. Although several GRPs have been characterised, the function of the glycine-rich domains in these proteins is poorly understood (Czolpinska and Rurek, 2018). GRPs are classified according to the arrangement of the glycine-rich repeats and the presence of additional domains (Sachetto-Martins *et al*., 2000*;* Fusaro *et al*., 2001;

Bocca *et al*., 2005; Mangeon *et al*., 2010). Class I GRPs share a high-glycine-content region with $(GGX)_n$ repeats. A C-terminal cysteine-rich region is present in the class II GRPs. The class III GRPs have a lower glycine content and may have an additional oleosin domain. Class IV GRPs are known as RNA-binding GRPs with either an RNA-recognition motif or a cold-shock domain and in some cases GRPs have additional zinc-finger motifs. Class V GRPs are similar to class I GRPs but show mixed patterns of glycine repeats. The expression patterns and the subcellular localisation of the different proteins within the GRP-superfamily are highly diverse thus suggesting that these proteins have different functions (Mangeon *et al*., 2010). GRPs with an apoplastic signal peptide have been proposed to be an important component of cell wall structures (Condit and Meagher, 1986, 1987; Keller *et al*., 1988). For example, the French bean PvGRP1.8 protein is part of the cell wall and forms a hydrophobic protein layer in the cell wall of protoxylem vessels. The protein was proposed to play a role in the protoxylem repair system (Ringli *et al*., 2001). According to microarray results GRPs could also be implicated in maintaining protoxylem structures (Yokoyama and Nishitani, 2006). Glycine-rich proteins have been proposed to connect the secondary cell wall thickenings between protoxylem elements (Ryser *et al*., 2004). The AtGRP9 protein from *A. thaliana* interacts with a cinnamyl alcohol dehydrogenase (AtCAD5) and may be involved in lignin biosynthesis (Chen *et al*., 2007). Besides class I GRPs also GRPs from other classes are plant cell wall components. The class V glycine-rich protein1 (BhGRP1) from *B*. *hygrometrica* was proposed to be important for cell wall integrity during dehydration, whereas the class II GRP NtCIG1 protein from tobacco was proposed to enhance callose deposition in cell walls (Ueki and Citovsky, 2002; Wang *et al*., 2009).

2.6 Cell wall-associated protein kinases and their interaction with glycine-rich proteins

The *C*. *plantagineum* glycine-rich protein1 (CpGRP1) belongs to the class II GRPs. CpGRP1 is highly abundant in the apoplast of desiccated leaves and interacts with the *C*. *plantagineum* cell wall-associated protein kinase1 (CpWAK1) (Giarola *et al*., 2016). WAKs contain an extracellular pectin binding domain and an intracellular serine/threonine protein kinase domain. WAKs have been suggested to link the cytoplasm to the extracellular matrix and to activate signalling pathways in response to pectin changes (He *et al*., 1999; Anderson *et al*., 2001; Kohorn and Kohorn, 2012). Many different receptor-kinases or receptor-like kinases have been identified to date

but WAKs are the only ones where direct binding to cell wall components has been demonstrated (Wolf, 2017). The CpGRP1-CpWAK1 complex may play a role in sensing dehydration-induced cell wall changes and thus activate dehydration-induced signalling pathways (Giarola *et al*., 2016). A similar complex is known from *A*. *thaliana* where the cysteine-rich region of AtGRP-3 interacts with the cell wall-associated kinase1 (AtWAK1). This complex has been proposed to be involved in pathogen-defence mechanisms (Park *et al.,* 2001).

2.7 Phosphatidic acid

Lipids are a major component of the plasma membrane and get modified upon dehydration in *C. plantagineum* (Gasulla *et al*., 2013). The CpGRP1 protein as part of the apoplast is also exposed to lipids. Gramegna *et al*. (2016) showed that the *A. thaliana* glycine-rich protein-3 is localised in the apoplast and at the plasma membrane. This observation suggests that AtGRP-3 could bind to the plasma membrane by an interaction with lipids. The negatively-charged head group of phosphatidic acid (PA) was described in the `electrostatic/hydrogen-bond switch model´ as an interaction partner for positively-charged amino acid residues (Kooijman *et al*., 2007). Phosphatidic acid was shown to bind to other proteins and thus modify the activity of proteins (Hou *et al*., 2015). Phosphatidic acid has different roles in plants and belongs to the group of phospholipids. The glycerol backbone carries a saturated fatty acid, an unsaturated fatty acid and a phosphate group (Hou *et al*., 2015). Phospholipase C and phospholipase D are involved in the synthesis of PA from phosphatidylinositol-(4,5)-bisphosphate (PIP2), phosphatidylcholine (PC) and phosphatidyl-ethanolamine (PE). These reactions are crucial for the maintenance of the PA pool, which serves as a source for the biosynthesis of other phospholipids (Munnik, 2001; Ufer *et al*., 2017). PA can also function as signalling molecule in response to environmental cues.

2.8 Objectives of the study

The cell wall is the outermost structure of a plant cell thus defining its shape. It is also the first structure to encounter environmental changes and different stresses. The aim of this study was to characterise the *C. plantagineum* cell wall during a desiccation/rehydration cycle, investigate how these changes in the cell wall are sensed by the plant and which cell wall modifying enzymes are important in cell wall remodelling processes. The work was divided in three objectives:

1. The first objective was to analyse *C. plantagineum* leaves on a morphological level with scanning electron microscopy and observe the folding of cell walls upon dehydration by staining them with silver nitrate. In a biochemical approach, different monoclonal antibodies against cell wall epitopes were utilised in ELISA assays to characterise changes in the cell wall composition during dehydration and rehydration.
2. The second objective was to analyse the amino acid sequence of CpGRP1 and search for amino acids which might be able to bind pectin. Blue-native page gel-shift assays, ELISA assays and dot-blot assays were used to test the ability of the CpGRP1 protein to interact with cell wall polysaccharides. The ability of CpGRP1 to interact with lipids was also tested by protein-lipid overlay assays and liposome-binding assays.
3. The third objective was to analyse transcriptome data of pectinmethylesterases and pectinmethylesterase inhibitor proteins. The aim was to further characterise candidates which were differentially expressed upon desiccation in terms of their amino acid sequence and their expression level during dehydration and rehydration.

3. MATERIALS AND METHODS

3.1 Cultivation of plants

C. *plantagineum* Hochst., *L*. *brevidens* Skan, and *L*. *subracemosa* De Wild plants were grown as described by Bartels *et al*. (1990) and Phillips *et al*. (2008). *C. plantagineum* plants were cultivated using clay pebbles for hydroculture (Original Lamstedt Ton, https://www.fiboexclay.de/) and *L. brevidens* and *L. subracemosa* were cultivated in soil. Plants were kept under a 16 h day/8 h night regime with a light intensity of 80 µE m^{-2} sec^{-1}. For dehydration, fully-grown plants were dehydrated in pots on tissue paper until partial dehydration (PD, RWC = 50%) or desiccation (D, RWC = 2%). Desiccated plants were rehydrated for either 24 h (R 1) or 48 h (R 2). The hydration status of leaves was determined by calculating the relative water content (RWC) with the formula: RWC [%] = (Initial weight-dry weight)/(full turgor weight-dry weight) x 100 (Bernacchia *et al*., 1996). Leaves from dehydrated and rehydrated plants were ground to a fine powder in liquid nitrogen with a mortar and pestle and stored at -80°C.

3.2 Molecular biology techniques and DNA sequencing

Molecular biology techniques were performed according to Green and Sambrook (2012). Polymerase chain reactions (PCR) were performed for expression analysis (RT-PCR), screening for positive colonies (colony-PCR), cloning and mutagenesis. For RT-PCR a sample (20 µL) consists of 11.8 µL water, 2 µL PCR 10 x buffer, 5 µL template, 0.5 µL forward primer (10 mM), 0.5 µL reverse primer (10 mM), 1 µL dNTPs (10 mM) and 0.2 µL *Taq* DNA-polymerase (2.5 U/µL). For colony-PCR 15.8 µL of water were used to prepare one sample and a colony was picked and used directly as a template. For RT-PCR and colony-PCR the following PCR programme was used: initial denaturation at 95°C for 90 s, [(denaturation at 95°C for 30 s, primer annealing at X °C for 1 min, elongation at 72°C for 1 min/kb) number of cycles varies], final elongation at 72°C for 5 min, storage at 4°C. PCR for cloning and mutagenesis was performed using Phusion DNA polymerase (ThermoScientific, https://www.thermofisher.com) according to the manufacturer's instructions. After PCR samples were analysed using agarose gel electrophoresis. Concentrations between 0.8% and 2% (w/v) of agarose were chosen depending on the size of the sample. Agarose gels were stained with 0.001 mg/ml ethidium bromide and evaluated under UV-light.

To extract plasmid-DNA a single bacterial clone was incubated overnight in 10 mL liquid LB-media supplemented with selective antibiotics at 200 rpm and 37°C. The bacteria were pelleted by centrifugation at 14000 *g* for 5 min and resuspended in 200 µL buffer B1 (50 mM Tris; 10 mM EDTA, pH 8; 100 µg/mL RNase A). 200 µL buffer B2 (200 mM NaOH; 1% (w/v) SDS) were added to the mixture and after addition of 300 µL buffer B3 (3 M potassium acetate, pH 5.5) the samples were inverted and incubated at RT for 3 min. After centrifugation at 14000 *g* for 10 min at RT, the supernatant was transferred to a new tube and 700 µL phenol/chloroform (1:1) were added and the samples were vortexed for 1 min. After centrifugation at 14000 *g* for 1 min at RT the upper phase was transferred to a new tube and 0.7 volumes isopropanol were added. The samples were incubated on ice for 15 min to precipitate the plasmid-DNA. The DNA was then pelleted by centrifugation at 16000 *g* for 30 min at 4°C. The pellet was washed two times with 70% (v/v) ethanol and then dried for 5 min at RT. Plasmid-DNA was then resuspended in 40 µL water and further purified with the PCR clean-up gel extraction kit (Macherey-Nagel, https://www.mn-net.com/) according to the manufacturer's instructions.

Total RNA was isolated according to Valenzuela-Avendaño *et al*. (2005). 200 mg of plant material were ground to fine powder and vortexed with RNA extraction buffer (38% (v/v) phenol; 0.8 M guanidine thiocyanate; 0.4 M ammonium thiocyanate; 0.1 M sodium acetate, pH 5). The suspension was incubated at RT for 10 min. The samples were centrifuged at 10000 *g* for 10 min at 4°C and the upper phase was precipitated with 375 µL ice-cold isopropanol and 375 µL 0.8 M sodium citrate/1 M sodium chloride for 10 min at RT. After centrifugation at 12000 *g* for 10 min at 4°C the RNA pellet was air-dried and resuspended in 100 µL sterile water. 167 µL 4 M LiCl were added and the samples were incubated on ice for 2 h. After centrifugation at 14000 *g* for 20 min at 4°C the pellets were washed with ice-cold 70% (v/v) ethanol. RNA samples were resuspended in 20 µL DEPC (diethylpyrocarbonate)-treated water.

Preparation of cDNA was performed as described by Giarola *et al*. (2015). Four µg of total RNA were treated with DNase I (1 U/µl) for 30 min (ThermoScientific, https://www.thermofisher.com) according to the manufacturer's instructions. Then two µg of treated RNA were reverse-transcribed using the RevertAid Reverse Transcriptase (ThermoScientific, https://www.thermofisher.com) following the manufacturer's instructions. Two µg of treated RNA were used as a negative control

for the reverse transcription reaction. For RT-PCR experiments the cDNA was diluted 15 times with water and 5 µL were used as a template for PCR-reactions.

DNA sequencing was carried out by GATC Biotech (https://www.gatc-biotech.com/en/index.html) and primer synthesis by Eurofins MWG Operon (http://www.eurofinsgenomics.eu). All primers used are listed in Table S1.

The mRNA coding sequence corresponding to the Cp_V2_contig_11593 was amplified from *C. plantagineum* cDNA using the primers CpPME_Full_F and CpPME_Full_R and cloned into the vector pJET1.2 (ThermoScientific, https://www.thermofisher.com). attB gateway sites were introduced into the Cp_V2_contig_11593 sequence by amplifying the sequence from pJET1.2 using a 2-step gateway protocol (developed by Invitrogen, https://www.embl.de/) with primers (attB1-adapter and attB2-adapter (for first step); CpPME_attB1 and CpPME_attB2 (for second step)). The amplified fragment was introduced with a BP-reaction (PCR fragment + Donor vector = Entry clone) into the pDONR201 vector (ThermoScientific, https://www.thermofisher.com) using the Gateway BP Clonase II enzyme mix (ThermoScientific, https://www.thermofisher.com) to generate the gateway entry clone which includes the attL sites. To introduce the Cp_V2_contig_11593 fragment into the pQLinkHD and generate the protein-overexpression clone a LR-reaction (Entry Clone + Destination Vector = Expression Clone) was performed using the Gateway LR Clonase II enzyme mix (ThermoScientific, https://www.thermofisher.com) (Scheich *et al*., 2007).

3.3 Scanning electron microscopy (SEM)

C. *plantagineum* leaves were frozen in liquid nitrogen and sputtered with palladium for 2 min using a sputter-coater (SCD 040, Balzer). Leaves were fixed on the sample holder and analysed under the electron microscope at 100x and 400x magnification to take surface images (Cambridge Stereoscan S 200, Cambridge Instrument Company, UK).

Cell walls were stained as follows: leaf material was cut with a razor blade and immediately immersed in cold FAA (10% (v/v) formalin; 10% (v/v) acetic acid; 30% (v/v) water and 50% (v/v) ethanol) solution for at least 24 h at 4°C. After fixation samples were incubated for 30 min in 85% (v/v) ethanol and sequentially in 50% (v/v) ethanol/50% (v/v) acetone and finally in 100% (v/v) acetone solutions.

Samples were embedded using the Agar Low Viscosity Kit (LVK) (Plano GmbH, Wetzlar, https://www.plano-em.de): Samples were treated in LVK/acetone using increasing concentrations of acetone (30% (v/v), 60% (v/v), 90% (v/v) and finally 100% (v/v) for 3 h each step. The leaf samples were embedded in fresh LVK-solution and polymerised at 70°C for 7 h. The LVK-blocks were cut using a microtome. Cell wall structures were stained with a 30% (w/v) silver nitrate solution for 10 min. The samples were incubated in 10% (v/v) HCl for 5 min after staining and sputtered with palladium for 2 min before analysing the surface under the SEM (Block-face imaging).

To preserve the surface structures of the specimens which could be damaged due to surface tension when changing form the liquid to gaseous state critical point drying (CPD 020; Balzers, http://www.oerlikon.com/balzers) was performed according to Svitkina *et al*. (1984) before analysing with the SEM.

3.4 Protein analyses

The DNA sequence encoding the N-terminal fragment (aa22-120) and the C-terminal fragment (aa121-156) of CpGRP1 (Genbank accession number ALQ43973.1) was amplified with primers from the pET28a CpGRP1His plasmid to add a *Nco*I site and a *Xho*I site at the 5' and 3' ends, respectively (CpGRP1_NTERM_R/T7 promoter and CpGRP1_CTERM_F/T7 terminator, Table S1). The sequence encoding the extracellular domain of CpWAK1 (aa31-315) was amplified with primers from a CpWAK1 cDNA clone (GenBank accession number KT893872.1; Giarola *et al*., 2016) to add a *Xho*I site at the 3' end (pJET1.2_F and CpWAK1_XhoI_R, Table S1). A *Nco*I site is already present in the CpWAK1 sequence. The sequence encoding the *C. plantagineum* germin-like protein1 (CpGLP1, Dulitz, 2016) without the signal peptide (aa27-226) was excised from a pAD vector using *Eco*RI and *Sal*I restriction enzymes.

N- and C-terminal fragments of CpGRP1 as well as the CpWAK1 extracellular fragment were cloned between the *Nco*I and the *Xho*I sites of the pET28a expression vector (NOVAGEN, http://www.novagen.com) to create the protein-His-tag translation fusion constructs (pET28a_CpGRP1_N-terminalHis, pET28a_CpGRP1_C-terminalHis, and pET28a_CpWAK1_extracellularHis, respectively). The CpGLP1 fragment was cloned using the *Eco*RI and *Sal*I sites of the pET28a vector to generate the pET28a_CpGLP1His fusion construct (CpGLP1, Dulitz, 2016). Overexpression

constructs were transformed into BL21 (DE3) *Escherichia coli* cells (Amersham Pharmacia Biotech, NJ, USA).

Protein overexpression was induced by adding isopropyl-1-thio-ß-D-galactopyranoside (IPTG) to a final concentration of 1 mM at an OD_{600} of 0.5. The recombinant proteins were purified from bacteria 5 h after IPTG induction using affinity chromatography with nickel-NTA resin columns (ThermoScientific, https://www.thermofisher.com) (Kirch and Röhrig, 2010). Bacterial samples were taken after 1 h and after 3 h and stored at -20°C. The main culture was harvested by centrifugation at 4000 *g* for 20 min at 4°C. The bacterial pellet was dissolved in 5 mL buffer A (50 mM NaH_2PO_4; 0.3 M NaCl; 5 mM imidazole; 10% (v/v) glycerol; 0.1% (v/v) Triton X-100; pH 8 (NaOH)) freshly supplemented with 1 mg/mL lysozyme and incubated on ice for 30 min. The suspension was sonicated with an ultrasonic processor for 6 x 20 s. Samples were centrifuged at 14000 *g* for 30 min at 4°C and the supernatant was sterile filtered. The lysate was loaded to a nickel-NTA resin column that was equilibrated with 3 mL water, 5 mL 50 mM $NiSO_4$, and 3 mL buffer A. After loading the column was washed with 10 mL buffer A and two times with 8 mL buffer B (50 mM NaH_2PO_4; 0.3 M NaCl; 10 mM imidazole; 10% (v/v) glycerol; 0.1% (v/v) Triton X-100; pH 8 (NaOH)). Elution of proteins was performed with 5 mL of buffer C (50 mM NaH_2PO_4; 0.3 M NaCl; 250 mM imidazole; 10% (v/v) glycerol; 0.1% (v/v) Triton X-100; pH 8 (NaOH)). The regeneration of the nickel-NTA resin was carried out with 3 mL regeneration buffer (20 mM Tris-HCl, pH 8; 0.3 M NaCl; 100 mM EDTA). The column was stored in 30% (v/v) ethanol.

Estimation of protein concentrations was performed according to Bradford (1976). In a 1 mL cuvette, 990 µL of 20% (v/v) Bradford reagent (BIORAD, https://www.bio-rad.com) was mixed with 10 µL of protein sample and inverted. The sample was incubated for 10 min and the absorbance was read at 595 nm with a spectrophotometer. The absorbance was correlated to a protein concentration with a standard curve prepared with 5 µg, 10 µg, 15 µg and 20 µg of BSA (Figure S1). Purified protein fragments were concentrated using Amicon Ultracel-10K centrifugal concentrators (MILLIPORE, http://www.millipore.com) and desalted with PD10-columns (http://www.gelifesciences.com) before freeze-drying in 100 mM ammonium bicarbonate buffer. Freeze-dried proteins were used for Blue-native page gel-shift assays, ELISA pectin binding assays and dot-blot assays.

The QuikChange II site-directed mutagenesis kit (Agilent, https://www.agilent.com) was used to mutate amino acid residues in the CpGRP1 N-term. fragment and the CpGRP1 full-length protein. The two arginine residues in the N-term. fragment (Arginine [118] and [120]) were mutated with primers (CpGRP1_NTERM _a352g_c358g_F and CpGRP1_NTERM _a352g_c358g_R, Table S1) to two glycine residues and the six cysteine residues in the CpGRP1 full-length protein (Cysteine [121], [125], [126], [135], [137] and [138]) were mutated in two steps with primers (CpGRP1_CTERM_MUT1_F and CpGRP1_CTERM_MUT1_R; CpGRP1_CTERM_ MUT2_F and CpGRP1_CTERM _MUT2_R) to six glycine residues to generate the mutated CpGRP1 N-term. fragment and the mutated CpGRP1 full-length protein.

Protein extraction was performed according to Laemmli (1970). The bacterial pellets were dissolved in 100 µL SDS-sample buffer (2% (w/v) SDS; 10% (w/v) glycerol; 60 mM Tris HCl, pH 6.8; 0.01% (w/v) bromophenol blue; 0.1 M DTT), boiled at 95°C for 10 min and centrifuged at 10000 *g* for 1 min. Samples were directly used for SDS-page or stored at -20°C. Separation of proteins was performed as described by He (2011) based on the method first described by Laemmli (1970). The SDS-gel contained a 4% (w/v) polyacrylamide stacking gel and a 15% (w/v) polyacrylamide separation gel. Electrophoresis was performed in 1 x running buffer (25 mM Tris; 192 mM glycine; 0.1% (w/v) SDS) for 2 h at 20 mA.

The separation of the CpGRP1 C-terminal fragment was performed as described by Schägger and Jagow (1987) using a peptide page. The polyacrylamide gel contained three different parts: The separating gel [6.7 mL water; 10 mL separating/spacer gel buffer (3 M trizma base; 1 M tricine; 1% (w/v) SDS; dilute 1:10 before use); 10 mL separating/spacer gel acrylamide (48 g acrylamide; 1.5 g *N,N*-methyl-ene-*bis*-acrylamide; bring to 100 mL); 3.2 mL glycerol; 10 µL TEMED; 100 µL 10% (w/v) ammonium persulfate], the spacer gel [6.9 mL water; 5 mL separating/spacer gel buffer; 3 mL separating/spacer gel acrylamide; 5 µL TEMED; 50 µL 10% (w/v) ammonium persulfate], and the stacking gel [10.3 mL water; 1.9 mL stacking gel buffer (1 M Tris-HCl, pH 6.8); 2.5 mL stacking gel acrylamide (30 g acrylamide; 0.9 g *N,N*-methylene-*bis*-acrylamide; bring to 100 mL); 150 µL EDTA; 7.5 µL TEMED; 150 µL 10% (w/v) ammonium persulfate]. Electrophoresis was performed in 1 x cathode running buffer (0.1 M trizma base; 0.1 M tricine; 0.1% (w/v) SDS) and 1 x anode running buffer (0.2 M trizma base, pH 8.9) at 7 W for 4 h. Proteins of acrylamide gels were

visualised with Coomassie Brilliant Blue R250 (0.1% (w/v) Coomassie R250; 50% (v/v) methanol; 10% (v/v) glacial acetic acid; 40% (v/v) water). Immunoblot analyses were performed according to Towbin *et al*. (1979). Proteins were transferred at 70 V for 1 h at 4°C in towbin buffer (25 mM Tris; 0.2 M glycine; 20% (v/v) methanol). Successful protein transfer to a nitrocellulose membrane was confirmed by staining with Ponceau red (0.2% (w/v) Ponceau S; 3% (w/v) TCA) for 10 min. The membrane was destained with water. The membrane was blocked in 4% (w/v) non-fat milk powder in TBST [TBS (20 mM Tris, pH 7.5; 0.15 M NaCl); 0.1% (v/v) Tween-20] for 1 h at RT. Then the membrane was incubated with the primary antibody in blocking solution for 1 h (RT) or overnight (4°C), depending on the antibody. The membrane was washed in TBST for 3 x 15 min and incubated in the secondary antibody (1:5000) for 45 min at RT. The membrane was again washed as described above. As primary antibodies the CpGRP1 or a 6x-His polyclonal antibody (http://www.thermofisher.com) was used. Detection of proteins was performed using the ECL Western Blotting detection kit (GE HEALTHCARE, http://www.gehealthcare.com). Signals were visualised using the Azure Biosystems c300 chemiluminescent detection system (http://www.biozym.com).

3.5 Extraction of cell wall components

Cell wall components were obtained by following extractions as described by Cornuault *et al*. (2014). The 1,2-cyclohexanediaminetetraacetic acid (CDTA) fraction was obtained by vortexing 1 mg freeze-dried material in 1 mL 50 mM CDTA pH 7.5 for 1 h. The sample was then centrifuged at 14000 *g* for 12 min and the supernatant was collected. The residue was further extracted by vortexing with 1 mL 4 M KOH, 1% (w/v) $NaBH_4$ solution for 1 h and the sample was again centrifuged and the supernatant was collected. 80% (v/v) acetic acid was used to neutralise the pH of the KOH fraction after extraction. All samples were stored at -20°C until use.

3.6 Enzyme-linked immunosorbent assays

The experiment was performed as described by Cornuault *et al*. (2014). Isolated CDTA and KOH fractions were incubated in microtiter plates (NUNC-Immuno MicroWell 96 well solid plates, flat bottom, http://www.sigmaaldrich.com) overnight at 4°C. Plate wells were washed vigorously six times with PBS (137 mM NaCl; 2.7 mM KCl; 10 mM Na_2HPO_4; 2 mM KH_2PO_4) and then blocked using 200 µL per well of 4% (w/v) non-fat milk powder in PBS for 2 h at room temperature. The plates were washed nine times

with PBS and padded dry. Primary antibodies were added and incubated overnight at 4°C. The plates were washed 12 times with PBS and shaken dry. Then 150 µL secondary peroxidase-coupled anti-rabbit or anti-rat IgG antibodies (http://www.sigmaaldrich.com) were added at a 5000-fold dilution in 4% (w/v) non-fat milk powder/PBS for 1 h at room temperature. After washing 12 times with PBS, microtiter plates were developed using 150 µL of substrate solution (0.1 M sodium acetate buffer, pH 6; 0.1% (w/v) tetramethyl benzidine; 0.006% (v/v) H_2O_2) in each well. The enzyme reaction was stopped by adding 40 µL of 2.5 M H_2SO_4 to each well, and the absorbance at 450 nm was determined for each well.

3.6.1 Analysis of cell wall composition

Nine different rat monoclonal antibodies (mAb) were used in this study: JIM5, JIM7, LM20, LM19, LM25, LM15, LM11, LM5 and LM6 (provided by J. Paul Knox, University of Leeds, UK, http://www.plantprobes.net/) and one rabbit mAb: 42-6 (provided by M. Kobayashi, Kyoto University, Japan) (Table 1).

Table 1. Monoclonal antibodies used in this study for pectin and hemicellulose characterisation.

	Antibody	Specificity	Reference
HG†	JIM5	partially or de-methylesterified HG	Knox *et al*. (1990)
	JIM7	partially methylesterified HG	Knox *et al*. (1990)
	LM20	methylesterified HG	Verhertbruggen *et al*. (2009)
	LM19	fully de-methylesterified HG	Verhertbruggen *et al*. (2009)
RG‡-II	42-6	B-RG-II, RG-II monomers, unknown pectic fragment	Zhou *et al*. (2018)
RG‡-I	LM6	α-(1,5)-arabinan	Willats *et al*. (1998)
	LM5	β-(1,4)-galactan	Jones *et al.* (1997)
Hemi-celluloses	LM25	Xyloglucan (XXLG, XLLG)	Pedersen *et al* (2012)
	LM15	Xyloglucan (XXXG)	Marcus *et al*. (2008)
	LM11	β-(1,4)-xylan	McCartney *et al*. (2005)

† Homogalacturonan, ‡ Rhamnogalacturonan

CDTA and KOH 1:5 dilutions were used for ELISA assays as they showed the most appropriate signal intensity (Figure S2). Tenfold dilution of hybridoma cell culture

supernatants in 4% (w/v) non-fat milk powder/PBS and a 1:10000 dilution for 42-6 were used as primary antibodies (150 µL each well).

3.6.2 Protein-pectin binding assays

After incubating CDTA and KOH fractions overnight in microtiter plates, the plates were washed 12 times with PBS and shaken dry. Recombinant proteins were dissolved in 4% (w/v) non-fat milk powder at a concentration of 1 µg/µL and incubated in the plates overnight at 4°C. After repeating the washing series, the proteins were detected using a 6x-His-tag polyclonal antibody (http://www.thermofisher.com) at a 1:5000 dilution. Pre-treatment of pectin was performed before adding recombinant proteins by incubating the plates with 50 mM CAPS-buffered solution at alkaline pH (adjusted between 7 and 11 with HCl and KOH) or with 0.1 M sodium carbonate (pH 9.6).

3.7 Determination of galacturonic acid

The galacturonic acid content was determined according to Blumenkrantz and Asboe-Hansen (1973) and Verma *et al*. (2014). All CDTA and KOH fractions were analysed for their galacturonic acid content by the m-hydroxydiphenyl method, using 0.05, 0.1, 0.2, 0.4 and 0.6 mg galacturonic acid as a standard (Figure S3). 200 µL of each fraction was transferred to a glass tube and 1.2 mL 0.0125 M tetraborate prepared in sulfuric acid was added. The samples were placed on ice for 10 min and then heated in a water bath at 100°C for 5 min. 20 µL 0.15% (w/v) m-hydroxydiphenyl reagent was added and the samples were shaken for 5 min before the absorbance was measured at 520 nm.

3.8 Blue-native page gel-shift assays

For gel-shift assays 0.5 µg of CpGRP1 protein were incubated with 0.5 µg of citrus pectin (http://www.sigmaaldrich.com) and different concentrations of $CaCl_2$ or $MgCl_2$ for 4 h at room temperature. The samples were mixed with 5x sample buffer (15.5 mL 1 M Tris-HCl, pH 6.8; 2.5 mL 1% (w/v) bromophenol blue solution; 7 mL water; 25 mL glycerol) and separated in 15% (w/v) polyacrylamide gels without SDS and without stacking gel. A Tris/boric acid buffer (89 mM Tris; 89 mM boric acid; pH 9.25) was used for gel preparation and gel electrophoresis. Gel-shift assays for the CpGRP1 C-term. fragment were performed in a peptide page (see 3.4) without SDS and without stacking and spacer gel. Gels were either stained with Coomassie Brilliant Blue or incubated in

50 mM Tris/1% (w/v) SDS buffer prior to immunoblotting. Proteins were detected using a 6x-His-tag polyclonal antibody (http://www.thermofisher.com) at a 1:5000 dilution.

3.9 Dot-blot pectin binding assays

Dot-blot assays were either based on proteins or pectin immobilised on a nitrocellulose membrane. Dots of 1.5 µL of either polygalacturonic acid (PGA) or of the CDTA-pectin fraction or of the CpGRP1 recombinant protein, the CpWAK1 recombinant protein, the CpGLP1 recombinant protein, the CpLEA-like 11-24 recombinant protein and BSA were spotted on a nitrocellulose membrane and allowed to dry. The amount of spotted PGA or recombinant proteins is indicated in the figures. Membranes were blocked with 4% (w/v) non-fat milk powder in TBST for 2 h and were then washed with TBST three times for 5 min. The membranes were incubated with different recombinant proteins (1 µg/mL; membranes with PGA and CDTA spots) or pectin (2 mg/mL; membranes with protein spots) in TBST overnight at 4°C followed by three washing steps. The membranes were incubated with 6x-His-tag antibody (1:5000 dilution) or JIM5 antibody (1:10 dilution) overnight at 4°C and then washed again three times with TBST. Immunodetection was performed as described above and quantification of dot intensity was done using *ImageJ* (http://www.imagej.net).

3.10 Protein-lipid overlay assays

Protein-lipid overlay assays were performed according to Deak *et al*. (1999) and Ufer *et al*. (2017) to analyse lipid binding properties of CpGRP1. Immobilised lipids (each 5 µg) on nitrocellulose membranes were provided by Prof. Dörmann (IMBIO, University of Bonn, Germany). The membrane was blocked for 1 h in 4% (w/v) BSA in TBST at RT. Then the recombinant protein at a concentration of 1 µg/mL prepared in 4% (w/v) BSA in TBST was added to the membrane and incubated overnight at 4°C. The membrane was washed three times with TBST for 5 min each time and incubated in the primary antibody prepared in 4% (w/v) BSA in TBST. The washing steps were repeated and the membrane was incubated with the secondary antibody prepared in 4% (w/v) BSA in TBST for 45 min and washed again prior to immunodetection.

3.11 Liposome-binding assays

Liposome-binding assays were performed according to Zhang *et al*. (2004) and Ufer *et al*. (2017) to analyse liposome-binding properties of CpGRP1. Phosphatidic acid

(PA) and phosphatidylcholine (PC) were dissolved in 2:1 chloroform/methanol to a final concentration of 4 µg/µL and stored at -20°C. 250 µg of lipids (150 µg PC + 100 µg PA) were transferred to fresh tubes and the solvents were evaporated under the fume hood. The pellet was resuspended in liposome-binding buffer (20 mM MES; 30 mM Tris-HCl, pH 7; 0.5 mM NaCl; 2 M urea; 0.5% (w/v) CHAPS; 1 mM DTT) and incubated at 37°C on a shaker and the resulting liposomes were vortexed for 5 min and subsequently centrifuged at 20000 *g* for 10 min at 4°C. Liposomes were resuspended in 250 µL liposome-binding buffer containing 0.1 µg/µL of the protein of interest. The mixture was incubated at 30°C for 30 min and spun down at 10000 *g* for 10 min at 4°C. Proteins of the supernatant and the pellet were analysed on polyacrylamide gels.

3.12 Electrostatic surface modelling

The *Phyre2* (http://www.sbg.bio.ic.ac.uk/phyre2/html/page.cgi?id=index) (Kelley *et al*., 2015) web service was used to create a PDB-file from the CpGRP1 and CpPME protein sequences, which were then used for electrostatic surface modelling using the website http://www.charmm-gui.org/?doc=input/pbeqsolver (Im *et al*., 1998; Jo *et al*., 2008a, 2008b) or 3D-modelling using *Phyre2*, respectively.

4. RESULTS

4.1 Morphological characterisation of leaf structures

Microscopic views of the *C*. *plantagineum* leaf surfaces and transverse sections during a desiccation/rehydration cycle are shown in Figure 5a and b. Untreated and rehydrated leaf tissues are almost identical suggesting that leaves can fully recover from desiccation-induced cellular changes after 48 h of rehydration. In contrast to the hydrated and rehydrated samples, the epidermis of the desiccated leaf is extensively folded. In this compact structure leaf glands are trapped in the epidermal folds. Leaf folding mainly occurs during late dehydration when the relative water content is below 60%. Cell walls in desiccated tissues were slightly thicker than cell walls in untreated and 48 h-rehydrated tissues as shown by cell wall staining (Figure 5c and d). These findings suggest that changes in pectin composition between the different samples might be involved in cell wall adaptations to water-stress conditions.

4.2 Pectin and hemicellulose profiles determined in a desiccation/rehydration cycle

Panels of monoclonal antibodies allow the monitoring of changes in cell wall polysaccharides (http://www.plantprobes.net/) (Table 1). In ELISA assays JIM5, JIM7, LM20 and LM19 were used to analyse differences in the methylesterification pattern of isolated *C*. *plantagineum* HG fractions upon desiccation and rehydration (Table 2). The abundance of the pectin and hemicellulose epitopes is correlated with colour intensity in the ELISA read-outs. JIM5, JIM7 and LM20 displayed a stronger binding to the untreated and rehydrated (1 and 2) samples than to the desiccated sample. LM19, which detects fully de-methylesterified HG, displayed a stronger signal to desiccated samples than to untreated samples. These results indicate changes in the HG methylesterification status during the desiccation/rehydration cycle and suggest homogalacturonan synthesis in the recovery process. Changes in the abundance of RG-II were analysed using the 42-6 antibody which binds RG-II monomers, crosslinked RG-II and an unknown pectic component (Table 1). The antibody bound more strongly to the untreated and rehydrated samples than to the desiccated samples (Table 2).

LM25, LM15, LM11, LM6 and LM5 monoclonal antibodies were used to analyse changes in the hemicelluloses and the rhamnogalacturonan-I (Table 1 and 2).

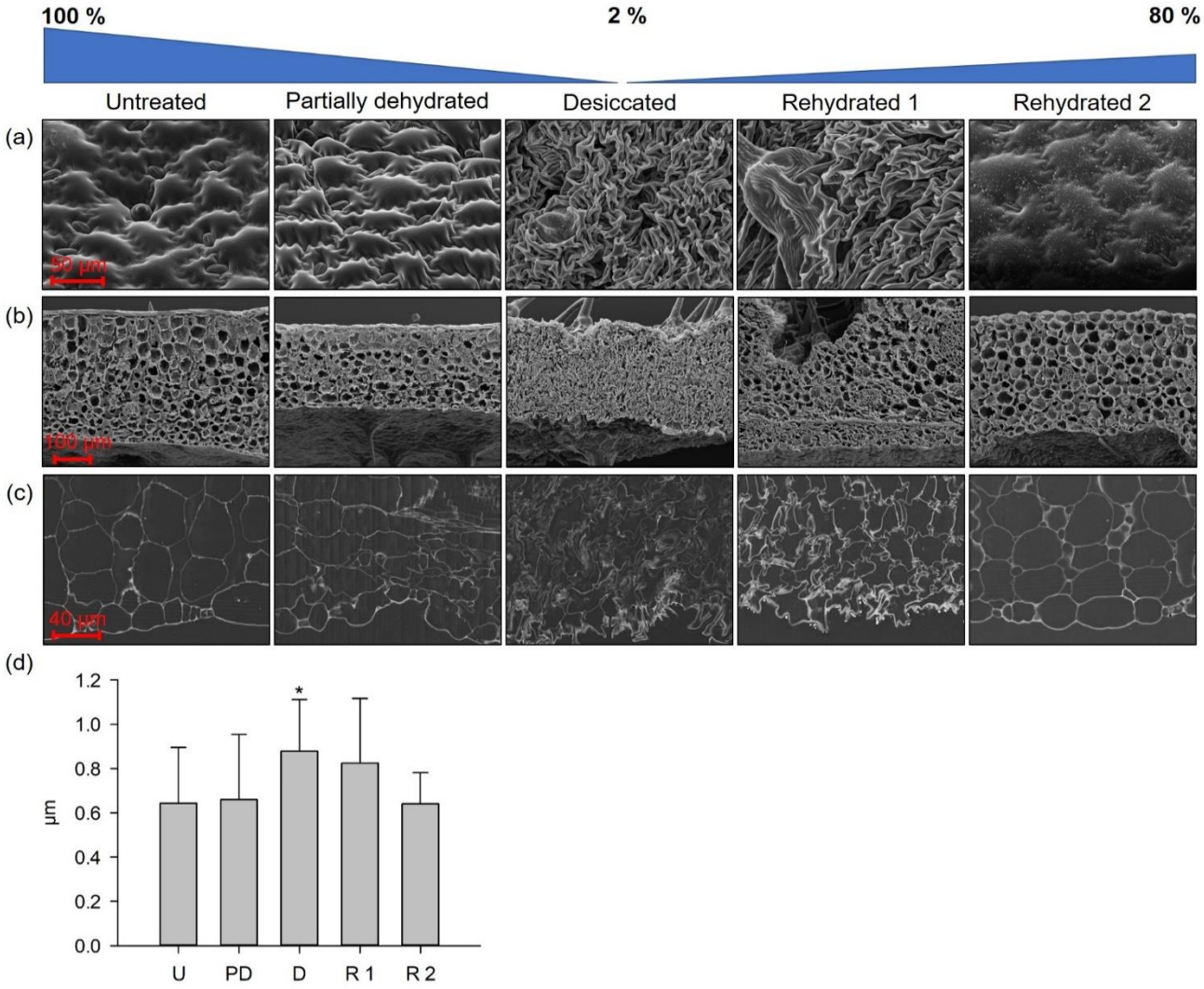

Figure 5 Morphological characterisation of *Craterostigma plantagineum* leaf structures using scanning electron microscopy: Surface images **(a)**, transverse section images **(b)** and images of cell walls stained with silver nitrate **(c)** are shown. Micrographs were taken in a desiccation/rehydration cycle. From left to right: Untreated (RWC = 100%), Partially dehydrated (RWC = 50%), Desiccated (RWC = 2%), 24 h after rehydration (Rehydrated 1) and 48 h after rehydration (Rehydrated 2). Representative micrographs are shown. Three different samples were used for the evaluation. **(d)**: Thickness of *C. plantagineum* cell walls in a desiccation/rehydration cycle. Images from **(c)** were used for the evaluation. Cell wall thickness increases slightly during dehydration and the starting point (untreated samples) is restored after 48 h of rehydration. U = Untreated, PD = Partially dehydrated, D = Desiccated, R 1 = Rehydrated 1, R 2 = Rehydrated 2. The star indicates the levels of significance in comparison to the untreated sample (OneWayANOVA, Holm-Sidak method): $*p < 0.05$.

LM25 and LM15 indicate strong signals for xyloglucan in desiccated leaves which are reversed during rehydration. LM11, which detects xylan, bound stronger to the desiccated samples, whereas LM6, which detects α-(1,5)-arabinan, displayed a slightly weaker binding to pectin of desiccated leaves than to pectin of untreated leaves. No significant changes were observed in the binding of the LM5 antibody which detects β-

(1,4)-galactan. Results obtained with RG-I, RG-II and hemicellulose antibodies suggest changes in the *C. plantagineum* cell wall composition during the desiccation/rehydration cycle.

Table 2. Analysis of changes in the cell wall composition of *Craterostigma plantagineum* leaves in a desiccation/rehydration cycle. JIM5, JIM7 and LM20 detect varying levels of methylesterification in HG. LM19 detects fully de-methylesterified HG. The 42-6 antibody detects RG-II, crosslinked RG-II and an unknown pectic epitope. LM6 and LM5 detect pectic arabinan and pectic galactan, epitopes present in the RG-I respectively. LM25 and LM15 detect xyloglucan and LM11 detects xylan. For specificity of different antibodies see Table 1. The colour scale in relation to absorbance values is shown at the bottom on the left-hand site. Results for HG were generated analysing the CDTA fractions in 1:5 dilutions and results for RG-I and RG-II were generated analysing the KOH fractions in 1:5 dilutions. Values shown are means of three biological replicates ± SD. The letters indicate the levels of significance (OneWayANOVA, Holm-Sidak method): abcd $p < 0.05$; ABCD $p < 0.01$; aA = significantly different from `Untreated´ sample, bB = significantly different from `Desiccated´ sample, cC = significantly different from `Rehydrated 1´ sample, dD = significantly different from `Rehydrated 2´ sample.

		Ab	Untreated	Desiccated	Rehydrated 1	Rehydrated 2
C. plantagineum	HG†	JIM5	0.85±0.14^{BCD}	0.37±0.09^{Ad}	0.33±0.06^{AD}	0.52±0.10^{AbC}
		JIM7	1.22±0.18^{BCD}	0.70±0.08^{AcD}	0.90±0.11^{Ab}	0.93±0.07^{AB}
		LM20	2.10±0.21^{BCd}	0.65±0.11^{ACD}	1.70±0.14^{AB}	1.83±0.16^{aB}
		LM19	0.77±0.12^{BCD}	1.32±0.17^{ACD}	0.46±0.05^{AB}	0.41±0.06^{AB}
	RG‡-II	42-6	3.49±0.27^{BCD}	0.41±0.11^{ACD}	1.63±0.26^{ABD}	2.55±0.23^{ABC}
	RG‡-I	LM6	1.66±0.31	1.33±0.25	1.50±0.22	1.45±0.19
		LM5	0.28±0.05	0.29±0.08^{d}	0.27±0.03	0.22±0.03^{b}
	Hemi-celluloses	LM25	1.30±0.10^{b}	1.50±0.19^{a}	1.35±0.11	1.34±0.14
		LM15	0.16±0.02^{B}	0.31±0.04^{ACD}	0.18±0.03^{B}	0.19±0.02^{B}
		LM11	0.15±0.07^{BCd}	0.65±0.11^{ACD}	0.42±0.09^{ABD}	0.26±0.08^{aBC}

† Homogalacturonan, ‡ Rhamnogalacturonan

0.00	0.50	1.00	1.50	2.00	2.50

4.3 Interaction between CpGRP1 and pectin

The glycine-rich cell wall protein CpGRP1 interacts with the CpWAK1 kinase protein in the apoplast and it has been hypothesised that CpGRP1 binds to pectin (Giarola *et al*., 2016). The objective of this chapter was to analyse the CpGRP1 amino acid sequence to search for residues which could be involved in an interaction with pectin and clone different polypeptide fragments and to investigate their possible interactions with cell wall polysaccharides. Three different approaches have been used to analyse a possible interaction of CpGRP1 and pectin: blue-native page gel-shift assays, ELISA

and dot-blot assays using either commercial pectin (from citrus peel, Sigma-Aldrich, USA) or the CDTA (1,2-cyclohexanediaminetetraacetic acid)-pectin fraction isolated from *C*. *plantagineum* or closely related species.

4.3.1 Cloning of CpGRP1 fragments

For pectin binding assays the CpGRP1 full-length recombinant protein and three CpGRP1 polypeptides have been used: N-term. fragment of CpGRP1, C-term. fragment of CpGRP1 and a mutated N-term. fragment with two arginines mutated to glycine (see Figure 7). The CpGRP1 full-length recombinant protein sequence was already cloned into pET28a resulting in the pET28a_CpGRP1His expression plasmid (Giarola *et al*., 2016). This plasmid has been used as a template to amplify the C-term. fragment and the N-term. fragment (Figure 6). The CpGRP1 full-length recombinant protein does not contain the signal peptide and carries an additional 6x-His-tag. The N-term. fragment does not contain the cysteine-rich region. The C-term. fragment is the smallest polypeptide and does not contain the glycine-rich domain of CpGRP1. For the mutated N-term. fragment arginines in position 118 and 120 were mutated to glycine. To investigate the migration behaviour of CpGRP1 in an SDS-page and to analyse changes in the hydrophobicity of the protein, six cysteine residues in the cysteine-rich domain have been mutated to glycine (CYS 121], CYS [125], CYS [126], CYS [135] CYS [137] and CYS [138]). Protein fragments and mutations are highlighted in Figure 7.

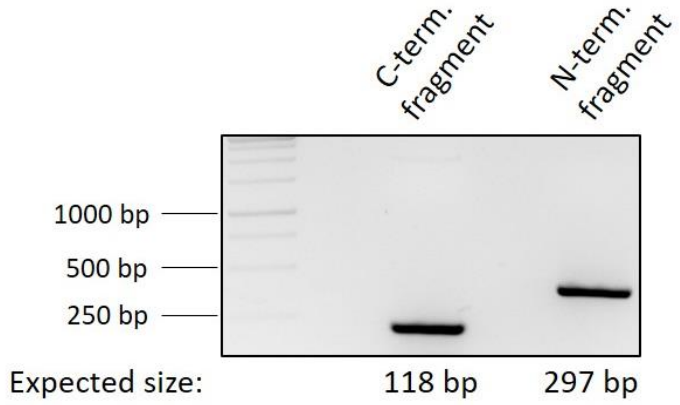

Figure 6 Amplification of CpGRP1 fragments from the pET28a_CpGRP1His plasmid. The C-term. fragment was amplified with the primers CpGRP1_CTERM_F and T7 terminator and the N-term. fragment with the primers CpGRP1_ NTERM_F and T7 promoter to add a *Nco*I site and a *Xho*I site at the 5' and 3' ends, respectively. The predicted amplicon size is indicated in the figure.

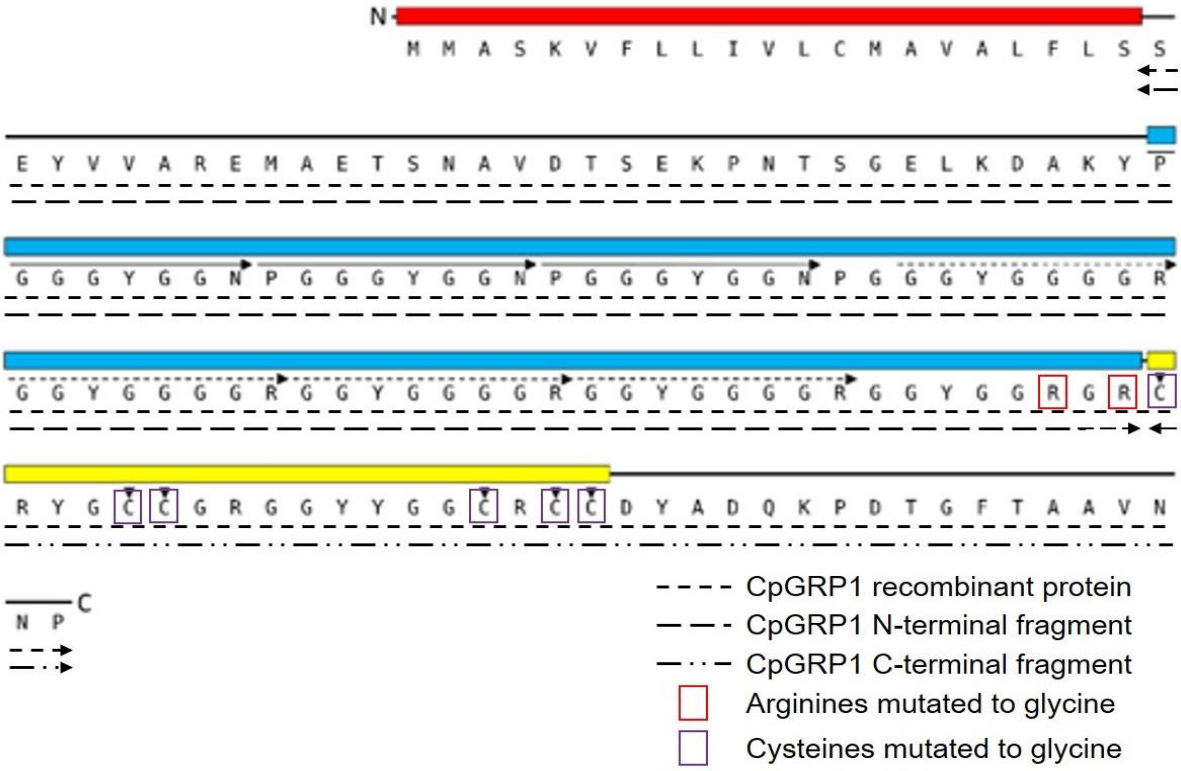

Figure 7 *Craterostigma plantagineum* CpGRP1 amino acid sequence and protein domains. The different protein domains of CpGRP1 are indicated by coloured boxes above the sequence. Red: predicted signal peptide; blue: semi-repetitive glycine-rich region; the two different amino acid tandem repeat motifs are shown with solid or dashed arrows respectively. Yellow: cysteine-rich region; the six cysteine residues are marked by black triangles. Different protein fragments are marked by dotted lines. Additionally, the full-length CpGRP1 recombinant protein and the other polypeptides carried six histidine residues at the C-terminus. The image was modified from Giarola *et al*. (2016).

4.3.2 Overexpression of CpGRP1 fragments

The different overexpression vectors pET28a_CpGRP1His plasmid, pET28a_CpGRP1_N-terminalHis, pET28a_CpGRP1_C-terminalHis, pET28a_Mutated_N-terminalHis and pET28a_Mutated_CpGRP1His were transformed into *E. coli* BL21 DE3 cells and overexpression was induced by adding IPTG to the culture. Samples were taken prior to IPTG induction and 1 h and 3 h after induction.

Successful overexpression was demonstrated by detecting the different proteins with a 6x-His-tag antibody (Figure 8). For all proteins no signal was detected before induction but after induction the protein was detected. The relatively small C-term. fragment was separated through a peptide page (see 3.4).

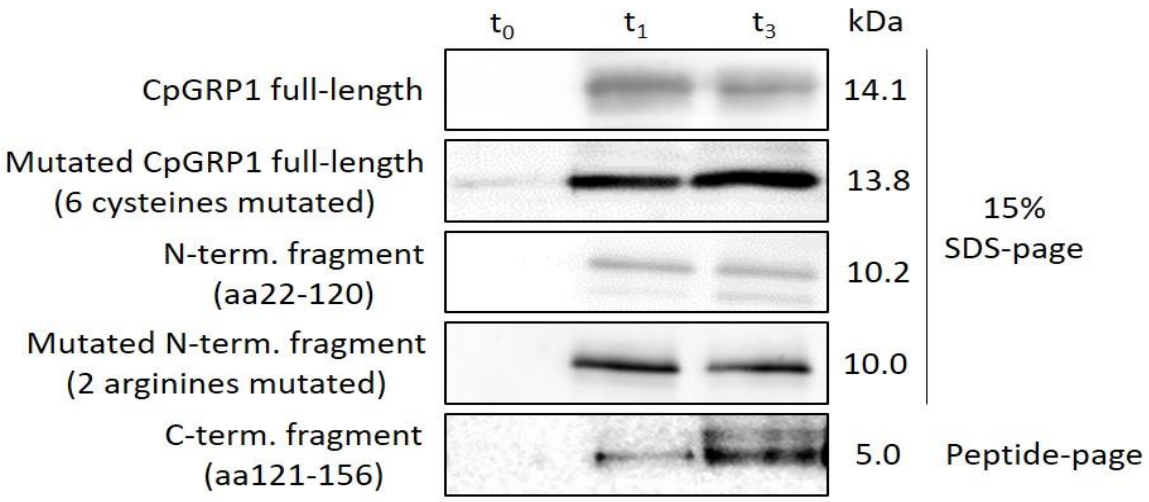

Figure 8 Overexpression of CpGRP1 full-length protein and polypeptides. Samples of overexpression culture were taken before inducing overexpression by adding IPTG (t_0) and 1 h (t_1) and 3 h (t_3) after IPTG induction. Total bacterial proteins were separated in SDS-gels and overexpressed proteins were detected with a 6x-His-tag antibody. The CpGRP1 full-length protein and the mutated CpGRP1 full-length protein, the N-term. fragment and the mutated N-term. fragment were separated from other proteins in a 15% (w/v) SDS-page and for the smaller C-term. fragment a peptide-page was used. The predicted size (kDa) of the proteins is indicated in the figure.

4.3.3 Electrostatic surface modelling of CpGRP1

Prior to investigating the pectin binding properties of the CpGRP1 full-length recombinant protein and the other purified polypeptide fragments, the electrostatic surface of the CpGRP1 protein was modelled to identify surface clusters which might be able to bind pectin (Figure 9). The electrostatic surface model revealed a positively charged cluster that contains six arginine residues and one lysine. All arginines present in this cluster were identified in the glycine-rich domain of the CpGRP1 protein (Figure 7).

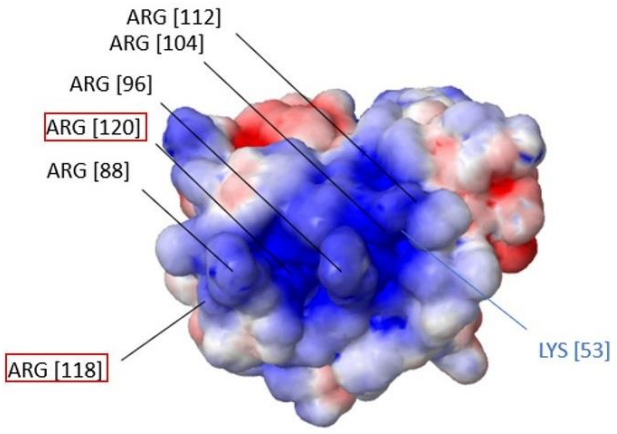

Figure 9 Electrostatic surface model of the recombinant CpGRP1 protein using CHARMM (http://www.charmm-gui.org/). Clustered arginines in the glycine-rich domain of the protein build up a positive cluster. Arginines at position 118 and 120 were mutated to glycine (red boxes).

The identified cluster strengthened the hypothesis, that CpGRP1 might be able to bind pectin. The ability of clustered positively charged amino acids to bind cell wall polysaccharides was reported previously (Spadoni *et al*., 2006).

4.3.4 Blue-native page gel-shift pectin binding assays

The full-length recombinant CpGRP1 protein or fragments of the CpGRP1 protein corresponding to N- or C-terminal domains or to the mutated N-terminal domain (two arginines mutated to glycine, a352g_c358g) were used for binding experiments (Figure 10). When the CpGRP1 full-length protein was incubated with commercial pectin and

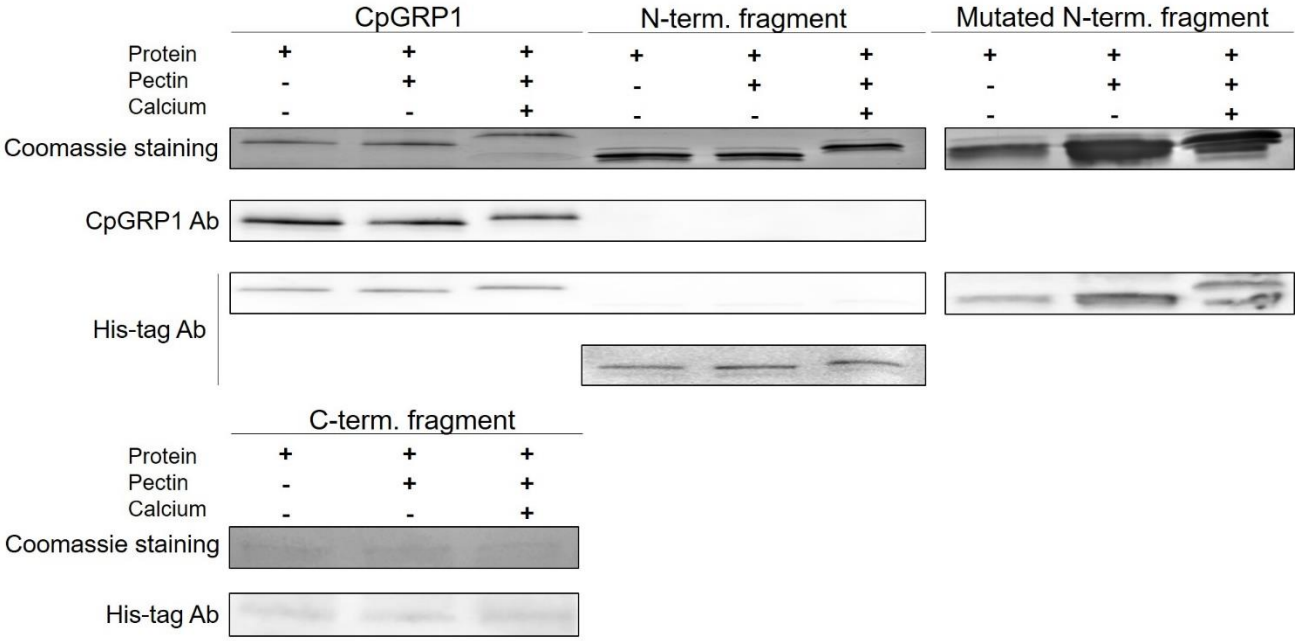

Figure 10 Analysis of CpGRP1-pectin interaction by Blue-native page gel-shift assay. The full-length recombinant CpGRP1 protein, the CpGRP1 N-terminal and C-terminal protein fragments and the mutated N-terminal protein fragment were used for this analysis. The proteins were detected with CpGRP1 or 6x-His-tag antibodies and gels were stained using Coomassie Brilliant Blue.

calcium, the electrophoretic mobility was retarded compared to the CpGRP1 protein in a native page. A similar mobility shift was observed for the N-terminal fragment, but not for the C-terminal fragment. The mutated N-terminal fragment did also show a mobility shift in the presence of pectin and calcium but in contrast to the non-mutated fragment, two protein bands were detected. No mobility shift for any of the proteins was observed in the absence of calcium. Different calcium concentrations were used

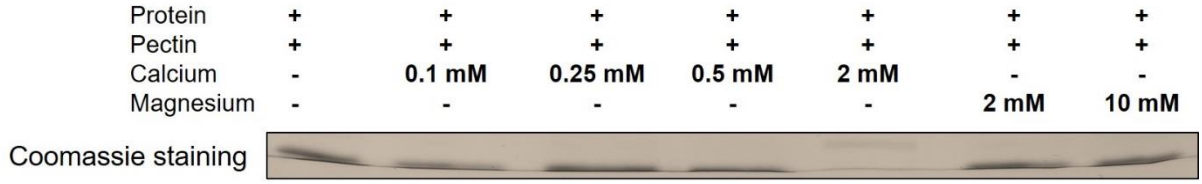

Figure 11 Effect of different calcium and magnesium concentrations on the interaction of CpGRP1 and pectin. The full-length recombinant CpGRP1 protein was used for this analysis. The gel was stained using Coomassie Brilliant Blue.

in a mobility-shift assay to determine the concentration crucial for the mobility shift (Figure 11). Low calcium concentrations between 0.1 mM and 0.5 mM were not sufficient to observe a retardation. The experiment confirmed the previous results (Figure 10) as a gel-shift was only observed in the presence of 2 mM calcium. Additionally, magnesium was tested in the gel-shift assay but no gel-shift was detected. This result demonstrates the specificity and importance of calcium in crosslinking pectin and formation of `egg-box´ structures (Plazinski, 2011).

4.3.5 ELISA pectin binding assays

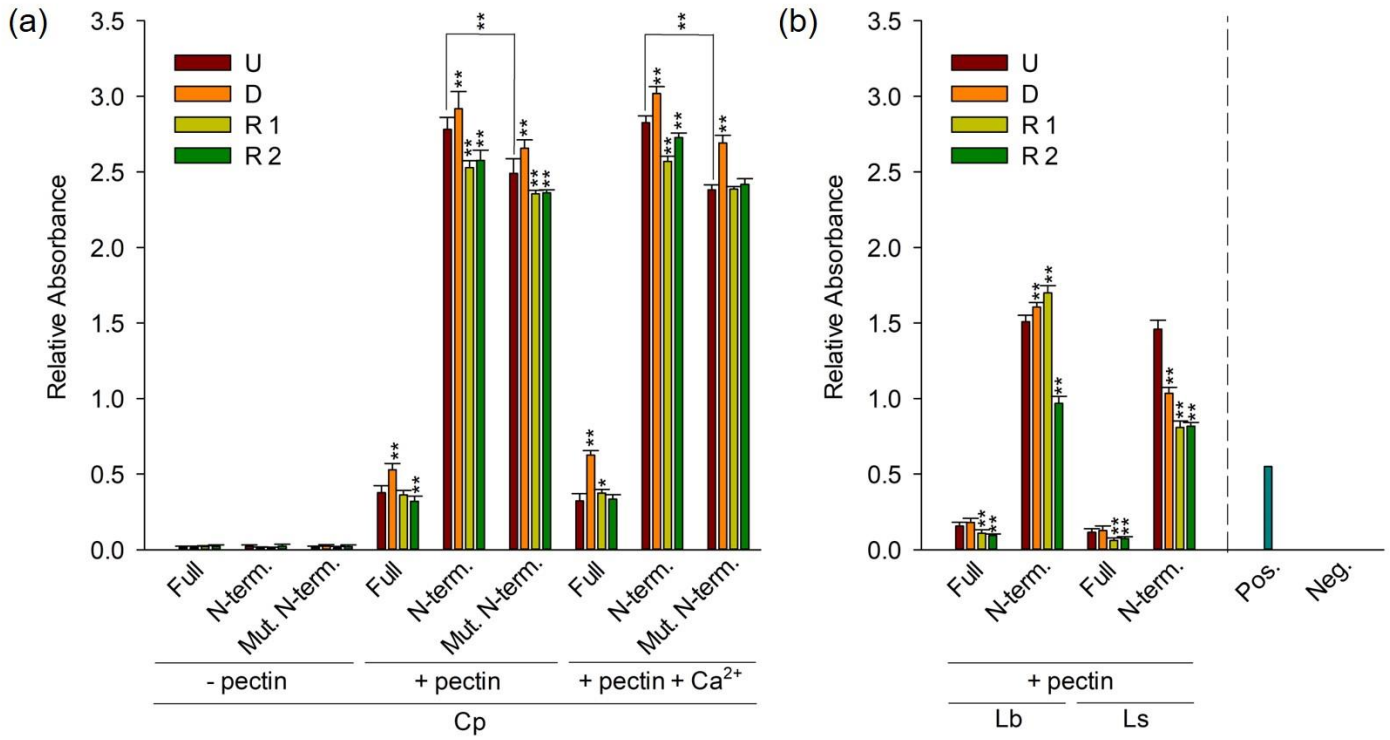

Figure 12 Quantification of the protein-pectin interaction using the CpGRP1 full-length protein, the N-term. fragment and the mutated N-term. fragment and pectin isolated from **(a)** *Craterostigma plantagineum* (Cp), **(b)** *Lindernia brevidens* (Lb) and *Lindernia subracemosa* (Ls) during dehydration and rehydration. All signals shown were detected using 1:5 dilutions of CDTA fractions. No signals were detected in KOH fractions. The CpLEA-like 11-24 protein was incubated with commercial pectin and 2 mM Ca^{2+} and used as a negative control (Neg.). The CpGRP1 full-length protein was incubated with commercial pectin and Ca^{2+} and used as a positive control (Pos.). U = Untreated, D = Desiccated, R 1 = Rehydrated 1, R 2 = Rehydrated 2. Values shown are means of three biological replicates ± SD. The star indicates the levels of significance in comparison to the untreated sample (OneWayANOVA, Holm-Sidak method): $*p < 0.05$; $**p < 0.01$.

After performing blue-native page gel-shift pectin binding assays the interaction between CpGRP1 and pectin was further investigated using pectin extracted from *C. plantagineum* leaves (Figure 12a). Microtiter plate wells were coated with CDTA-

soluble pectin or KOH-soluble cell wall fractions from *C. plantagineum* and then incubated with the full-length CpGRP1 protein, the N-terminal polypeptide or the mutated N-terminal polypeptide. No complex was observed between CpGRP1 and the KOH cell wall fractions. The strongest interaction was observed with the N-terminal polypeptide, followed by the mutated N-terminal polypeptide and the full-length protein. Each of the tested proteins showed the highest value for the CDTA-pectin fraction isolated from desiccated *C. plantagineum* leaves. No differences were observed in the presence or absence of calcium. In addition, pectin fractions from the two closely related species differing in desiccation tolerance, *L*. *brevidens* and *L*. *subracemosa,* were prepared and the CpGRP1 binding to those fractions was analysed (Figure 12b). The CpGRP1 full-length protein and the N-terminal polypeptide showed the strongest interaction with *C*. *plantagineum* pectin, followed by pectin from *L*. *brevidens* and *L*. *subracemosa*.

4.3.6 Quantification of galacturonic acid content

To confirm that the differences in CpGRP1-pectin binding between the different species are due to the pectin composition and not due to the amount of isolated homogalacturonan the galacturonic acid content was determined for all different fractions. As shown in Table 3 no significant differences in the galacturonic acid content were detected which supports comparable HG contents.

Table 3. Quantification of galacturonic acid content in the different CDTA-pectin fractions in µg/µL. Values shown are means of three biological replicates ± SD. The star indicates the levels of significance in comparison to the untreated sample (OneWayANOVA, Holm-Sidak method): *$p < 0.05$.

	Untreated	**Desiccated**	**Rehydrated 1**	**Rehydrated 2**
C. plantagineum	2.01±0.31	2.12±0.22	2.00±0.24	1.62±0.41
L. brevidens	1.81±0.24	1.55±0.26	1.58±0.27	1.60±0.21
L. subracemosa	2.05±0.25	1.92±0.21	1.65±0.27*	2.02±0.20

4.3.7 Cell wall methylesterification status in *L. brevidens* and *L. subracemosa*

To analyse the HG methylesterification status in *L. brevidens* and *L. subracemosa* the JIM5, JIM7, LM20 and LM19 antibodies were used to analyse the *L*. *brevidens* and *L*. *subracemosa* HG fractions. The methylesterification profile of HG for the desiccation tolerant plant *L*. *brevidens* was similar to the one of *C*. *plantagineum* (Table 4). For *L*.

subracemosa the signal intensity detected with the antibodies in the rehydrated samples was lower than the signal in the untreated sample suggesting that this plant is not able to restore cell wall composition during rehydration which is consistent with the phenotype (Table 4). No significant differences in the galacturonic acid content and no differences in the cell wall methylesterification status that would explain the differences in the ELISA CpGRP1-pectin binding experiments were detected, suggesting that additional factors besides the HG methylesterification status are important for protein-pectin interaction.

Table 4. Analysis of changes in cell wall methylesterification of *Lindernia brevidens* (Lb) and *Lindernia subracemosa* (Ls) leaves in a desiccation/rehydration cycle. JIM5, JIM7 and LM20 detect varying levels of methylesterification in HG. LM19 detects fully de-methylesterified HG. For specificity of different antibodies see Table 1. The colour scale in relation to absorbance values is shown at the bottom on the left-hand site. Results were generated analysing the CDTA fractions in 1:5 dilutions. Values shown are means of three biological replicates ± SD. The letters indicate the levels of significance (OneWayANOVA, Holm-Sidak method): abcd $p < 0.05$; ABCD $p < 0.01$; aA = significantly different from `Untreated´ sample, bB = significantly different from `Desiccated´ sample, cC = significantly different from `Rehydrated 1´ sample, dD = significantly different from `Rehydrated 2´ sample.

		Ab	Untreated	Desiccated	Rehydrated 1	Rehydrated 2
HG†	Lb	JIM5	0.77±0.14^{BCd}	0.31±0.08^{AcD}	0.45±0.11^{Abd}	0.62±0.15^{aBc}
		JIM7	1.42±0.21^{BCd}	0.67±0.17^{AcD}	1.02±0.22^{Ab}	1.14±0.19^{aB}
		LM20	2.05±0.28^{BC}	0.87±0.18^{ACD}	1.52±0.20^{ABd}	1.89±0.16^{Bc}
		LM19	0.58±0.09^{BCd}	1.52±0.15^{ACD}	0.36±0.07^{AB}	0.45±0.06^{aB}
	Ls	JIM5	0.67±0.18^{BCD}	0.22±0.02^{A}	0.31±0.06^{A}	0.24±0.04^{A}
		JIM7	1.36±0.16^{BCD}	0.88±0.18^{A}	0.74±0.11^{A}	0.81±0.14^{A}
		LM20	2.41±0.33^{BCD}	0.99±0.25^{A}	0.84±0.17^{A}	0.88±0.18^{A}
		LM19	0.61±0.09^{BCD}	1.44±0.17^{ACD}	1.02±0.22^{AB}	0.97±0.21^{AB}

† Homogalacturonan

0.00	0.50	1.00	1.50	2.00	2.50

4.3.8 Dot-blot pectin binding assays

To confirm the ELISA analyses a series of dot-blot experiments was carried out. The interaction of the CpGRP1 protein and pectin was either detected using a 6x-His-tag antibody or the JIM5 antibody (Figure 13a). The dot-blot analyses confirmed the interaction between the CpGRP1 full-length protein and the two N-terminal protein fragments with pectin. BSA (Carl Roth, Karlsruhe, Art.-Nr. 8076.2) and the CpLEA-like 11-24His recombinant protein (Petersen *et al*., 2012) were used as negative controls and did not show any interaction. Figure 13b presents the species-specific interactions

between the CpGRP1 full-length protein, the N-terminal peptide fragment and the mutated N-terminal peptide fragment with the CDTA fractions of *C*. *plantagineum*, *L*. *brevidens* and *L*. *subracemosa.*

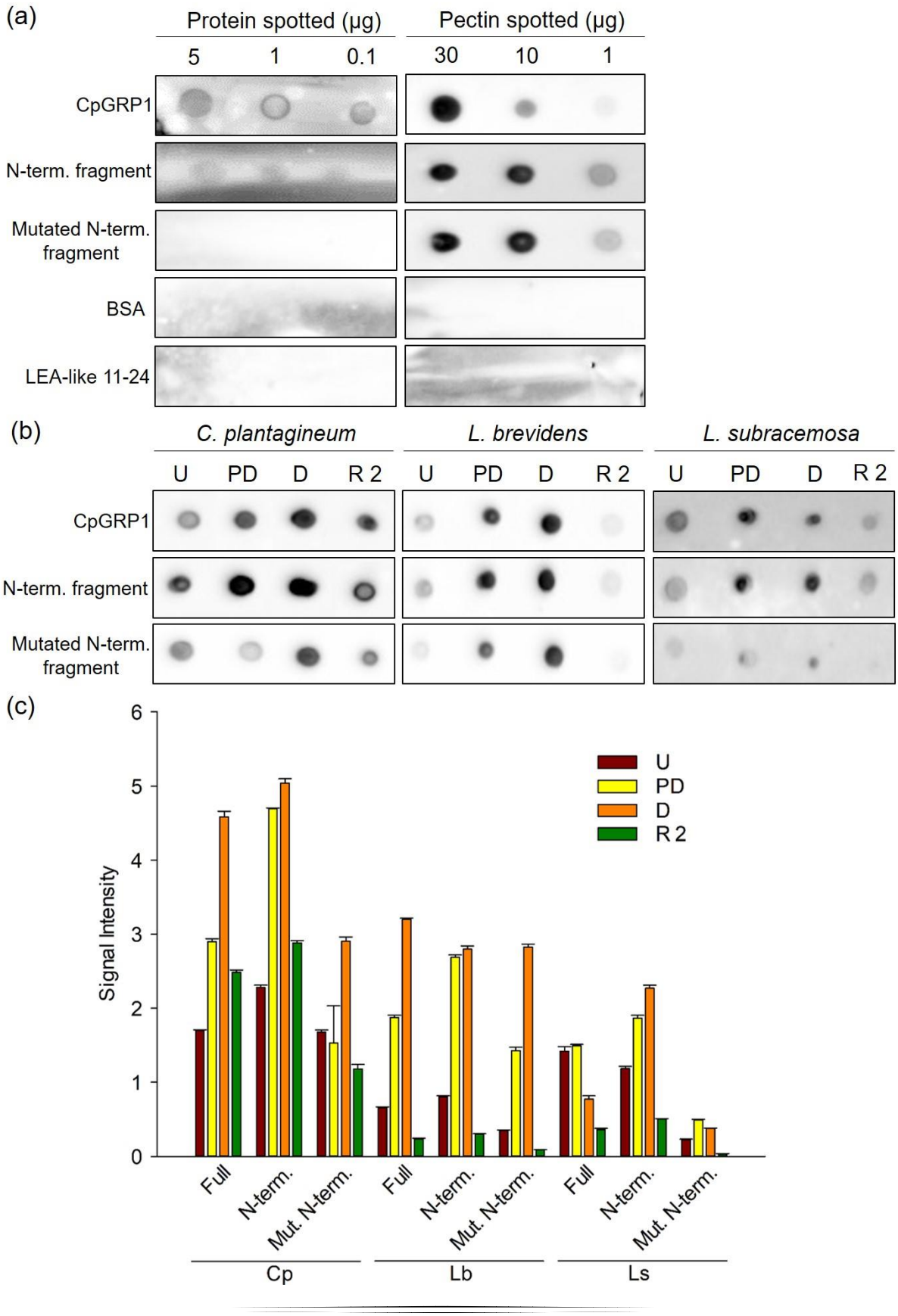

Figure 13 Evaluation of CpGRP1 interaction with *Craterostigma plantagineum* (Cp), *Lindernia brevidens* (Lb) and *Lindernia subracemosa* (Ls) pectin fractions during dehydration and rehydration by dot-blot analyses. **(a)**: Binding of CpGRP1 full-length, N-terminal fragment and mutated N-terminal fragment to commercial pectin. BSA and the CpLEA-like 11-24 protein were used as negative controls. In the left-hand column the protein was spotted on the membrane first and then incubated with pectin, the right-hand column represents the opposite experiment, the pectin was spotted first and then the protein was added. **(b)**: Interaction of CpGRP1 full-length, N-terminal fragment. and mutated N-terminal fragment with CDTA fractions. From each fraction 1 µg of pectin was spotted. Quantification of signals from **(b)** is shown in **(c)**. U = Untreated, PD = Partially dehydrated, D = Desiccated, R 2= Rehydrated 2. Values shown are means of three technical replicates ± SD.

Mutation of arginines in the N-terminal fragment led to weaker interactions with pectin. Quantification of signal intensities of the dot-blots fully supports the ELISA results (Figure 13c). The binding of CpGRP1 and CpGRP1 protein fragments to pectin from the desiccated samples was stronger than the binding to pectin from the untreated or rehydrated samples in all experiments. The highest signal intensity was obtained for pectin isolated from *C*. *plantagineum*. To investigate and compare the CpGRP1-pectin interaction, the pectin binding of two other apoplastic proteins, CpWAK1 (Giarola *et al*., 2015, 2016) and the *C. plantagineum* germin-like protein1 (CpGLP1) (Dulitz, 2016), was investigated. Figure 14 demonstrates that the CpGRP1 interacts stronger with pectin than CpWAK1 or CpGLP1.

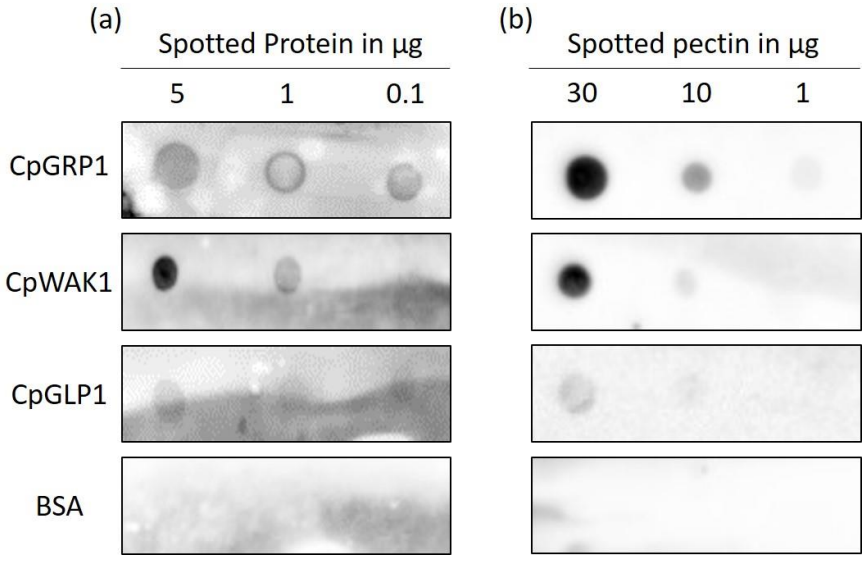

Figure 14 Evaluation of CpGRP1-pectin interaction in comparison to the apoplastic proteins CpWAK1 and CpGLP1. **(a, b)**: Binding of CpGRP1, CpWAK1 and CpGLP1 to commercial pectin. BSA was used as negative control. In the left-hand column **(a)** the protein was spotted on the membrane first and then incubated with pectin, the right-hand column **(b)** represents the opposite experiment, the pectin was spotted first and then the protein was added.

4.3.9 Effect of pectin de-methylesterification on CpGRP1-pectin interaction

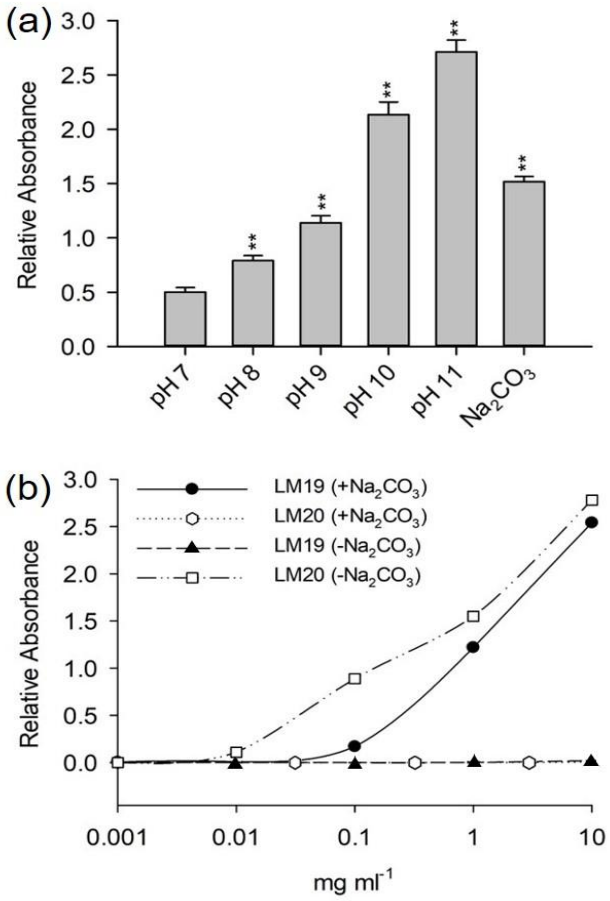

Figure 15 Quantification of CpGRP1-pectin interaction after pectin de-methylesterification. **(a)**: ELISA-assay to quantify CpGRP1-pectin interaction after pre-treatment of coated homo-galacturonan with CAPS-buffers (pH 7–11) or with sodium carbonate. **(b)**: Binding of LM19 and LM20 to different concentrations of apple pectin with and without sodium carbonate pre-treatment. Values shown are means of three biological replicates ± SD. The star indicates the levels of significance in comparison to the untreated sample (OneWayANOVA, Holm-Sidak method): $^{**}p < 0.01$.

The protein-pectin binding assays demonstrated a stronger binding of the CpGRP1 fragments to pectin isolated from desiccated samples than to untreated and rehydrated samples (Figure 12 and 13). Pectin profiles in a desiccation/rehydration cycle did reveal a lower degree of homogalacturonan methylesterification upon desiccation (Table 2). These results suggest a role of pectin methylesterification in the interaction between CpGRP1 and pectin. Therefore, the influence of pectin de-methylesterification on the CpGRP1-pectin interaction was investigated.

Pre-treatment of pectin with CAPS-buffered solutions (pH 7–11) or with 0.1 M sodium carbonate reduced the extent of HG methylesterification. The CpGRP1 full-length protein bound more strongly to de-methylesterified than to methylesterified commercial apple pectin (Apple Pectin Powder, Solgar, USA) (Figure 15a). I hypothesise that the de-methylesterification of HG provides more binding sites for the CpGRP1 protein. Highly methylesterified commercial apple pectin was used to confirm the effect of the de-methylesterification procedure as shown by the specificities of the LM19 and LM20 probes. Figure 15b shows that untreated apple pectin is recognised by the LM20 antibody but not by LM19, whereas the sodium carbonate-treated and hence de-methylesterified apple pectin is recognised by the LM19 antibody and not by LM20.

4.3.10 Effect of cysteine mutations on CpGRP1 migration behaviour in SDS-page

The CpGRP1 full-length recombinant protein has a predicted molecular weight of 14.1 kDa but the protein does not run at this level in SDS-page. The unexpected running behaviour of CpGRP1 was already described by Giarola *et al*. 2016. Two different buffers were used to fully denature the CpGRP1 full-length recombinant protein prior to SDS-page (Figure 16). Both buffers contained SDS and one buffer contained

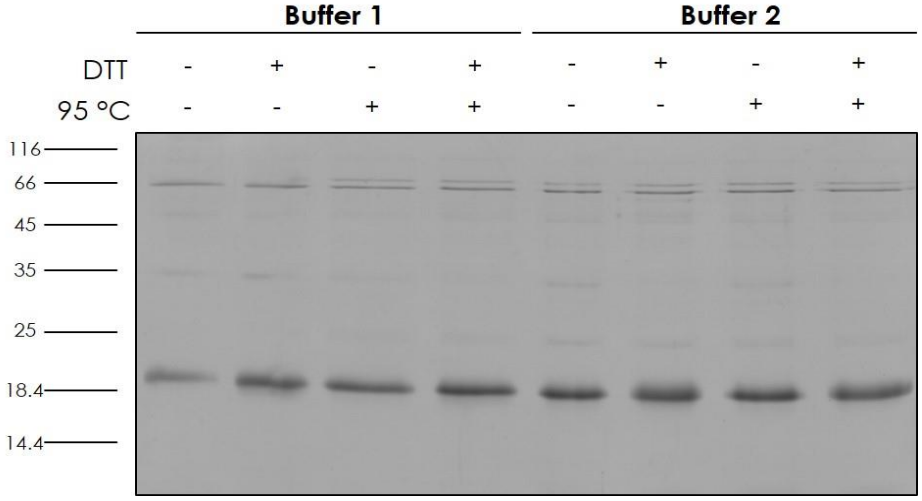

Figure 16 Evaluation of CpGRP1 migration behaviour in SDS-page. 1 µg of protein was loaded per lane. Two different buffers were used for this experiment: 2 x buffer 1 (4% (w/v) SDS; 20% (v/v) glycerol; 120 mM Tris, pH 6.8; 0.01% (w/v) bromophenol blue and 2 x buffer 2 (2% (w/v) SDS; 7% (v/v) glycerol; 50 mM Tris, pH 6.8; 8 M urea; 2% (v/v) ß-mercaptoethanol; 0.01% (w/v) bromophenol blue. The SDS-gel was stained using Coomassie Brilliant Blue.

additionally urea and ß-mercaptoethanol. Some of the samples were additionally heated at 95°C and supplemented with DTT. No combination of different buffers, heating and DTT was sufficient to change the running behaviour of the CpGRP1 full-length recombinant protein. Cysteine residues might be responsible for intermolecular disulfide bonds which could have been masked by the spatial confirmation of the protein but this assumption could not be confirmed because even strong degradation treatments with SDS, DTT and heat did not change the result. This was also confirmed by mutating six cysteine residues and testing the mutated protein in SDS-page (Figure 17a). The mutated CpGRP1 full-length recombinant protein does also migrate more slowly than the predicted 13.8 kDa (Figure 17a). Hydrophobicity plots of the CpGRP1 full-length recombinant protein and the mutated CpGRP1 recombinant protein were performed as described by Kyte and Doolittle (1982) and revealed that the six cysteine residues in the C-terminal part make the non-mutated protein more hydrophobic than

the mutated protein (Figure 17b). A stronger hydrophobic character might increase the binding of SDS molecules to the native protein. This could lead to an increased negative charge and a faster migration. 3D-modelling of both proteins predicted a more compact protein for the CpGRP1 recombinant protein than for the mutated CpGRP1 recombinant protein (Figure 17c). This observation also supports a faster migration of the native protein. The reason for the unexpected running behaviour could not be clarified but it can be hypothesised that the strong hydrophobic character of the protein at the N-terminus and the C-terminus is important for the migration behaviour. Mutating six cysteines to glycine makes the protein less compact and less hydrophobic than the native protein. Although it has a lower molecular weight the protein migrates more slowly. This demonstrates the importance of protein hydrophobicity for SDS-page.

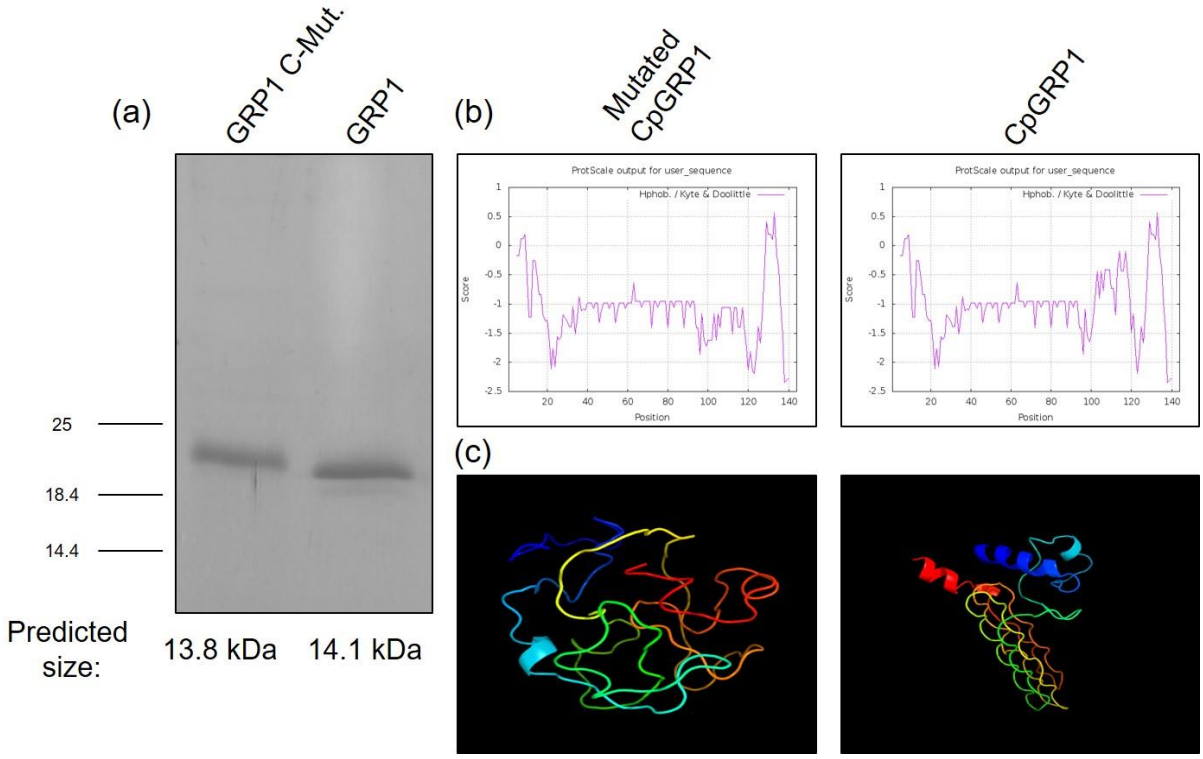

Figure 17 Evaluation of the effect of cysteine mutations on the CpGRP1 migration behaviour in SDS-page. **(a)**: SDS-page using the mutated CpGRP1 full-length and the CpGRP1 full-length protein. 1 µg of protein was loaded per lane. The SDS-gel was stained using Coomassie Brilliant Blue. **(b)**: Hydrophobicity plot for the mutated CpGRP1 full-length and the CpGRP1 full-length protein (Kyte and Doolittle, 1982). **(c)**: Prediction of a 3D-model for the mutated CpGRP1 full-length and the CpGRP1 full-length protein using *Phyre2* (http://www.sbg.bio.ic.ac.uk/phyre2 /html/page.cgi?id=index).

4.4 Interaction between CpGRP1 and lipids

As lipids are a major component of cell membranes and are modified during desiccation/rehydration in *C. plantagineum* (Gasulla *et al*., 2013) the aim was to

analyse whether CpGRP1 may also bind to lipids. In a first approach a protein-lipid overlay assay was performed. This is a quick possibility to investigate binding of a target protein to different lipids (Deak *et al*., 1999). In a second approach liposome-binding assays were performed. Liposome-binding assays reflect a more natural environment of lipids than protein-lipid overlay assays because the cellular state of lipids is considered.

4.4.1 Protein-lipid overlay assays

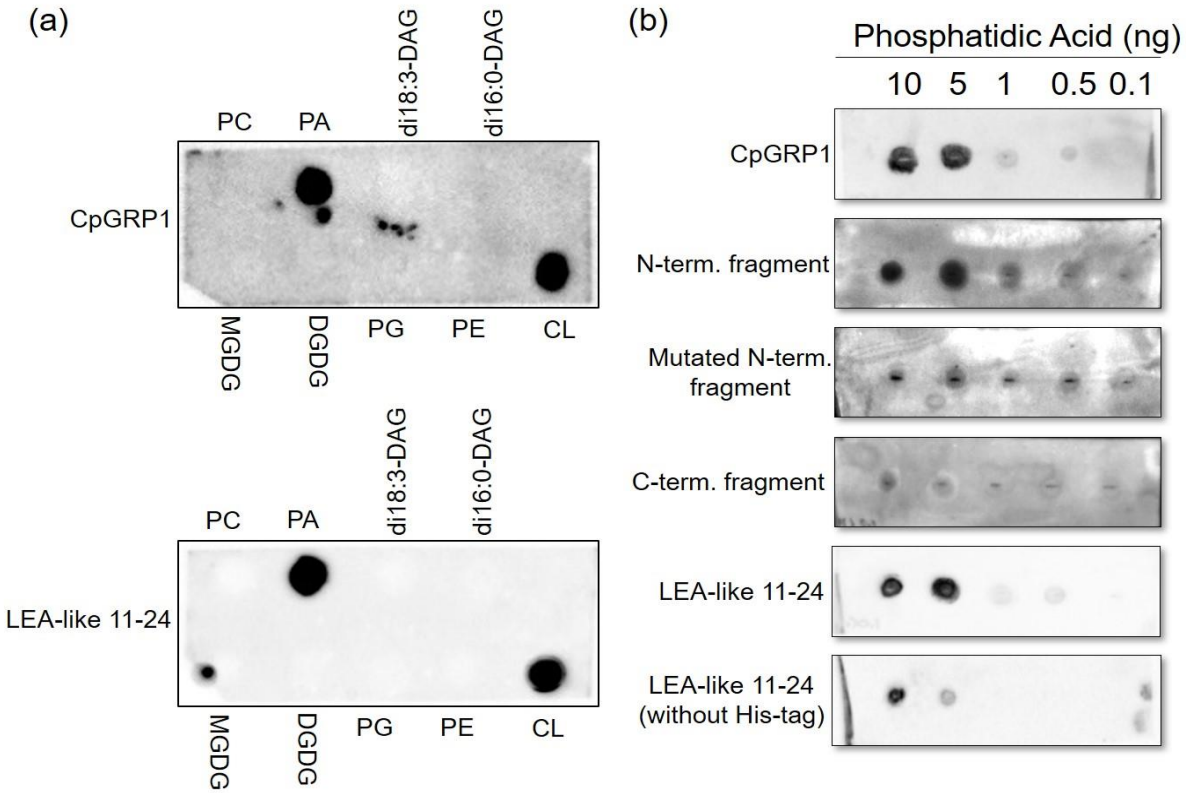

Figure 18 Protein-lipid overlay assays using the recombinant CpGRP1 full-length protein, the N-term. polypeptide, the mutated N-term. polypeptide and the C-term. polypeptide. A 6x-His antibody was used to detect the different protein fragments. The CpLEA-like 11-24 protein (with and without His-tag) served as a positive control and was detected with an antibody specific to CpLEA-like 11-24. **(a)**: Investigation of CpGRP1 binding properties to different lipids: phospatidylcholine (PC), phosphatidic acid (PA), diacylglycerol 18:3 (di18:3-DAG), diacylglycerol 16:0 (di16:0-DAG), monogalactosyldiacylglyceride (MGDG), digalactosyldiacylglyceride (DGDG), phosphatidylglycerine (PG), phosphatidylethanolamine (PE) and cardiolipin (CL). **(b)**: Evaluation of differences in PA binding strength of protein fragments using filters containing 10, 5, 1, 0.5 and 0.1 ng of PA.

CpGRP1 binding to different lipids was analysed in protein-lipid overlay assays (Figure 18a). The CpLEA-like 11-24 protein was used as a positive control and it was used with or without an additional His-tag to account for possible His-tag background binding

(Petersen *et al*., 2012). The CpGRP1 full-length recombinant protein showed strong binding to phosphatidic acid (PA) and cardiolipin (CL), but not to any other lipid tested (Figure 18a). The N-terminal fragment of CpGRP1 and the full-length CpGRP1 showed similar binding to PA, whereas the binding of the C-terminal fragment of CpGRP1 to PA was very weak (Figure 18b). These results indicate that the binding of CpGRP1 to PA is mainly mediated by the N-terminal part of the protein. Mutations of two arginines in this part led to weaker binding, suggesting the involvement of positively charged arginines in the CpGRP1-PA interaction.

4.4.2 Liposome-binding assays

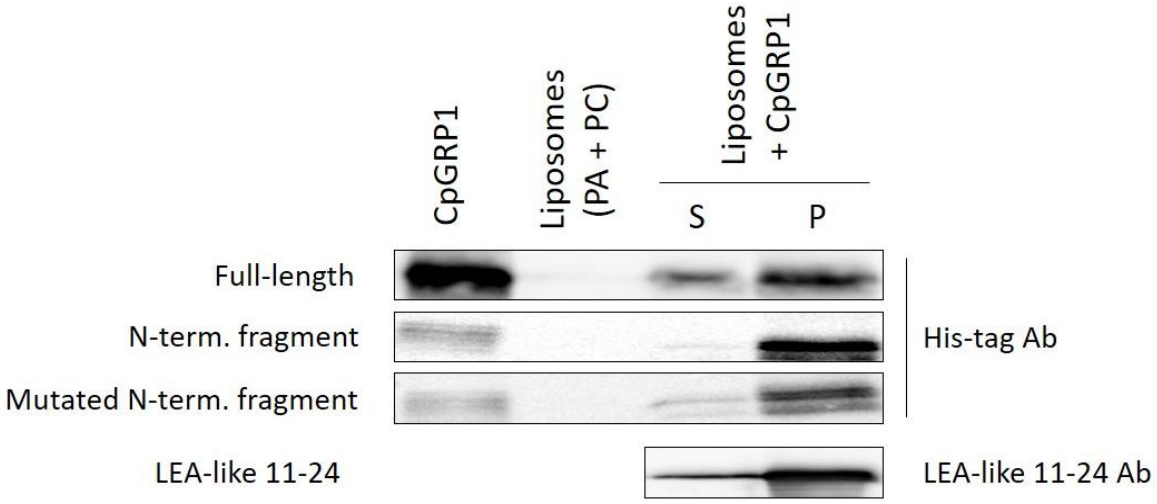

Figure 19 Liposome-binding assays with CpGRP1. Binding of liposomes (PA + PC) to the CpGRP1 full-length protein, the N-term. fragment and the mutated N-term. fragment was tested. Pure liposomes were used as negative binding control and the CpLEA-like 11-24 protein was used as a positive binding control. CpGRP1 full-length protein and protein fragments were detected using an 6x-His-tag antibody and CpLEA-like 11-24 was detected with a protein specific polyclonal antibody. S = supernatant, P = pellet.

The binding properties of the CpGRP1 full-length protein, the N-term. fragment and the mutated N-term. fragment to liposomes which contain phosphatidic acid and phosphatidylcholine were tested (Figure 19). The CpLEA-like 11-24 protein was used as a positive control. Unbound proteins were detected in the supernatant (S) and liposome-bound proteins were detected in the pellet fractions (P). For all three proteins tested, liposome-protein complexes were detected in the pellet fraction, which confirms an interaction between CpGRP1 and liposomes. For the mutated N-term. fragment the signal detected for the pellet fraction was slightly weaker than the signal for the N-term. fragment. *Vice versa*, more proteins were retained in the supernatant for the mutated N-term. fragment. This result again demonstrates the importance of arginines for lipid binding.

4.5 Pectinmethylesterases in *C. plantagineum*

Pectin profiling with ELISA assays in a desiccation/rehydration cycle revealed changes in the homogalacturonan, rhamnogalacturonan-I and rhamnogalacturonan-II in *C. plantagineum* (Table 2). Particularly the changes in the methylesterification profile are important to describe the interaction between proteins and pectin. Desiccation leads to a lower degree of homogalacturonan methylesterification and a stronger binding of the CpGRP1 protein to pectin isolated from desiccated samples. This suggests a direct link between a higher degree of de-methylesterified homogalacturonan stretches and more CpGRP1 proteins binding to pectin (Figure 15). Homogalacturonan de-methylesterification is taking place in the apoplast and the reaction is catalysed by pectinmethylesterases (Fleischer *et al*., 1999; Le Gall *et al*., 2015). The objective of the experiments was to analyse pectinmethylesterases in *C. plantagineum* and to identify possible candidates which might be important in regulating homogalacturonan changes upon desiccation.

4.5.1 Transcriptome analysis of pectinmethylesterases and pectinmethylesterase inhibitors in *C. plantagineum*

The starting point was a transcriptome analysis of *C. plantagineum* which provided expression data for four different stages upon dehydration and rehydration (Giarola *et al*., unpublished). 33 contigs were identified as possible pectinmethylesterases (Figure 20a) and 48 contigs were identified as pectinmethylesterase inhibitors (Figure 20b). The contigs in Figure 20a were divided into four clusters according to similarities in their expression patterns. The first cluster contains transcripts which were higher expressed in the untreated samples and upon rehydration. The second cluster contains transcripts of which some were upregulated upon dehydration. The third cluster contains transcripts which are downregulated upon desiccation (RWC = 2%). Transcripts in the last cluster were present in the untreated samples and were downregulated upon dehydration, the transcript abundance did not fully recover after rehydration. Contigs in the second cluster were especially interesting. A higher expression of pectinmethylesterases upon dehydration and desiccation could be an important factor in explaining the detected changes in homogalacturonan methylesterification. The Cp_V2_contig_11593 was chosen as a promising candidate because the transcriptome data suggests a higher expression already at a relative water content of 60% and the transcript is even more abundant upon desiccation.

Figure 20 Transcriptome data of different *Craterostigma plantagineum* contigs which were identified as **(a)** pectinmethylesterases (PME) or **(b)** pectinmethylesterase inhibitors (PMEI). The expression was measured through a dehydration/rehydration cycle at four different stages. The Cp_V2_contig_11593, representing a PME, is marked with a red box (Giarola *et al*., unpublished). The expression (log2) is represented by a colour scale shown at the bottom left hand side. U = Untreated, R = Rehydrated.

This transcript was the only one with a strong increase in expression upon early dehydration and desiccation. The contigs in Figure 20b were divided into five clusters. The first cluster represents transcripts downregulated upon dehydration and the expression level recovered upon rehydration. In the second cluster the transcripts are only downregulated upon desiccation. The third and fourth cluster represents PMEIs with more fluctuating expression patterns. PMEIs clustered in the last group are upregulated in early dehydration and rehydration, but downregulated upon desiccation.

4.5.2 Sequence analysis of Cp_V2_contig_11593

The amino acid sequence of Cp_V2_contig_11593 was used to perform a protein blast at the NCBI database (https://www.ncbi.nlm.nih.gov/). The blast result showed sequence similarities of Cp_V2_contig_11593 to the pectinmethylesterase31 protein from different species (Figure S4).

For further analysis the *A*. *thaliana* pectinmethylesterase31 (AtPME31) was chosen for comparison. The sequence similarity between Cp_V2_contig_11593 and AtPME31 is 79%. The AtPME31 protein was described previously by Dedeurwaerder *et al*. (2009). An alignment of the Cp_V2_contig_11593 and the AtPME31 amino acid sequences demonstrates the similarities (Figure 21). Pectinmethylesterases often contain characteristic segments and conserved amino acid residues in their protein sequences

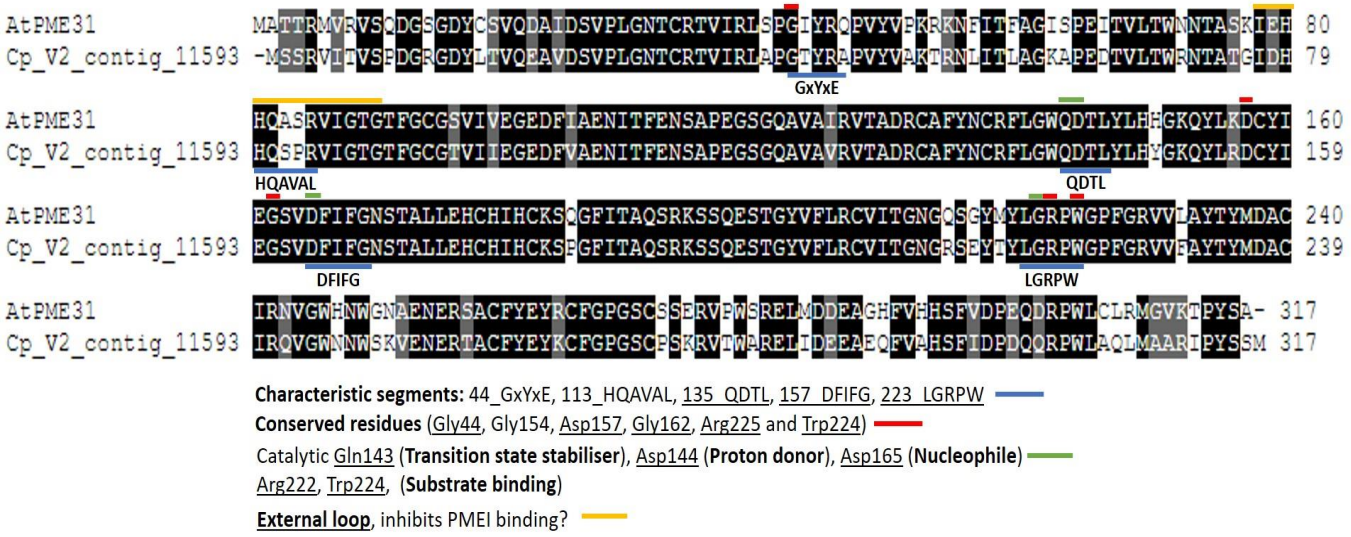

Figure 21 Alignment of AtPME31 and Cp_V2_contig_11593 amino acid sequences (https://www.bioinformatics.org/sms2/). Characteristic segments for pectinmethylesterases are marked in blue, conserved residues between different pectinmethylesterases are marked in red, amino acids important for enzyme activity are marked in green and amino acids important for the formation of an external loop are marked in yellow (Markovic and Janecek, 2004). Underlined motifs or residues are conserved between AtPME31 and Cp_V2_contig_11593.

(Markovic and Janecek, 2004). Three out of five of these characteristic segments (135_QDTL, 157_DFIFG and 223_LGRPW) are conserved between Cp_V2_contig_11593 and AtPME31 and five out of six conserved residues (Gly44, Asp157, Gly162, Arg225 and Trp224) are present in both sequences. The amino acids which are required for the catalytic activity of the enzyme are present in the Cp_V2_contig_11593. The sequence analysis identifies Cp_V2_contig_11593 as a pectinmethylesterase which is very similar to AtPME31 and which could be the homolog to PME31 in other species.

4.5.3 3D-modelling of Cp_V2_contig_11593

After searching for similarities in the sequences between AtPME31 and Cp_V2_contig_11593 the *Phyre2* web service was used to compare the predicted 3D-structure of both proteins. A 3D-modelling for AtPME31 was performed by Dedeurwaerder *et al*. 2009. This study proposed the presence of an external loop which is composed of the aa78-90 (Figure 21). The external loop seems to play a role in preventing the binding of pectinmethylesterase inhibitor (PMEI) proteins to AtPME31.

The region between amino acid 78 and amino acid 90 is highly similar between AtPME31 and Cp_V2_contig_11593. 3D-modelling of Cp_V2_contig_11593 did also predict a similar external loop (Figure 22). The presence of an external loop is a rare feature in pectinmethylesterases (Dedeurwaerder *et al.,* 2009).

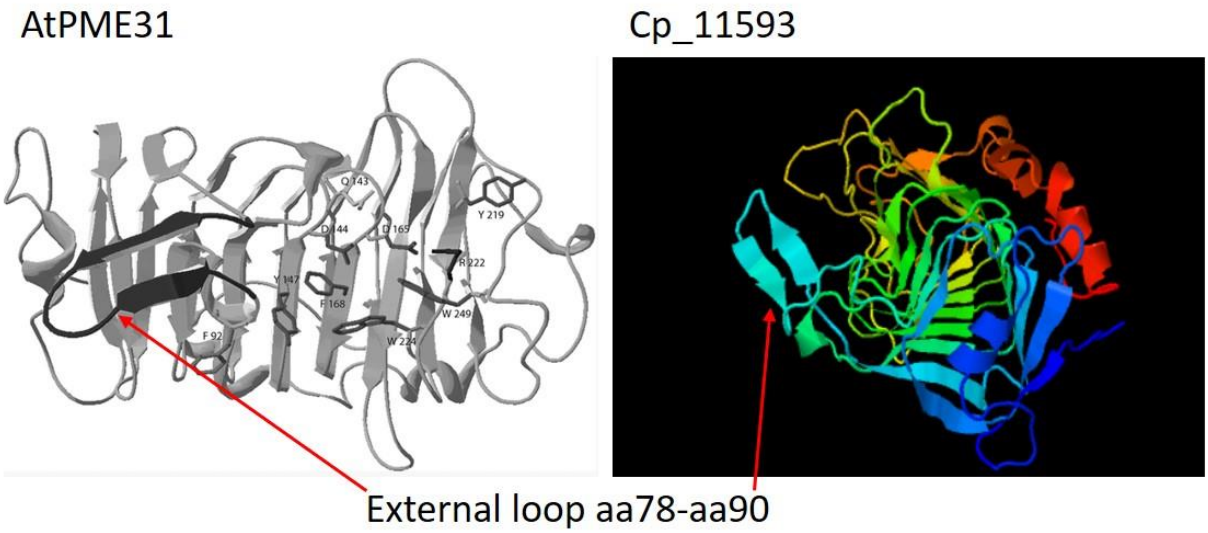

Figure 22 3D-modeling of Cp_V2_contig_11593 with *Phyre2*. Left picture shows the 3D-model of AtPME31 (Dedeurwaerder *et al*., 2009). A predicted external loop is marked with red arrows.

4.5.4 Expression analysis of Cp_V2_contig_11593

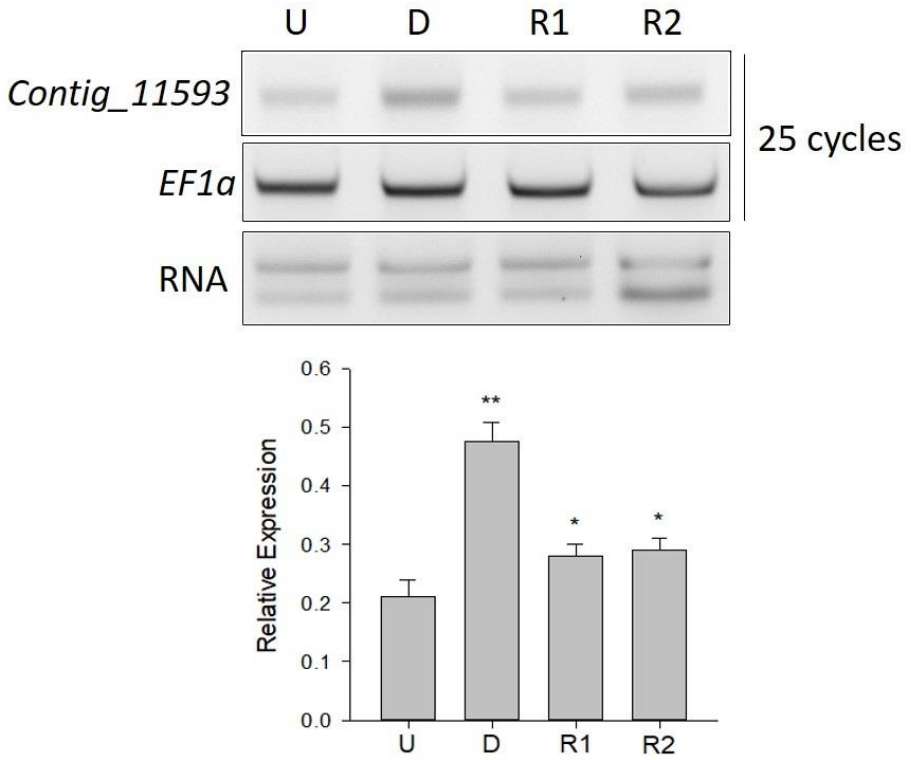

Figure 23 RT-PCR analysis of Cp_V2_contig_11593 transcript abundance within dehydration and rehydration. Part of the Cp_V2_contig_11593 coding sequence was amplified using CpPME_RT_F/CpPME_RT_R primers. *CpEF1α* was amplified as housekeeping control using CpEF1α_RT_F/CpEF1α_RT_R primers. U = Untreated, D = Desiccated, R1 = Rehydrated 1, R2 = Rehydrated 2. The relative expression was measured with *ImageJ*. The star indicates the levels of significance in comparison to the untreated sample (OneWayANOVA, Holm-Sidak method): *$p < 0.05$; **$p < 0.01$.

The transcriptome data suggest a higher abundance of the Cp_V2_contig_11593 transcript in desiccated samples and again a decrease in gene expression upon rehydration. RT-PCR was used to evaluate the expression of *Cp_V2_contig_11593*. Samples from untreated, desiccated and rehydrated *C. plantagineum* leaves were collected and used for RNA-extraction, cDNA-synthesis and RT-PCR.

The relative expression of the transcript was normalised with the housekeeping gene *CpEF1a* (Figure 23). The RT-PCR analysis fully supports the transcriptome data. The relative expression increases by a factor of more than two and upon rehydration the expression is decreasing.

4.5.5 Amplification of Cp_V2_contig_11593 sequence from *C. plantagineum* cDNA

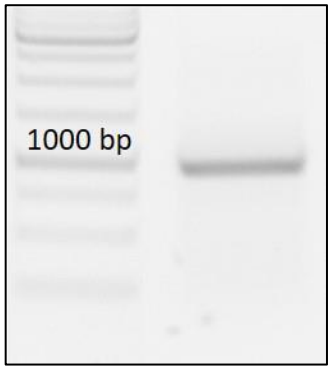

Figure 24 Amplification of Cp_V2_contig_11593 coding sequence from *C. plantagineum* cDNA using CpPME1_Full_F/CpPME1_Full_R primers.

The previous experiments confirmed that the pectinmethylesterase encoded by the Cp_V2_contig_11593 sequence could be a candidate to catalyse de-methylesterification in the homogalacturonan upon dehydration in *C. plantagineum*. The aim of this experiment was to amplify the full Cp_V2_contig_11593 sequence from *C. plantagineum* cDNA and clone it in the vector pJET1.2. The amplification from cDNA yielded in a band with the expected size (Figure 24). The amplicon was purified from the gel and cloned into pJET1.2. Positive clones were send for DNA sequencing and the sequencing result was compared to the reference sequence (Figure S5). Sequencing confirmed successful cloning of the full Cp_V2_contig_11593 sequence with a few mismatches. The nucleotide sequences of the Cp_V2_contig_11593 and the sequencing result were translated to their corresponding amino acid sequences and the protein sequences were aligned to each other (Figure 25). Two amino acids are different, namely at the positions aa199 and aa214. In both cases a single nucleotide was different (Figure S5). The pJET1.2_Cp_V2_contig_11593Clone9 vector was used for subsequent experiments.

```
CpPME Clone9      MSSRVITVSPDGRGDYLTVQEAVDSVPLGNTCRTVIRLAPGTYRAPVYVAKTRNLITLAG  60
CpPME Ref         MSSRVITVSPDGRGDYLTVQEAVDSVPLGNTCRTVIRLAPGTYRAPVYVAKTRNLITLAG  60
                  ************************************************************

CpPME Clone9      KAPEDTVLTWRNTATGIDHHQSPRVIGTGTFGCGTVIIEGEDFVAENITFENSAPEGSGQ  120
CpPME Ref         KAPEDTVLTWRNTATGIDHHQSPRVIGTGTFGCGTVIIEGEDFVAENITFENSAPEGSGQ  120
                  ************************************************************

CpPME Clone9      AVAVRVTADRCAFYNCRFLGWQDTLYLHYGKQYLRDCYIEGSVDFIFGNSTALLEHCHIH  180
CpPME Ref         AVAVRVTADRCAFYNCRFLGWQDTLYLHYGKQYLRDCYIEGSVDFIFGNSTALLEHCHIH  180
                  ************************************************************

CpPME Clone9      CKSPGFITAQSRKSSQESSGYVFLRCVITGNGRPEYTYLGRPWGPFGRVVFAYTYMDACI  240
CpPME Ref         CKSPGFITAQSRKSSQESTGYVFLRCVITGNGRSEYTYLGRPWGPFGRVVFAYTYMDACI  240
                  ****************:*********** ************************

CpPME Clone9      RQVGWNNWSKVENERTACFYEYKCFGPGSCPSKRVTWARELIDEEAEQFVAHSFIDPDQQ  300
CpPME Ref         RQVGWNNWSKVENERTACFYEYKCFGPGSCPSKRVTWARELIDEEAEQFVAHSFIDPDQQ  300
                  ************************************************************

CpPME Clone9      RPWLAQLMAARIPYSSM     317
CpPME Ref         RPWLAQLMAARIPYSSM     317
                  *****************
```

Figure 25 Alignment of pJET1.2_CpPMEClone9 sequencing result with the CpPME reference sequence (https://www.bioinformatics.org/sms2/). The alignment contains two mismatches at aa199 and aa224.

4.5.6 Gateway-cloning of Cp_V2_contig_11593

The pJET1.2_Cp_V2_contig_11593Clone9 vector was taken as a template to amplify the Cp_V2_contig_11593 coding sequence in a two-step gateway protocol and introduce the attB sites (Figure 26). The PCR-reaction resulted in several bands. The upper band corresponds to the correct size of the coding sequence + attB sites and was purified from the gel. A BP-reaction (PCR fragment + Donor vector = Entry clone) was performed to introduce the fragment into the entry clone vector pDONR201 which resulted in the pDONR201_Cp_ V2_contig_11593 vector. After transforming the plasmid into *E. coli* DH10B positive clones were screened by colony-PCR. The plasmid was extracted from pDONR201_Cp_ V2_contig_11593Clone9 and used for PCR and sequencing. Sequencing the insert in the pDONR201 vector did not work and the sequencing quality was low. Sequencing the insert + attB sites did not give results either. When using the pDONR201_Cp_V2_contig_11593Clone9 vector as a template for PCR positive results were obtained (Figure 27).

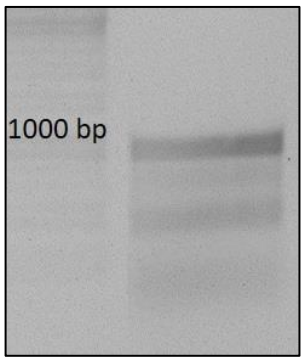

Figure 26 Amplification of Cp_V2_contig_11593 coding sequence from pJET1.2_CpPMEClone9 using a 2-step gateway protocol to introduce attB sites.

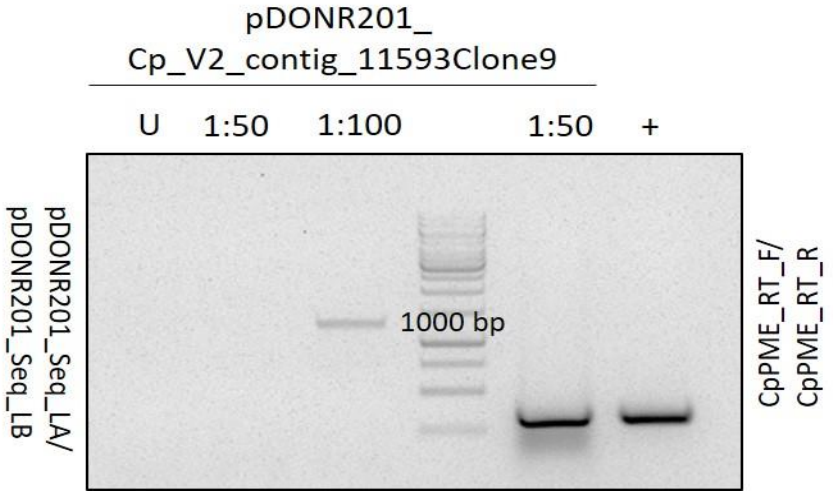

Figure 27 Amplification of the full insert from pDONR201_Cp_V2_contig_11593Clone9 using pDONR201_Seq_LA /pDONR201_Seq_LB primers and amplification of the partial coding sequence of Cp_V2_contig_11593Clone9 from pDONR201_Cp_V2_contig_11593Clone9 using CpPME_RT_F/CpPME_RT_R primers. The plasmid was used in different dilutions as a template which are indicated in the figure. The pJET1.2_CpPMEClone9 plasmid was used as a positive control (+). U = undiluted.

Amplifying the complete sequence of the insert did work when the template was diluted 1:100 and amplifying a part of the coding sequence did also work. The reason why the sequencing did not work remains unknown. The sequence was classified as a complex

sequence which is rich in repeats (https://www.eurofinsgenomics.eu/). However, a modified sequencing protocol for repeat-rich sequences did not provide a sequencing result with higher quality. To create a vector for Cp_V2_ contig_11593 overexpression a LR-reaction was performed to subclone the insert into the pQLinkHD vector resulting in the pQLinkHD_Cp_V2_contig_11593 construct. No positive colonies were screened after transformation. Sequencing the pQLinkHD_Cp_V2_contig_11593 construct did also not work. The experiments identified a promising pectinmethylesterase in *C. plantagineum* and follow-up experiments should be performed to provide more insights into homogalacturonan remodelling upon dehydration.

5. DISCUSSION

5.1 Pectin fractions are remodelled upon dehydration

Folding of cell walls and changing of texture and chemical composition is an adaptation to desiccation in resurrection plants (Bartels and Hussain, 2011). Intensive cell wall folding of desiccated cells is in place in *C*. *plantagineum* as shown by scanning electron microscopy (Figure 5). Similar observations have been made for *L. brevidens* and *L. subracemosa*, which are closely related to *C. plantagineum* and *C. wilmsii* (Farrant, 2000; Phillips *et al*., 2008). Although the leaves of the desiccation sensitive plant *L. subracemosa* are folded upon dehydration, they became brown and necrotic and did not recover after re-watering. The folding and unfolding of cell walls in a dehydration/rehydration cycle in *C. plantagineum* and *L. brevidens* points to alterations in the composition of the cell wall. To address this question pectin and hemicelluloses associated with cell wall flexibility were analysed.

C. plantagineum showed a lower degree of methylesterification in HG upon dehydration, which is reversed during rehydration (Table 2). *L. brevidens* did show a similar methylesterification status as *C*. *plantagineum*, which is in agreement with the fact that this plant is also desiccation tolerant. In contrast, no significant changes in the HG fraction were detected for the desiccation sensitive plant *L. subracemosa* upon rehydration (Table 4). The degree of methylesterification may be important for desiccation tolerance, at least among the Linderniaceae. HG is thought to be synthesised in the Golgi-apparatus in a highly methylesterified form and is de-methylesterified in the cell wall (Zhang and Staehelin, 1992; Staehelin and Moore, 1995; Sterling *et al*., 2001). Thus, the de-methylesterification of HG in the cell wall is a one-way process and there is no evidence of methylesterification of pectin in cell walls. The increasing binding of antibodies detecting methylesterified HG in rehydrated samples suggests that pectin is synthesised *de novo* in *C. plantagineum* and *L. brevidens* during the recovery process (Table 2 and 4).

Pectin de-methylesterification is catalysed by pectinmethylesterases (PMEs) which are organised in a large gene family (Fleischer *et al*., 1999; Le Gall *et al*., 2015). Little is known about the activities of PMEs in *C. plantagineum*. PMEs are thought to be crucial in influencing cell wall properties and to be important for the modulation of apoplastic

Ca^{2+} concentrations (Micheli, 2001; Wu and Jinn 2010; Wu *et al*., 2010; Wu *et al*., 2018). Ca^{2+} mediates the interaction between de-methylesterified pectin chains leading to the formation of `egg-box´ pectin structures (Grant *et al*., 1973; Jarvis, 1984; Moore *et al*., 1986; Lloyd, 1991). The importance of Ca^{2+} is supported by the observation that apoplastic Ca^{2+} increases in *C. wilmsii* upon dehydration suggesting enhanced cell wall strength in *Craterostigma* upon dehydration (Vicré *et al*., 1999).

Besides the methylesterification patterns of pectic polysaccharides the patterning of *O*-acetylation plays an important role in the modulation of cell wall extensibility. De-acetylation of cell wall polysaccharides has been proposed to increase the association between pectin and cellulose and therefore leads to stiffer cell walls (Gou *et al*., 2012; Orfila *et al*., 2012). The *O*-acetylation status of the *C. plantagineum* cell wall components has not been analysed so far but should be done in the future to gain more insights into cell wall stability.

RG-II is crosslinked by borate (Kobayashi *et al*., 1996). The interaction between RG-II, borate and HG is important for the physical and biochemical properties of the cell wall (O'Neill *et al*., 2001). The antibody 42-6 detects RG-II monomers, borate-crosslinked RG-II and an unknown pectic component (Zhou *et al*., 2018). The analysis revealed significant changes in RG-II during desiccation/rehydration in *C. plantagineum* (Table 2). The decrease in the 42-6 signals in response to dehydration suggests pectin remodelling which could affect cell wall rigidity.

Xyloglucan connects cellulose fibrils and contributes to cell wall extensibility (Moore *et al.,* 1986; Fry, 1989). Higher abundance of xyloglucan and de-methylesterified pectin are both known to strengthen the cell wall. This fits well with the increase in xyloglucan and de-methylesterified pectin in desiccated *C. plantagineum* leaves (Table 2) and *C. wilmsii* (Vicré *et al.,* 1999). Increased xylan, mostly present in secondary cell walls, was observed upon dehydration in *C. plantagineum*. Higher xylan contents may contribute to cell wall strength, as xylan together with xyloglucan connects cellulose fibrils. *A*. *thaliana* plants with reduced xylan contents have weakened cell walls (Brown *et al*., 2007; Wu *et al*., 2009). β-(1,4)-galactan, the most flexible component of the cell wall, decreases the ability of pectin molecules to crosslink and also α-(1,5)-arabinan side chains are motile (Ha *et al*,. 1996; Jones *et al*., 1997; Moore *et al*., 2008). These

components do not change or even decrease upon dehydration in *C. plantagineum* (Table 2).

Another compound or parameter which regulates cell wall flexibility is auxin (Majda and Robert, 2018). Auxin induces the expression of genes encoding cell wall-related proteins and stimulates the synthesis of proton pumps (Perrot-Rechenmann, 2010). This leads to an acidification of the apoplast and the activation of wall loosening proteins. Auxin signalling is involved in pectin polymerisation, increases pectin viscosity and depolymerisation of xyloglucan (Nishitani and Masuda, 1981). Not much is known about the changes in auxin concentration in *C. plantagineum* upon desiccation. In *A. thaliana* no changes in auxin were measured upon dehydration and biosynthetic genes were significantly downregulated, suggesting that auxin is not increasing upon dehydration and thus auxin signalling is most likely not involved in dehydration related cell wall processes (Urano *et al*., 2017). However, the leaf apoplast is known to alkalise during dehydration which counteracts `acid-growth´ (Geilfus, 2017).

Our results demonstrate major changes in cell wall components. The flexible cell wall components are not changing or even decreasing upon drying. On the other hand, components associated with stiffer and stronger cell walls increase. These findings are in agreement with the results published by Vicré *et al*. (1999) but are different to the results by Jones and McQueen-Mason (2004). The latter found an increase in cell wall flexibility and a higher activity of expansins. I propose that the *C. plantagineum* cell wall folds in a distinct way and this process is tightly controlled by cell wall modifying enzymes. Some connections are strengthened, while more flexibility is added to others. Different mechanisms need to be in place to protect the cells from being damaged by the mechanical tension during the dehydration process. How the expression and activity of cell wall modifying enyzmes in resurrection plants are controlled is another major question which has to be answered.

In this study changes in the cell wall were analysed in total cell wall extracts. However, it is important and necessary to analyse changes in the cell wall composition and in the activity of cell wall modifying enzymes in cell wall microdomains. The cell wall folding process is very complex and most likely modifications are not the same in every domain of the cell wall. Maybe the folding needs `hotspots´ from where the folding

process is initiated and where the cell wall needs to be more flexible than in the regions between those `hotspots´. A `hotspot´-theory is also discussed for the hemicellulose-cellulose interaction. This cell wall model proposes a limited number of load-bearing contact sides, which are possible targets for cell wall loosening proteins such as expansins (Cosgrove, 2016). The surface image upon partial dehydration in Figure 5a shows regions with distinct spacing where the folding seems to be initiated. Analysing the cell wall microdomains and finding differences between certain regions (e.g. distribution of pectin/activity of enzymes) is a challenging task but might be a crucial step to further unravel the folding process.

The different cell wall fractions were analysed with monoclonal antibodies detecting epitopes and not the abundance of a cell wall component. This approach was able to reveal differences in the cell wall composition for the different samples tested but other methods have to be utilised and combined in future experiments to get a more detailed picture of cell wall changes. It is possible that the extraction method and the solvents are not equally effective across all samples and epitopes could be masked, modified or even destroyed. Every antibody has different affinities and avidities which makes it not possible to compare signals from different epitopes to each other. Other oligosaccharide profiling techniques which could be used additionally are OLIMP (oligosaccharide mass profiling), HPAEC (high-performance anion exchange chromatography), NMR (nuclear magnetic resonance), CE (capillary electrophoresis) or PACE (polyacrylamide gel electrophoresis). Advantages and disadvantages of the different methods were reviewed in Persson *et al*. (2011).

5.2 CpGRP1 binds to de-methylesterified pectin through clustered arginines

Glycine-rich proteins have been connected with cell wall properties of plants (Condit and Meagher, 1986, 1987; Keller *et al*., 1988). In *C. plantagineum* the class II glycine-rich protein CpGRP1 accumulates in the apoplast of dehydrated leaf tissues (Giarola *et al*., 2016). The glycine-rich protein1 from the resurrection plant *B*. *hygrometrica* (BhGRP1) was proposed to be correlated with cell wall flexibility (Wang *et al*., 2009). The *A. thaliana* glycine-rich protein-3 (AtGRP-3), structurally similar to CpGRP1, interacts with a cell wall-associated protein kinase1 (AtWAK1). This interaction is involved in plant-pathogen defence mechanisms and requires the C-terminal cysteine-rich domain (Park *et al*., 2001). AtWAK1 does also interact with a cytoplasmic plasma membrane-localised kinase-associated protein phosphatase (KAPP) but a similar

interaction partner in *C. plantagineum* has not been identified so far. Gramegna *et al*. (2016) proposed a negative function of AtGRP-3 and AtKAPP in the oligogalacturonide-triggered expression of defence genes. Giarola *et al*. (2016) showed that CpGRP1 binds to a WAK protein of *C. plantagineum*, CpWAK1, and proposed that the CpGRP1-CpWAK1 complex could be involved in dehydration-induced mechanisms. WAKs can bind to cell wall pectin (Kohorn and Kohorn, 2012) but a GRP-pectin interaction has not been characterised so far.

It is shown in this thesis that the CpGRP1 protein binds to pectin which requires the glycine-rich domain of CpGRP1 (Figure 10). The substitution of two arginines within the glycine-rich domain by glycine was sufficient to reduce the protein-pectin interaction (Figure 10, 12 and 13). Glycine is a small and uncharged amino acid, whereas arginine contains a positively charged side chain. The involvement of an arginine cluster in pectin binding was also shown for *Phaseolus vulgaris* polygalacturonase inhibitor proteins (Spadoni *et al*., 2006). The glycine-rich domain of the CpGRP1 protein is important for pectin binding. The repetitive character of this domain leads to multiple arginines with a distinct spacing. This spacing could be important for the spatial organisation of a positive amino acid cluster, which plays a crucial role in pectin binding.

The role of Ca^{2+} in the protein-pectin binding is not clear. The gel-shift assay suggests Ca^{2+} to be important for the interaction but the ELISA assays showed that Ca^{2+} was not essential for the interaction between CpGRP1 and pectin (Figure 10 and 12). One explanation could be that in gel-shift assays Ca^{2+} might be required to crosslink pectin and thus increasing the strength of the interaction. Gel-shift assays are performed in an aqueous solution containing only pectin, the protein of interest and calcium; whereas ELISA assays contain complex cell wall fractions and all components get in close proximity to the ELISA plate surface and to each other, maybe decreasing the importance of Ca^{2+} for an interaction. Substituting Ca^{2+} by Mg^{2+} in the gel-shift assay did not lead to a mobility-shift, which supports the importance of Ca^{2+} ions as part of the pectin matrix (Figure 11). In *A. thaliana* a Ca^{2+}-induced modification of the pectin structure supports the interaction with AtWAK1 (Decreux and Messiaen, 2005). Ca^{2+} seems not to be necessary for CpGRP1-pectin binding *in vitro*, at least in ELISA assays. A role of Ca^{2+} *in planta* is possible, as also other components may be present besides the ones investigated here.

To compare the CpGRP1-pectin interaction with other apoplastic proteins, CpWAK1 and CpGLP1 were used. CpWAK1 and CpGLP1 were chosen, because they are exposed to pectin in a similar way as CpGRP1 due to their localisation. CpWAK1 has a wall-associated receptor kinase galacturonan-binding domain, an EGF-like domain signature 2, a calcium-binding EGF-like domain signature, a transmembrane domain and a protein kinase domain (Giarola *et al*., 2016). CpGLP1 might be involved in detoxifying reactive-oxygen species as a superoxide-dismutase activity was shown in in-gel assays (König, unpublished). Both proteins are able to bind pectin (Figure 14) but the interaction of CpGRP1 with pectin is stronger. To exclude that the pectin binding of CpGRP1, CpWAK1 and CpGLP1 is just due to a high electrostatic charge, two other proteins with high lysine and arginine frequencies were used as additional controls (Figure 12 and 14). The recombinant CpLEA-like 11-24 protein (Petersen *et al.*, 2012) has a lysine frequency of 9.1% which is more than double compared to CpGRP1, which has a lysine frequency of 3% and an arginine frequency of 7.4%. BSA (UniProtKB accession number P02769) has a lysine frequency of 9.9% and an arginine frequency of 4.3%. Despite the high lysine and arginine frequencies CpLEA-like 11-24 and BSA did not show interactions with pectin, proving that a high electrostatic charge alone is not sufficient for a protein-pectin interaction and that a particular spatial arrangement of the amino acid residues is required. The strong pectin binding of CpGRP1 seems to be specific, as other apoplastic proteins or proteins with a high electrostatic charge did not show any or a weaker pectin binding.

After identifying the protein domains important for pectin binding, the pectin fractions from differently treated plants with regards to CpGRP1 binding were tested. Both, the CpGRP1 full-length protein and the N-term. fragment, showed a slightly stronger binding to pectin samples isolated from desiccated *C. plantagineum* leaves than to pectin isolated from untreated leaves (Figure 12a). This could be due to the methylesterification level of HG which decreased upon dehydration. Previous reports demonstrated the importance of de-methylesterified HG stretches for protein binding (Spadoni *et al*., 2006; Chevalier *et al*., 2019). Pectin with a lower degree of methylesterification provides more binding sites for proteins. The N-term. polypeptide of CpGRP1 showed always a higher signal in ELISA pectin binding assays than the full-length CpGRP1 protein (Figure 12a and b). Likely, more of the protein molecules can bind to the de-methylesterified pectin which explains the stronger signal. To

demonstrate a link between the degree of pectin methylesterification and protein binding, the *C. plantagineum* pectin was treated with solutions of different pH-values to stepwise de-methylesterify the HG. The results demonstrate that de-methylesterification of HG provides more binding sites for CpGRP1 (Figure 15a). Reduced methylesterification of HG in the *C. plantagineum* cell wall during dehydration might be responsible for the reduction of mechanical stress and might provide more binding sites for proteins. However, the protein binding experiments using pectin from *L. brevidens* and *L. subracemosa* suggest that other factors in the structure of pectin also contribute to protein-pectin interactions. No significant changes were detected in the degree of methylesterification between *C. plantagineum*, *L. brevidens* and *L. subracemosa* (Table 2 and 4), but the binding of the CpGRP1 protein to the pectin fractions from the three species was different (Figure 12 and 13). A correlation seems to exist between desiccation tolerance and the CpGRP1-binding capacity to pectin, as the signal is strongest for the *C. plantagineum* pectin, weaker for the *L. brevidens* pectin and even weaker for the pectin isolated from the non-tolerant *L. subracemosa*. The reasons for these differences are unknown. Galacturonic acid residues can be unsubstituted, methylesterified or acetylated. The status of galacturonic acid acetylation was not determined in any of the three species but should be done in future experiments. It could be possible that *C. plantagineum* has more unsubstituted galacturonic acid residues than the other two species and *L. brevidens* and *L. subracemosa* have more acetylated galacturonic acid residues. Structural proteins or other cell wall components could also affect the accessibility of protein binding sites within pectin. Due to the spatial organisation of pectin the binding sites for CpGRP1 could be more accessible in *C. plantagineum* than in *L. brevidens* and *L. subracemosa*. Maybe structural proteins like hydroxyproline-rich glycoproteins, arabinogalactan proteins, glycine-rich proteins, proline-rich proteins and extensins are expressed at different levels in the three species and affect the CpGRP1-pectin interaction in combination with the homogalacturonan methylesterification/acetylation status.

5.3 CpGRP1 binds to phosphatidic acid and liposomes

Lipids are a major part of the plasma membrane. CpGRP1, as an apoplastic protein, is localised in close proximity to the plasma membrane. Therefore, it was tested whether CpGRP1 can bind to lipids. Lipid binding experiments revealed that CpGRP1 is not just able to bind to pectin, but also lipids (Figure 18 and 19). The binding to PA

seems also to be mediated through the N-terminal domain of the protein and the arginine cluster. There is evidence suggesting that arginine and lysine residues are important for proteins to bind PA (Kooijman *et al*., 2007; Kooijman and Testerink, 2010; Petersen *et al*., 2012). The N-term. fragment shows a strong binding to PA and mutation of arginines in the N-term. fragment leads to a weaker binding. The C-term. fragment shows no interaction to PA. The results of the protein-lipid overlay assays were confirmed by liposome-binding assays which represent a natural environment because they also consider the cellular state of lipids as liposomes.

PA has multiple functions in plants and is known to be rapidly generated in response to different stresses like dehydration, salt, temperature stress, abscisic acid and pathogen attack (Munnik *et al*., 2000; Katagiri *et al*., 2001; Ruelland *et al*., 2002; Hong *et al*., 2008; Arisz *et al*., 2009; Yu *et al*., 2010; Uraji *et al*., 2012; Zhao, 2015). PA serves as a cellular signalling molecule but how exactly PA is involved in the regulation of downstream effects is not known (Ohlrogge and Browse, 1995; Testerink and Munnik, 2011). Different target proteins of PA have been identified and PA was proposed to function as a membrane-localised signal which is able to bind and recruit target proteins, that change their conformation and activity upon binding (Hou *et al*., 2015). The CpGRP1-PA interaction should be investigated further because the possibility of CpGRP1 to bind PA *in vitro* does not necessarily mean that they also interact *in vivo*. However, multiple binding capacities of CpGRP1 suggest that this protein may coordinate different ligands in the regulation of cell wall/membrane modifications during the folding process. Maybe pectin and PA compete for CpGRP1 binding depending on the abundance of PA and de-methylesterified homogalacturonan stretches. How CpGRP1, pectin, CpWAK1 and PA interact and how these interactions are regulated in a stress-dependent manner is important to investigate to gain further insights in the activation of dehydration-stress responses.

5.4 Identification and characterisation of a pectinmethylesterase in *C. plantagineum* similar to AtPME31

Pectinmethylesterases and pectinmethylesterase inhibitor proteins play a central role in the modulation of homogalacturonan. Homogalacturonan gets transported to the apoplast in a highly methylesterified form and can be de-methylesterified by pectinmethylesterases and by alkalisation of the apoplast (Harholt *et al*., 2010, Lampugnani *et al*., 2018). The interplay between pectinmethylesterases and

pectinmethylesterase inhibitors is crucial for cell adhesion, cell wall porosity and elasticity (Wormit and Usadel, 2018). Pectinmethylesterases produce either non-blockwise or blockwise methylesters in discrete cell wall microdomains (Willats *et al*., 2001). Random de-methylesterification makes homogalacturonan a target for polygalacturonases and pectin lyases. This leads to depolymerisation and generation of oligosaccharides, finally resulting in cell wall loosening. Blockwise de-methylesterification leads to the formation of `egg-boxes´, which results in a stiffer cell wall (Wormit and Ursadel, 2018). This is the reason why different expression levels of pectinmethylesterase enzymes cannot be directly correlated with cell wall loosening or hardening as the mode of action determines the result.

Analysing the transcriptome data of *C. plantagineum* identified the Cp_V2_contig 11593 which was the only transcript significantly up-regulated upon desiccation within the pectinmethylesterases (Figure 20). The sequence analysis demonstrated a high similarity between Cp_V2_contig_11593 and the pectinmethylesterase31 from *A. thaliana* (AtPME31) (Figure 21). AtPME31 has a blockwise mode (see Figure 4) of pectin methylesterification, is highly abundant in *A. thaliana* seeds but not in the vegetative tissue and is localised in the plasma membrane (Dedeurwaerder *et al*., 2009; Yan *et al*., 2018). Yan *et al*. (2018) also demonstrated that PME31 positively modulates the expression of salt stress-induced genes and that *pme31*-mutants are hypersensitive to salt stress. RT-PCR confirmed the transcriptome result and demonstrated that the Cp_V2_contig_11593 transcript was more abundant upon desiccation and that the gene in *C. plantagineum* is present in vegetative plant tissues (Figure 23). The fact that the Cp_V2_contig_11593 is the only up-regulated pectinmethylesterase upon desiccation in *C. plantagineum* and the fact that the most similar transcript in *A. thaliana* is highly abundant in dry seeds makes this gene an interesting candidate to study in the context of desiccation tolerance. It is a common observation that seed specific genes or pathways were re-established in the vegetative tissue of resurrection plants and these results follow the same pattern (Giarola *et al*., 2017). AtPME31 and Cp_V2_contig_11593 share also a structural feature: both enzymes have a predicted external loop in their 3D-predictions (Figure 22). AtPME31 was not inhibited in activity assays by a kiwi pectinmethylesterase inhibitor and the external loop was proposed to prevent the binding of inhibitors (Dedeurwaerder *et al*., 2009). The pectinmethylesterase encoded by the Cp_V2_contig_11593 could be involved in increasing cell wall stiffness in *C. plantagineum* upon desiccation as the

enzyme is supposed to show a blockwise mode of homogalacturonan de-methylesterification. However, further studies are necessary to analyse the activity and the localisation of the enzyme.

5.5 The CpGRP1-CpWAK1-pectin complex

Pectin and hemicelluloses of the *C. plantagineum* cell wall are modified, especially the HG and xyloglucan. These modifications strengthen the cell wall. A higher proportion of de-methylesterified HG provides more binding sites for the CpGRP1 protein. CpGRP1 interacts through arginines with HG or PA and via cysteines in the C-terminal part with the extracellular domain of CpWAK1. These results are now integrated in a model how CpGRP1, CpWAK1, pectin and PA may interact and what are their possible roles in regulating cell shrinkage and expansion (Figure 28).

I propose, that CpGRP1 is an essential factor in cell wall adaptations to desiccation. The data provide a first step to understand cell wall adaptations during desiccation and rehydration in the resurrection plant *C*. *plantagineum* and it is now possible to identify additional components. However, the mechanism of how CpGRP1 affects signalling of CpWAK1 is not known so far. In *A. thaliana* GRP-3 was proposed to negatively regulate WAK1 signalling (Gramegna *et al*., 2016). As CpGRP1 is high expressed upon dehydration stress and strongly binds to the cell wall, it could influence the CpWAK1-pectin interaction and modify the signalling cascade. CpGRP1 as a structural modulator in the extracellular matrix could influence the physical properties of the cell wall. Together with the fact that CpWAK1 is also lower expressed upon dehydration-stress than under control conditions, both might decrease the expression of genes which regulate cell expansion and dehydration-stress responses are increasing.

The findings of this thesis together with the observations of Vicré *et al*. (1999), (2004) suggest pectin modifications in resurrection plants which lead to a more rigid cell wall. However, Jones and McQueen-Mason, (2004) proposed an increase in cell wall flexibility together with a higher activity of expansins upon desiccation. Together, these studies give a first insight in the complex cell wall folding mechanism of resurrection plants. The understanding of the activity and regulation of cell wall modifying enzymes such as pectinmethylesterases, expansins and xyloglucan endotransglycosylases /hydrolases is crucial to decipher the folding process. The activation of pathways leading to more flexible components on the one hand, and other pathways adding more

stability to the cell wall on the other hand upon desiccation, suggests a tightly controlled folding process which finally enables the conservation and protection of the plasmalemma and the photosynthetic apparatus in resurrection plants.

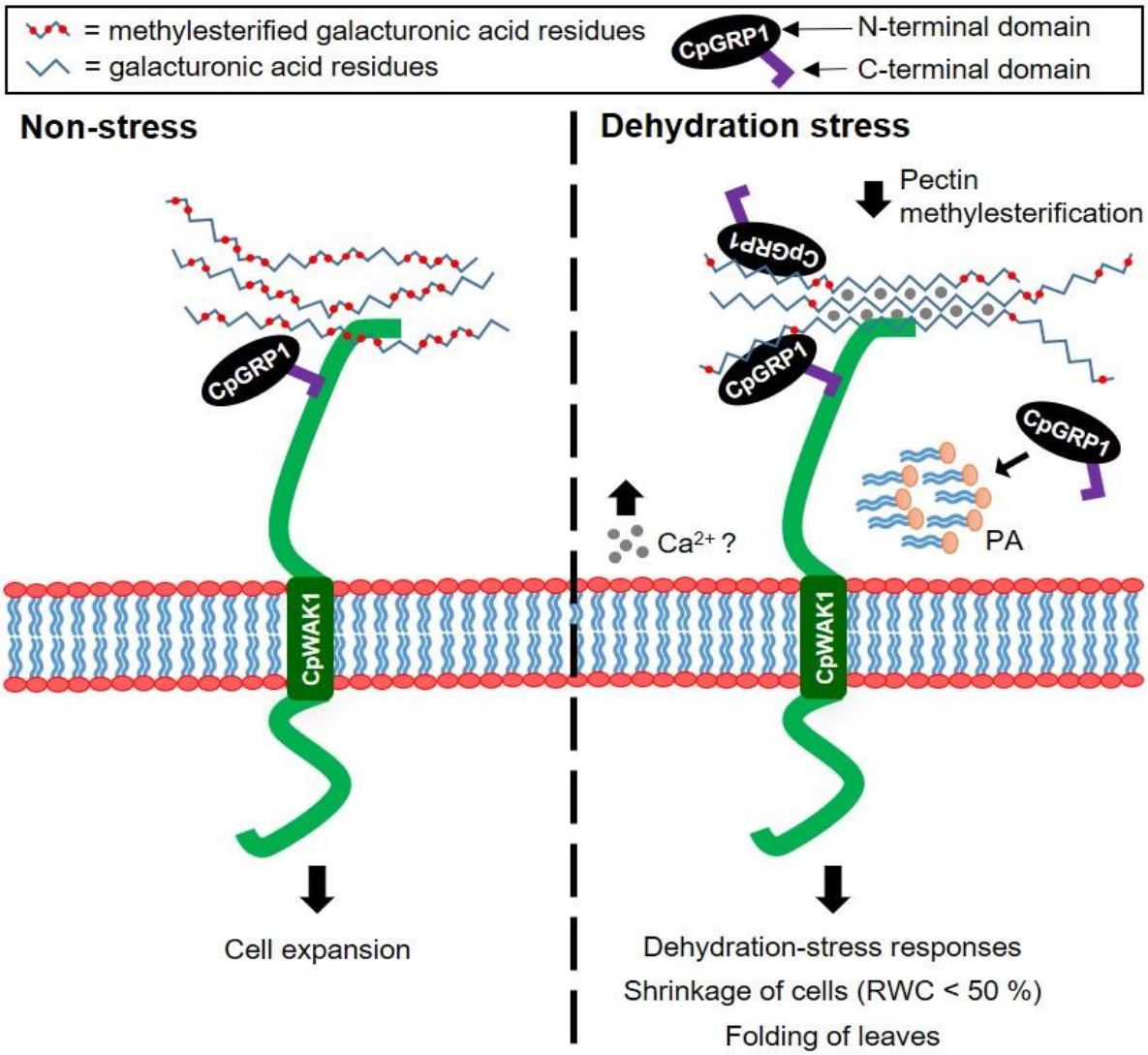

Figure 28 Model depicting the interaction between the *Craterostigma plantagineum* glycine-rich protein1 (CpGRP1), the *C. plantagineum* cell wall associated protein kinase1 (CpWAK1) and cell wall pectin and their role in regulating growth and dehydration-stress responses (modified from Giarola *et al*., 2016). CpGRP1 is a part of the pectin matrix. Under non-stress conditions cell wall pectin (jagged blue lines) with a high degree of methylesterification (red dots) is bound to CpWAK1 and involved in cell expansion. Upon dehydration, CpGRP1 is more abundant. Clustered arginines in the N-terminal domain of CpGRP1 are involved in binding PA and de-methylesterified stretches of pectin, which are more abundant upon dehydration. The binding of CpGRP1 to CpWAK1 is most likely mediated by cysteines in the C-terminal domain of CpGRP1. CpGRP1 might be either bound to PA or pectin with both competing for CpGRP1 binding. Ca^{2+} levels increase upon dehydration which may lead to the formation of `egg-box´ structures resulting in an increase in rigidity of the cell walls.

6. APPENDIX

Table S1. List of primers used in this study.

Primer	Sequence (5'-3')
CpGRP1_NTERM_R	ACCATACTCGAGACGCCCTCTTCCACCATAAC
CpGRP1_NTERM_a352g_c358g_F	GGTTATGGTGGAGGAGGGGGTCTCGAGCACC
CpGRP1_NTERM_a352g_c358g_R	GGTGCTCGAGACCCCCTCCTCCACCATAACC
CpGRP1_CTERM_F	TGGAACCATGGGTTGCCGCTATGGTTGCTGT
CpGRP1_CTERM_MUT1_F	GCGGATATTATGGAGGTGGCAGAGGCGGTGA TTACGCTGACCAG
CpGRP1_CTERM_MUT1_R	CTGGTCAGCGTAATCACCGCCTCTGCCACCTC CATAATATCCGC
CpGRP1_CTERM_MUT2_F	GAAGAGGGCGTGCCCGTTATGGTGGCGGTGG GCCGAGGC
CpGRP1_CTERM_MUT2_R	GCCTCGCCCACCGCCACCATAACGGGCACG CCCTCTTC
pJET1.2_F	CGACTCACTATAGGGAGAGCGGC
pJET1.2_R	AAGAACATCGATTTTCCATGGCAG
CpWAK1_XhoI_R	ATACTGCTCGAGACACGTGAAAGAGC
T7 promoter	TAATACGACTCACTATAGGG
T7 terminator	GCTAGTTATTGCTCAGCGG
CpPME_RT_F	TTTCTGGGTTGGCAGGATAC
CpPME_RT_R	TGGGAGGATTTTCTGCTTTG
CpEF1α_RT_F	AGTCAAGTCCGTCGAAATGC
CpEF1α_RT_R	CACTTGGCACCCTTCTTAGC
CpPME_Full_F	CCAAATGAGCTCAAGGGTCA
CpPME_Full_R	TATTTGCCTCAGCCATCACA
CpPME_attB1	AAAAAGCAGGCTTAATGAGCTCAAGGGTCATA
CpPME_attB2	AGAAAGCTGGGTACATTGATGAGTATGGTAT
attB1-adapter	GGGGACAAGTTTGTACAAAAAAGCAGGCT
attB2-adapter	GGGGACCACTTTGTACAAGAAAGCTGGGT
pDONR201_Seq_LA	TCGCGTTAACGCTAGCATGGATCTC
pDONR201_Seq_LB	GTAACATCAGAGATTTTGAGACAC
pQLinkHD_pQE276	GGCAACCGAGCGTTCTGAAC
pQLinkHD_pQE65	TGAGCGGATAACAATTTCACACAG

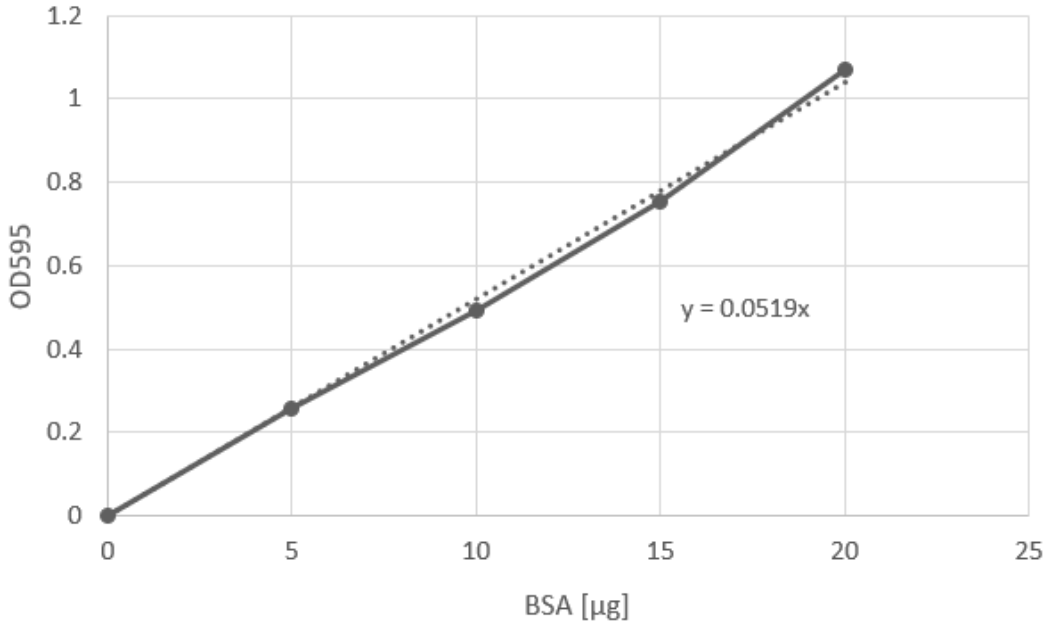

Figure S1 Standard-curve to calculate the protein content using a BSA standard curve.

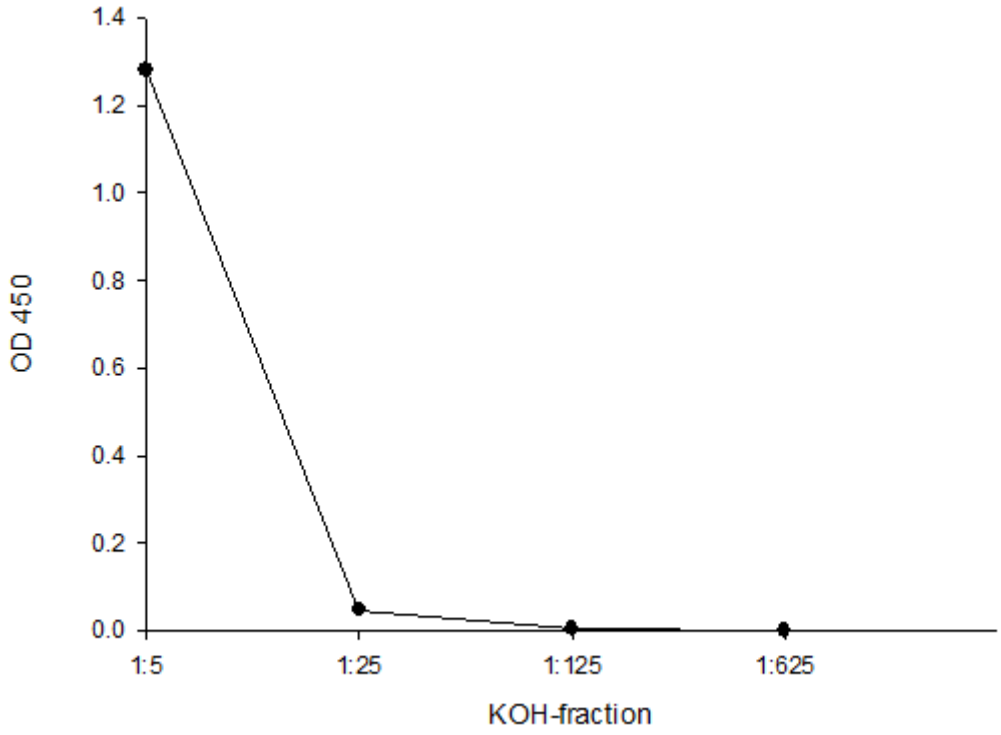

Figure S2 LM25 binding to different dilutions of the KOH fraction extracted from *C. plantagineum* to determine the most appropriate dilution for ELISA studies.

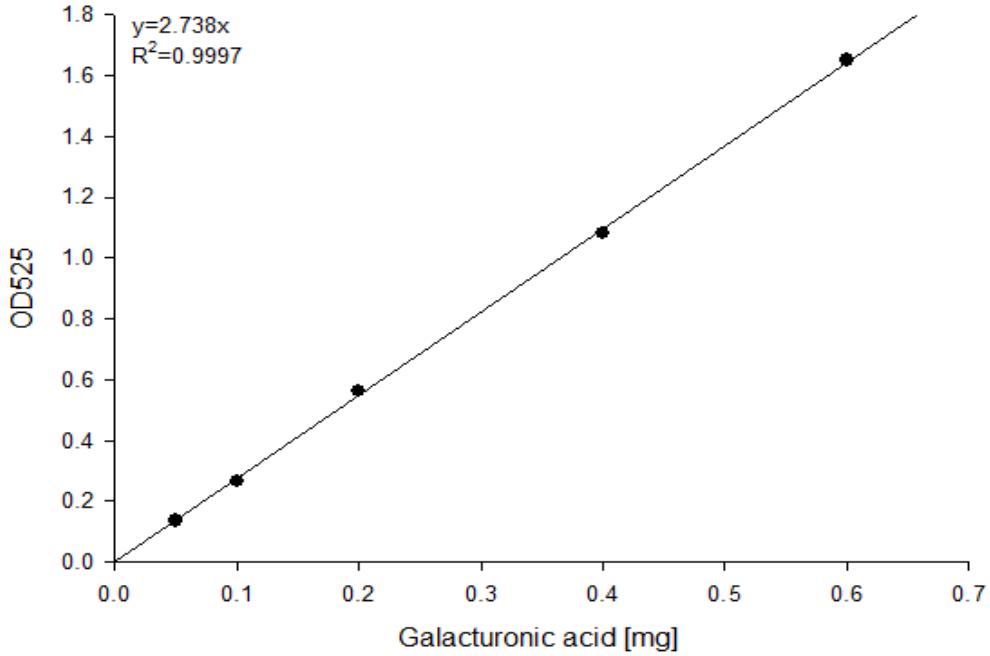

Figure S3 Standard-curve to calculate the galacturonic acid (GA) content in the different pectin fractions.

Description	Max Score	Total Score	Query Cover	E value	Per. Ident	Accession
pectinesterase 31 [Sesamum indicum]	582	582	100%	0.0	84.23%	XP_011085738.2
PREDICTED: pectinesterase 31-like [Populus euphratica]	573	573	100%	0.0	82.97%	XP_011011322.1
pectinesterase 31 [Dorcoceras hygrometricum]	580	580	99%	0.0	83.54%	KZV15962.1
hypothetical protein EUGRSUZ_G02070 [Eucalyptus grandis]	579	579	99%	0.0	83.23%	KCW64453.1
pectinesterase 31 isoform X2 [Jatropha curcas]	578	578	99%	0.0	84.18%	XP_012084742.1
pectinesterase 31 [Olea europaea var. sylvestris]	577	577	99%	0.0	84.81%	XP_022884094.1
pectinesterase 31 [Ricinus communis]	576	576	99%	0.0	84.81%	XP_002530008.1
PREDICTED: pectinesterase 31 [Eucalyptus grandis]	575	575	99%	0.0	83.23%	XP_010066543.1
pectinesterase 31 [Syzygium oleosum]	575	575	99%	0.0	83.54%	XP_030468128.1
pectinesterase 31 [Populus trichocarpa]	572	572	99%	0.0	83.54%	XP_002305315.1
pectinesterase 31-like [Populus alba]	571	571	99%	0.0	83.54%	TKS09466.1
pectinesterase 31 isoform X1 [Jatropha curcas]	571	571	99%	0.0	82.61%	XP_012084740.1
PREDICTED: pectinesterase 31 [Fragaria vesca subsp. vesca]	570	570	99%	0.0	83.60%	XP_004304276.1
PREDICTED: pectinesterase 31 [Vitis vinifera]	570	570	99%	0.0	83.23%	XP_002283941.1
Pectinesterase, catalytic [Corchorus olitorius]	570	570	99%	0.0	82.28%	OMP03547.1
Pectinesterase 31 [Vitis vinifera]	569	569	99%	0.0	83.23%	RVW80869.1
pectinesterase 31-like isoform X2 [Rosa chinensis]	568	568	99%	0.0	82.91%	XP_024184835.1
Pectinesterase, catalytic [Corchorus capsularis]	568	568	99%	0.0	82.28%	OMO79346.1
pectinesterase 31-like [Hevea brasiliensis]	568	568	99%	0.0	82.28%	XP_021647229.1
hypothetical protein EZV62_015419 [Acer yangbiense]	568	568	99%	0.0	82.97%	TXG57590.1
pectinesterase 31 [Citrus clementina]	567	567	99%	0.0	82.91%	XP_006431211.1
PREDICTED: pectinesterase 31 isoform X2 [Nelumbo nucifera]	566	566	99%	0.0	82.59%	XP_010258408.1
hypothetical protein CDL15_Pgr004536 [Punica granatum]	566	566	99%	0.0	82.91%	OWM74769.1
Pectinesterase 31 [Capsicum baccatum]	566	566	99%	0.0	82.65%	PHT35232.1
PREDICTED: pectinesterase 31 [Nicotiana tomentosiformis]	566	566	99%	0.0	82.33%	XP_009596023.1
pectinesterase 31 isoform X1 [Morus notabilis]	565	565	99%	0.0	81.33%	XP_024025308.1
PREDICTED: pectinesterase 31 [Capsicum annuum]	565	565	99%	0.0	82.65%	XP_016573230.1

Figure S4 Protein blast for Cp_V2_contig_11593 at NCBI (https://www.ncbi.nlm.nih.gov/).

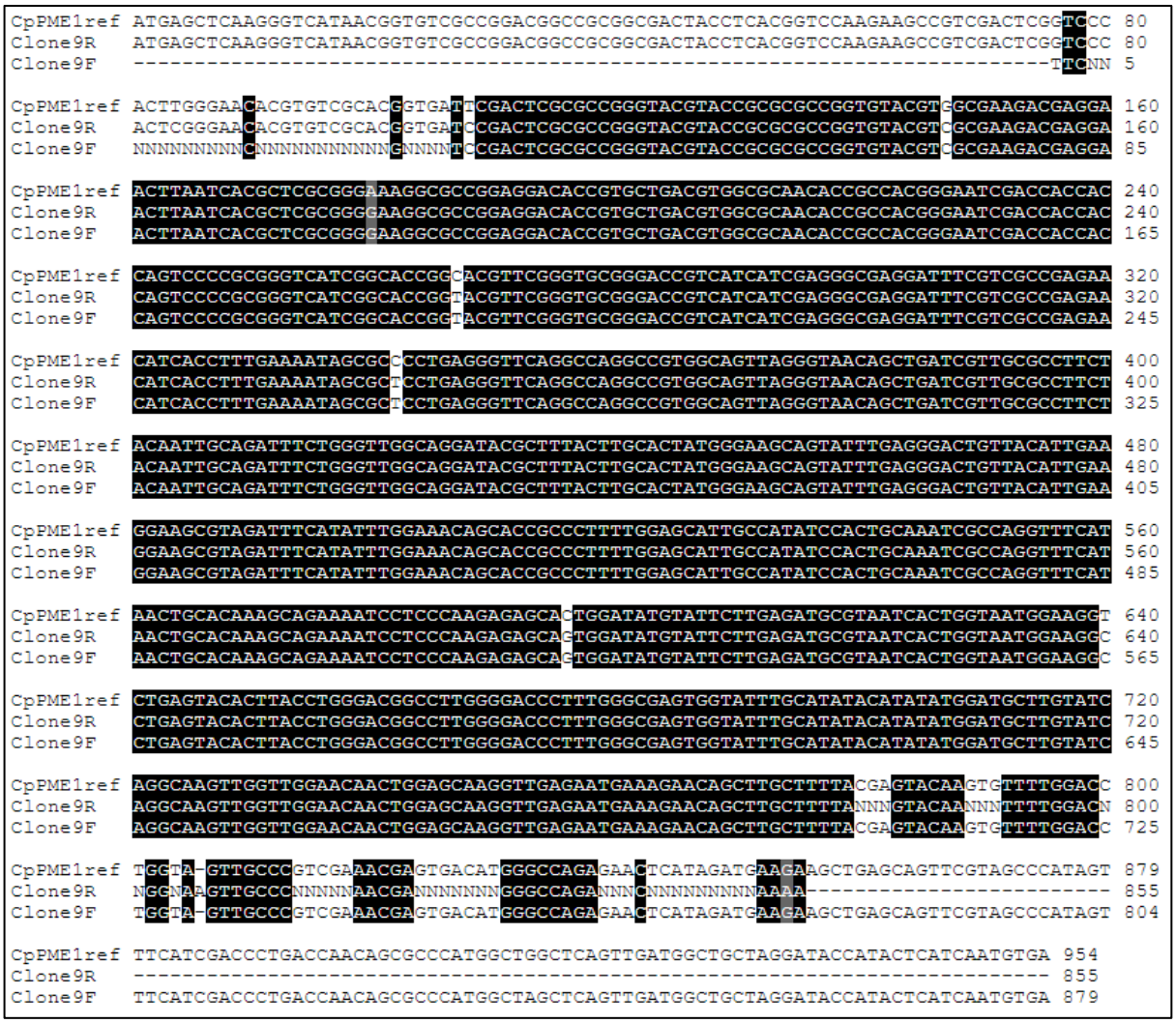

Figure S5 Sequencing result of pJET1.2_CpPME1Clone9_F and pJET1.2_CpPME1 Clone9_R. Both sequencing results were aligned to the CpPME1 reference sequence (https://www.bioinformatics.org/sms2/).

7. REFERENCES

Alamillo, J.M. and Bartels, D. (2001) Effects of desiccation on photosynthesis pigments and the ELIP-like dsp 22 protein complexes in the resurrection plant *Craterostigma plantagineum*. *Plant Sci*ence, **160**, 1161–1170. https://doi.org/10.1016/S0168-9452(01)00356-9

Albach, D.C., Meudt, H.M. and Oxelman, B. (2005) Piecing together the „new" Plantaginaceae. *American Journal of Botany*, **92**, 297–315. https://doi.org/10.3732/ajb.92.2.297

Almeida, E.M., Wanderley, A.M., De Souza Santos, A., De Melo, J.I.M., Souza, G., Da Costa Batista, F.R., Christenhusz, M.F.M. and Felix, L.P. (2019) Two new genera and species of Linderniaceae (Lamiales) from inselbergs in northeastern Brazil: morphological and karyological evidence. *Phytotaxa*, **400**, 215–226. http://dx.doi.org/10.11646/phytotaxa.400.4.1

Alpert, P. (2005) The limits and frontiers of desiccation-tolerant life. *Integrative and Comparative Biology*, **45**, 685–695. https://doi.org/10.1093/icb/45.5.685

Alpert, P. (2006) Constraints of tolerance: why are desiccation-tolerant organisms so small or rare? *Journal of Experimental Biology*, **209**, 1575–1584, https://doi.org/10.1242/jeb.02179

Anderson, C.M., Wagner, T.A., Perret, M., He, Z.H., He, D. and Kohorn, B.D. (2001) WAKs. Cell wall-associated kinases linking the cytoplasm to the extracellular matrix. *Plant Molecular Biology*, **47**, 197–206. https://doi.org/10.3389/fpls.2012.00088

Arisz, S.A., Testerink, C. and Munnik, T. (2009) Plant PA signalling via diacylglycerol kinase. *Molecular and Cell Biology of Lipids*, **1791**, 869–875. https://doi.org/10.1016/j.bbalip.2009.04.006

Bartels, D., Schneider, K., Terstappen, G., Piatkowski, D. and Salamini, F. (1990) Molecular cloning of abscisic acid-modulated genes which are induced during desiccation of the resurrection plant *Craterostigma plantagineum*. *Planta*, **181**, 27–34. https://doi.org/10.1007/BF00202321

Bartels, D. (2005) Desiccation tolerance studied in the resurrection plant *Craterostigma plantagineum*. *Integrative and Comparative Biology*, **45**, 696–701. https://doi.org/10.1093/icb/45.5.696

Bartels, D. and Hussain, S.S. (2011) Resurrection plants: physiology and molecular biology. In: *Plant Desiccation Tolerance* (Lüttge, U., Beck, E., Bartels, D. eds). Berlin: Springer, pp. 339–357

Bernacchia, G., Salamini, F. and Bartels, D. (1996) Molecular characterization of the rehydration process in the resurrection plant *Craterostigma plantagineum*. *Plant Physiology*, **111**, 1043–1050. https://doi.org/10.1104/pp.111.4.1043

Bewley, J.D. (1979) Physiological aspects of desiccation tolerance. *Annual Review of Plant Physiology and Plant Molecular Biology*, **30**, 195–238. https://doi.org/10.1146/annurev.pp.30.060179.001211

Blumenkrantz, N. and Asboe-Hansen, G. (1973) New method for quantitative determination of uronic acids. *Analytical Biochemistry*, **54**, 484–489. https://doi.org/10.1016/0003-2697(73)90377-1

Bocca, S.N., Magioli, C., Mangeon, A., Junqueira, R.M., Cardeal, V., Margis, R. and Sachetto-Martins, G. (2005) Survey of glycine-rich proteins (GRPs) in the Eucalyptus expressed sequence tag database (ForEST). *Genetics and Molecular Biology*, **28**, 608–624. http://dx.doi.org/10.1590/S1415-47572005000400016

Bradford, M.M. (1976) A rapid and sensitive method for the quantification of microgram quantities of protein utilizing the principle of protein-dye. *Analytical Biochemistry*, **72**, 248–254. https://doi.org/10.1016/0003-2697(76)90527-3

Brown, D.M., Goubet, F., Wong, V.W., Goodacre, R., Stephens, E., Dupree, P. and Turner, S.R. (2007) Comparison of five xylan synthesis mutants reveals new insight into the mechanisms of xylan synthesis. *The Plant Journal*, **52**, 1154–1168. https://doi.org/10.1111/j.1365-313X.2007.03307.x

Caffall, K.H. and Mohnen, D. (2009) The structure, function, and biosynthesis of plant cell wall pectic polysaccharides. *Carbohydrate Res*earch, **344**, 1879–1900. https://doi.org/10.1016/j.carres.2009.05.021

Caffal, K.H., Pattathil, S., Phillips, S.E., Hahn, M.G. and Mohnen, D. (2009) *Arabidopsis thaliana* T-DNA mutants implicate GAUT genes in the biosynthesis of pectin and xylan in cell walls and seed testa. *Molecular Plant*, **2**, 1000–1014. https://doi.org/10.1093/mp/ssp062

Challabathula, D., Puthur, J.T. and Bartels, D. (2016) Surviving metabolic arrest: photosynthesis during desiccation and rehydration in resurrection plants. *Annals of the New York Academy of Sciences*, **1365**, 89–99. https://doi.org/10.1111/nyas.12884

Chen, A.P., Zhong, N.Q., Qu, Z.L., Wang, F., Liu, N. and Xia, G.X. (2007) Root and vascular tissue-specific expression of glycine-rich protein AtGRP9 and its interaction with AtCAD5, a cinnamyl alcohol dehydrogenase, in *Arabidopsis thaliana*. *Journal of Plant Research*, **120**, 337–343. https://doi.org/10.1007/s10265-006-0058-8

Chevalier, L.M., Rioux, L.E., Angers, P. and Turgeon, S.L. (2019) Study of the interactions between pectin in a blueberry puree and whey proteins. Functionality and application. *Food Hydrocolloids*, **87**, 61–70. https://doi.org/10.1016/j.foodhyd.2018.07.038

Condit, C.M. and Meagher, R.B. (1986) A gene encoding a novel glycine-rich structural protein of petunia. *Nature*, **323**, 178–181. https://doi.org/10.1038/323178a0

Condit, C.M. and Meagher, R.B. (1987) Expression of a gene encoding a glycine-rich protein in petunia. *Molecular and Cellular Biology*, **7**, 4273–4279. https://doi.org/10.1128/MCB.7.12.4273

Cho, S.K., Kim, J.E., Park, J-A., Eom, T.J. and Kim, W.T. (2006) Constitutive expression of abiotic stress-inducible hot pepper CaXTH3, which encodes xyloglucan endotransglucosylase/hydrolase homolog, improves drought and salt tolerance in transgenic Arabidopsis plants. *FEBS Letters*, **580**, 3136–3144. https://doi.org/10.1007/s00299-010-0989-3

Choi, J.Y., Seo, Y.S., Kim, S.J., Kim, W.T. and Shin, J.S. (2011) Constitutive expression of *CaXTH3*, a hot pepper xyloglucan endotransglucosylase /hydrolase, enhanced tolerance to salt and drought stresses without phenotypic defects in tomato plants (*Solanum lycopersicum cv. Dotaerang*). *Plant Cell Reports*, **30**, 867–877. https://doi.org/10.1007/s00299-010-0989-3

Collett, H., Butowt, R., Smith, J., Farrant, J. and Illing N. (2003) Photosynthetic genes are differentially transcribed during the dehydration-rehydration cycle in the resurrection plant, *Xerophyta humilis*. *Journal of Experimental Botany*, **54**, 2593–2595. https://doi.org/10.1093/jxb/erg285

Cornuault, V., Manfield, I.W., Ralet, M.C. and Knox J.P. (2014) Epitope detection chromatography: a method to dissect the structural heterogeneity and inter-connections of plant cell-wall matrix glycans. *The Plant Journal*, **78**, 715–722. https://doi.org/10.1111/tpj.12504

Cosgrove, D.J. (1999) Enzymes and other agents that enhance cell wall extensibility. *Annual Review of Plant Physiology and Plant Molecular Biology*, **50**, 391–417. https://doi.org/10.1146/annurev.arplant.50.1.391

Cosgrove, D.J. (2015) Plant expansins: diversity and interactions with plant cell walls. *Current Opinion in Plant Biology*, **25**, 162–172. https://doi.org/10.1016/j.pbi.2015.05.014

Cosgrove, D.J. (2016) Plant cell wall extensibility: connecting plant cell growth with cell wall structure, mechanics, and the action of wall-modifying enzymes. *Journal of Experimental Botany*, **67**, 463–476. https://doi.org/10.1093/jxb/erv511

Czolpinska, M. and Rurek, M. (2018) Plant glycine-rich proteins in stress response. An emerging, still prospective story. *Frontiers in Plant Science*, **9**, 302. https://doi.org/10.3389/fpls.2018.00302

De Storme, N. and Geelen, D. (2014) Callose homeostasis at plasmodesmata: molecular regulators and developmental relevance. *Frontiers in Plant Science*, **5**, 138. https://doi.org/10.3389/fpls.2014.00138

Deak, M., Casamayor, A., Currie, R.A., Downes, C.P. and Alessi, D.R. (1999) Characterisation of a plant 3-phosphoinositide-dependent protein kinase-1 homologue which contains a pleckstrin homology domain. *FEBS Letters*, **451**, 220–226. https://doi.org/10.1016/S0014-5793(99)00556-6

Decreux, A. and Messiaen, J. (2005) Wall-associated kinase WAK1 interacts with cell wall pectins in a calcium-induced conformation. *Plant & Cell Physiology*, **46**, 268–278. https://doi.org/10.1093/pcp/pci026

Dedeurwaerder, S., Menu-Bouaouiche, L., Mareck, A., Lerouge, P. and Guerineau, F. (2009) Activity of an atypical *Arabidopsis thaliana* pectin methyl-esterase. *Planta*, **229**, 311–321. https://doi.org/10.1007/s00425-008-0831-0

Dekkers, B.J., Costa, M.C., Maia, J., Bentsink, L., Ligterink, W. and Hilhorst, H.W. (2015) Acquisition and loss of desiccation tolerance in seeds: from experimental model to biological relevance. *Planta*, **241**, 563–577. https://doi.org/10.1007/s00425-014-2240-x

Dinakar, C. and Bartels, D. (2013) Desiccation tolerance in resurrection plants: new insights from transcriptome, proteome and metabolome analysis. *Frontiers in Plant Science*, **4**, 482. https://doi.org/10.3389/fpls.2013.00482

dos Santos, H.P., Purgatto, E., Mercier, H. and Buckeridge, M.S. (2004) The control of storage xyloglucan mobilisation in cotyledons of *Hymenaea courbaril*. *Plant Physiology*, **135**, 287–299. https://doi.org/10.1104/pp.104.040220

Dulitz, J.S. (2016) Isolation and characterization of the *Craterostigma plantagineum* germin-like protein 1 CpGLP1. Master Thesis, University of Bonn, Germany

Edwards, M., Dea, I.C.M., Bulpin, P.V. and Reid, J.S.G. (1985) Xyloglucan (amyloid) mobilisation in the cotyledons of *Tropaeolum majus* L. seeds following germination. *Planta*, **163**, 133–140. https://dx.doi.org/10.1007/BF00395907

Farrant, J.M. (2000) Comparison of mechanisms of desiccation tolerance among three angiosperm resurrection plants. *Plant Ecology*, **151**, 29–39. https://doi.org/10.1023/A:1026534305831

Farrant, J.M., Bartsch, S., Loffell, D., Vander Willigen, C. and Whittaker, A. (2003) An investigation into the effects of light on the desiccation of three resurrection plants species. *Plant, Cell & Environment*, **26**, 1275–1286. https://doi.org/10.1046/j.0016-8025.2003.01052.x

Farrant, J.M. and Moore, J.P. (2011) Programming desiccation-tolerance: from plants to seeds to resurrection plants. *Current Opinion in Plant Biology*. **14**, 340–345. https://doi.org/10.1016/j.pbi.2011.03.018

Fischer, E. (1992) Systematik der afrikanischen Lindernieae (Scrophulariaceae). *Tropische und subtropische Pflanzenwelt*, **81**, 1–365.

Fischer, E. (1995) Revision of the Lindernieae (Scrophulariaceae) in Madagascar. 1. The genera *Lindernia Allioni* and *Crepidorhopalon*. *Bulletin du Musèum National d'Histoire Naturelle, section B, Adansonia: Botanique Phytochemie ser*. 4, **17**, 227–257

Fischer E., Schäferhoff, B. and Müller, K. (2013) The phylogeny of Linderniaceae-The new genus *Linderniella*, and new combinations within *Bonnaya*, *Craterostigma*, *Lindernia*, *Micranthemum*, *Torenia* and *Vandellia*. *Willdenowia-Annals of the Botanic Garden and Botanical Museum Berlin-Dahlem*, **43**, 209–238.

Fleischer, A., O'Neill, M.A. and Ehwald, R. (1999) The pore size of non-graminaceous plant cell walls is rapidly decreased by borate ester cross-linking of the

pectic polysaccharide rhamnogalacturonan II. *Plant Physiology*, **121**, 829–838. https://doi.org/10.1104/pp.121.3.829

Fry, S.C. (1989) The structure and functions of Xyloglucan. *Journal of Experimental Botany*, **40**, 1–11. https://doi.org/10.1093/jxb/40.1.1

Fry, S.C., Smith, R.C., Renwick, K.F., Martin, D.J., Hodge, S.K. and Matthews, K.J. (1992) Xyloglucan endotransglycosylase, a new wall-loosening enzyme activity from plants. *Biochemical Journal*, **282**, 821–828. https://doi.org/10.1042/bj2820821

Fusaro, A., Mangeon, A., Junqueira, R.M., Rocha, C.A.B., Coutinho, T.C., Margis, R. and Sachetto-Martins, G. (2001) Classification, expression pattern and comparative analysis of sugarcane expressed sequences tags (ESTs) encoding glycine-rich proteins (GRPs). *Genetics and Molecular Biology*, **24**, 263–273. http://dx.doi.org/10.1590/S1415-47572001000100035

Gaff, D.F. (1971) Desiccation-tolerant flowering plants in southern Africa. *Science*, **174**, 1033–1034. https://doi.org/10.1126/science.174.4013.1033

Gasulla, F., Dorp, K., Dombrink, I., Zähringer, U., Gisch, N., Dörmann, P. and Bartels, D. (2013) The role of lipid metabolism in the acquisition of desiccation tolerance in *Craterostigma plantagineum*: a comparative approach. *The Plant Journal*, **75**, 726–741. https://doi.org/10.1111/tpj.12241

Gasulla, F., Barreno, E., Parages, M., Camara, J., Jimenez, C., Dörmann, P. and Bartels, D. (2016) The role of Phospholipase D and MAPK signalling cascades in the adaptation of lichen microalgae to desiccation: changes in membrane lipids and phosphoproteome. *Plant and Cell Physiology*, **57**, 1908–1920. https://doi.org/10.1093/pcp/pcw111

Gechev, T.S., Benina, M., Obata, T., Tohge, T., Sujeeth, N., Minkov, I., Hille, J., Temanni, M.R., Marriott, A.S., Bergström, E., Thomas-Oates, J., Antonio, C., Mueller-Roeber, B., Schippers, J.H., Fernie, A.R. and Toneva, V. (2013) Molecular mechanisms of desiccation tolerance in the resurrection glacial relic *Haberlea rhodopensis*. *Cellular and Molecular Life Sciences*, **70**, 689–709. https://doi.org/10.1007/s00018-012-1155-6

Geilfus, C.M. (2017) The pH of the apoplast: dynamic factor with functional impact under stress. *Molecular Plant*, **10**, 1371–1386. https://doi.org/10.1016/j.molp.2017.09.018

Georgieva, T., Christov, N.K. and Djilianov, D. (2012) Identification of desiccation-regulated genes by cDNA-AFLP in *Haberlea rhodopensis*: a resurrection plant. *Acta physiologiae plantarum*, **34**, 1055–1066. https://doi.org/10.1007/s11738-011-0902-x

Giarola, V., Krey, S., Frerichs, A. and Bartels, D. (2015) Taxonomically restricted genes of *Craterostigma plantagineum* are modulated in their expression during dehydration and rehydration. *Planta*, **241**, 193–208. https://doi.org/10.1007/s00425-014-2175-2

Giarola, V., Krey, S., von den Driesch, B. and Bartels, D. (2016) The *Craterostigma plantagineum* glycine-rich protein CpGRP1 interacts with a cell wall-

associated protein kinase 1 (CpWAK1) and accumulates in leaf cell walls during dehydration. *New Phytologist*, **210**, 535–550. https://doi.org/10.1111/nph.13766

Giarola, V., Hou, Q. and Bartels, D. (2017) Angiosperm plant desiccation tolerance: hints from transcriptomics and genome sequencing. *Trends in Plant Science*, **22**, 705–717. https://doi.org/10.1016/j.tplants.2017.05.007

Giarola, V., Jung, N.U., Singh, A., Satpathy, P. and Bartels, D. (2018) Analysis of pcC13-62 promoters predicts a link between cis-element variations and desiccation tolerance in Linderniaceae. *Journal of Experimental Botany*, **69**, 3773–3784. https://doi.org/10.1093/jxb/ery173

Gou, J.Y., Miller, L.M., Hou, G., Yu, X.H., Chen, X.Y. and Liu, C.J. (2012) Acetylesterase-mediated deacetylation of pectin impairs cell elongation, pollen, germination, and plant reproduction. *The Plant Cell*, **24**, 50–65. https://doi.org/10.1105/tpc.111.092411

Gramegna, G., Modesti, V., Savatin, D.V., Sicilia, F., Cervone, F. and De Lorenzo, G. (2016) GRP-3 and KAPP, encoding interactors of WAK1, negatively affects defence responses induced by oligogalacturonides and local response to wounding. *Journal of Experimental Botany*, **67**, 1715–1729. https://doi.org/10.1093/jxb/erv563

Grant, G.T., Morris, E.R., Rees, D.A., Smith, P.J.C., Thom, D. (1973) Biological interactions between polysaccharides and divalent cations: The egg-box model. *FEBS Letters*, **32**, 195–198. https://doi.org/10.1016/0014-5793(73)80770-7

Green, M.R. and Sambrook, J. (2012) *Molecular cloning. A laboratory manual*. Cold Spring Harbor: Cold Spring Harbor Laboratory Press.

Ha, M.A., Evans, B.W., Jarvis, M.C., Apperley, D.C. and Kenwright, A.M. (1996) CP-MAS NMR of highly mobile hydrated biopolymers. Polysaccharides of *Allium* cell walls. *Carbohydrate Research*, **288**, 15–23. https://doi.org/10.1016/S0008-6215(96)90771-5

Harholt, J., Suttangkakul, A. and Scheller, H.V. (2010) Biosynthesis of Pectin. *Plant Physiology*, **153**, 384–395. https://doi.org/10.1104/pp.110.156588

He, F. (2011) Laemmli-SDS-PAGE. *Bio-Protocol*, **1**. https://doi.org/10.21769/BioProtoc.80

He, Z.H., Cheeseman, I., He, D. and Kohorn, B.D. (1999) A cluster of five cell wall-associated receptor kinase genes, Wak1-5, are expressed in specific organs of *Arabidopsis*. *Plant Molecular Biology*, **39**, 1189–1196. https://doi.org/10.1023/A:1006197318246

Herburger, K., Xin, A.Z. and Holzinger, A. (2019) Homogalacturonan accumulation in cell walls of the green alga *Zygnema* sp. (Charophyta) increases desiccation resistance. *Frontiers in Plant Science*, **10**, 540. https://doi.org/10.3389/fpls.2019.00540

Hirt, H. and Shinozaki, K. (2004) Plant responses to abiotic stress. Springer Verlag Berlin

Hong, Y., Zheng, S. and Wang, X. (2008) Dual functions of phospholipase Da1 in plant response to drought. *Molecular Plant*, **1**, 262–269. https://doi.org/10.1093/mp/ssm025

Hou, Q., Ufer, G. and Bartels, D. (2015) Lipid signalling in plant responses to abiotic stress. *Plant, Cell & Environment*, **39,** 1029–1048. https://doi.org/10.1111/pce.12666

Iljin, W.S. (1957) Drought resistance in plants and physiological processes. *Annual Review of Plant Physiology*, **8**, 257–274. https://doi.org/10.1146/annurev.pp.08.060157.001353

Im, W., Beglov, D. and Roux, B. (1998) Continuum solvation model. Computation of electrostatic forces from numerical solutions to the Poisson-Boltzmann equation. *Computer Physics Communications*, **111**, 59–75. https://doi.org/10.1016/S0010-4655(98)00016-2

Jarvis, M.C. (1984) Structure and properties of pectin gels in plant cell walls. *Plant, Cell & Environment*, **7**, 153–164. https://doi.org/10.1111/1365-3040.ep11614586

Jo, S., Kim, T., Iyer, V.G. and Im, W. (2008a) CHARMM-GUI: a web-based graphical user interface for CHARMM. *Journal of Computational Chemistry,* **29**, 1859–1865. https://doi.org/10.1002/jcc.20945

Jo, S., Vargyas, M., Vasko-Szedlar, J., Roux, B. and Im, W. (2008b) PBEQ-Solver for online visualization of electrostatic potential of biomolecules. *Nucleic Acids Research*, **36**, W270–5. https://doi.org/10.1093/nar/gkn314

Jones, L., Seymour, G.B. and Knox, J.P. (1997) Localization of pectic galactan in tomato cell walls using a monoclonal antibody specific to (1[->]4)-[beta]-D-Galactan. *Plant Physiology*, **113**, 1405–1412. https://doi.org/10.1104/pp.113.4.1405

Jones, L. and McQueen-Mason, S. (2004) A role for expansins in dehydration and rehydration of the resurrection plant *Craterostigma plantagineum*. *FEBS Letters*, **559**, 61–65. https://doi.org/10.1016/S0014-5793(04)00023-7

Katagiri, T., Takahashi, S. and Shinozaki, K. (2001) Involvement of a novel Arabidopsis phospholipase D, AtPLDδ, in dehydration-inducible accumulation of phosphatidic acid in stress signalling. *The Plant Journal*, **26**, 595–605. https://doi.org/10.1046/j.1365-313x.2001.01060.x

Keller, B., Sauer, N. and Lamb, C.J. (1988) Glycine-rich cell wall proteins in bean. Gene structure and association of the protein with the vascular system. *The EMBO Journal,* **7**, 3625–3633. https://doi.org/10.1002/j.1460-2075.1988.tb03243.x

Kelley, L.A., Mezulis, S., Yates, C.M., Wass, M.N. and Sternberg, M.J.E. (2015) The *Phyre2* web portal for protein modeling, prediction and analysis. *Nature Protocols*, **10**, 845 EP. https://doi.org/10.1038/nprot.2015.053

Kirch, H.H., Nair, A. and Bartels, D. (2001) Novel ABA-and dehydration inducible-aldehyde dehydrogenase genes isolated from the resurrection plant *Craterostigma*

plantagineum and *Arabidopsis thaliana*. *The Plant Journal*, **28**, 555–567. https://doi.org/10.1046/j.1365-313X.2001.01176.x

Kirch, H.H. and Röhrig, H. (2010) Affinity purification and determination of enzymatic activity of recombinantly expressed aldehyde dehydrogenases. *Methods in Molecular Biology*, **639**, 282–291. https://doi.org/10.1007/978-1-60761-702-017

Knox, J.P., Linstead, P.J., King, J., Cooper, C. and Roberts, K. (1990) Pectin esterification is spatially regulated both within cell walls and between developing tissues of root apices. *Planta*, **181**, 512–521. https://doi.org/10.1007/BF00193004

Kobayashi, M., Matoh, T. and Azuma, Ji. (1996) Two chains of rhamnogalacturonan II are cross-linked by borate-diol ester bonds in higher plant cell walls. *Plant Physiology*, **110**, 1017–1020. https://doi.org/10.1104/pp.110.3.1017

Kohorn, B.D. and Kohorn, S.L. (2012) The cell wall-associated kinases, WAKs, as pectin receptors. *Frontiers in Plant Science*, **3**, 88. https://doi.org/10.3389/fpls.2012.00088

Kooijman, E.E., Tieleman, D.P., Testerink, C., Munnik, T., Rijkers, D.T., Burger, K.N. and De Kruijff, B. (2007) An electrostatic/hydrogen bond switch as the basis for the specific interaction of phosphatidic acid with proteins. *Journal of Biological Chemistry*, **282**, 11356–11364. https://doi.org/10.1074/jbc.M609737200

Kooijman, E. and Testerink, C. (2010) Phosphatidic acid: an electrostatic/hydrogen-bond switch? In: *Lipid Signaling in Plants*. Berlin: Springer, pp. 203–222.

Kranner, I., Beckett, R.P., Wornik, S., Zorn, M. and Pfeifhofer, H.W. (2002) Revival of a resurrection plant correlates with its antioxidant status. *The Plant Journal*, **31**, 13–24. https://doi.org/10.1046/j.1365-313X.2002.01329.x

Kyte, J. and Doolittle, R.F. (1982) A simple method for displaying the hydropathic character of a protein. *Journal of Molecular Biology*, **158**, 105–132. https://doi.org/10.1016/0022-2836(82)90515-0

Laemmli, U.K. (1970) Cleavage of structural proteins during the assembly of the head of bacteriophage T4. *Nature*, **227**, 680–685. https://doi.org/10.1038/227680a0

Lampugnani, E.R., Khan, G.A., Somssich, M. and Persson, S. (2018) Building a plant cell wall at a glance. *Journal of Cell Science*, **131**, jcs207373. https://doi.org/10.1242/jcs.207373

Le Gall, H., Philippe, F., Domon, J.M., Gillet, F., Pelloux, J. and Rayon, C. (2015) Cell wall metabolism in response to abiotic stress. *Plants*, **4**, 112–166. https://doi.org/10.3390/plants4010112

Levesque-Tremblay, G., Pelloux, J., Braybrook, S.A. and Müller, K. (2015) Tuning of pectin methylesterification: consequences for cell wall biomechanics and development. *Planta*, **242**, 791–811. https://doi.org/10.1007/s00425-015-2358-5

Levitt, J. (1980) Responses of plant to environmental stresses. 2nd edn. Academic Press, New York.

Lloyd, C.W. (1991) The cytoskeletal basis of plant growth and form. Academic Press London.

Ma, C., Wang, H., Macnish, A.J., Estrada-Melo, A.C., Lin, J., Chang, Youhong., Reid, M.S. and Jiang, C-Z. (2015) Transcriptomic analysis reveals numerous diverse protein kinases and transcription factors involved in desiccation tolerance in the resurrection plant *Myrothamnus flabellifolia*. *Horticulture Research*, **2**, 15034. https://doi.org/10.1038/hortres.2015.34

Majda, M. and Robert, S. (2018) The role of auxin in cell wall expansion. *International Journal of Molecular Sciences*, **19**, 951. https://doi.org/10.3390/ijms19040951

Mangeon, A., Junqueira, R.M. and Sachetto-Martins, G. (2010) Functional diversity of the plant glycine-rich proteins superfamily. *Plant Signaling & Behavior*, **5**, 99–104. https://doi.org/10.4161/psb.5.2.10336

Marcus, S.E., Verhertbruggen, Y., Hervé, C., Ordaz-Ortiz, J.J., Farkas, V., Pedersen, H.L., Willats, W.G. and Knox, J.P. (2008) Pectic homogalacturonan masks abundant sets of xyloglucan epitopes in plant cell walls. *BMC Plant Biology*, **8**, 60. https://doi.org/10.1186/1471-2229-8-60

Markovic, O. and Janecek, S. (2004) Pectin methylesterase: sequence-structural features and phylogenetic relationships. *Carbohydrate Research*, **339**, 2281–2295. https://doi.org/10.1016/j.carres.2004.06.023

Maron, L. (2019) Water status signaling in resurrection plants: a possible role for cell wall glycine-rich proteins. *The Plant Journal*, **100**, 659–660. https://doi.org/10.1111/tpj.14582

McCartney, L., Marcus, S.E. and Knox, J.P. (2005) Monoclonal antibodies to plant cell wall xylans and arabinoxylans. *The Journal of Histochemistry and Cytochemistry*, **53**, 543–546. https://doi.org/10.1369/jhc.4B6578.2005

McQueen-Mason, S.J. and Cosgrove, D.J. (1995) Expansin mode of action on cell walls. Analysis of wall hydrolysis, stress relaxation, and binding. *Plant Physiology*, **107**, 87–100. https://doi.org/10.1104/pp.107.1.87

Micheli, F. (2001) Pectin methylesterases. Cell wall enzymes with important roles in plant physiology. *Trends in Plant Science*, **6**, 414–419. https://doi.org/10.1016/S1360-1385(01)02045-3

Mohnen, D. (2008) Pectin structure and biosynthesis. *Current Opinion in Plant Biology*, **11**, 266–277. https://doi.org/10.1016/j.pbi.2008.03.006

Molhoj, M., Pagant, S. and Höfte, H. (2002) Towards understanding the role of membrane-bound endo-ß-1,4-glucanases in cellulose biosynthesis. *Plant and Cell Physiology*, **43**, 1399–1406. https://doi.org/10.1093/pcp/pcf163

Moore, P.J., Darvill, A.G., Albersheim, P. and Staehelin, L.A. (1986) Immunogold localization of xyloglucan and rhamnogalacturonan I in the cell walls of suspension-

cultured sycamore cells. *Plant Physiology*, **82**, 787–794. https://doi.org/10.1104/pp.82.3.787

Moore, J.P., Nguema-Ona, E., Chevalier, L., Lindsey, G.G., Brandt, W.F., Lerouge, P., Farrant, J.M. and Driouich, A. (2006) Response of the leaf cell wall to desiccation in the resurrection plant *Myrothamnus flabellifolius*. *Plant Physiology*, **141**, 651–662. https://doi.org/10.1104/pp.106.077701

Moore, J.P., Farrant, J.M. and Driouich, A. (2008) A role for pectin-associated arabinans in maintaining the flexibility of the plant cell wall during water deficit stress. *Plant Signaling & Behavior*, **3**, 102–104. https://doi.org/10.4161/psb.3.2.4959

Moore, J.P., Nguema-Ona, E.E., Vicré-Gibouin, M., Sørensen, I., Willats, W.G., Driouich, A. and Farrant, J.M. (2013) Arabinose-rich polymers as an evolutionary strategy to plasticize resurrection plant cell walls against desiccation. *Planta*, **237**, 739–754. https://doi.org/10.1007/s00425-012-1785-9

Mowla, S.B., Thomson, J.A., Farrant, J.M. and Mundree, S.G. (2002) A novel stress-inducible antioxidant enzyme identified from the resurrection plant *Xerophyta viscosa* Baker. *Planta*, **215**, 716–726. https://doi.org/10.1007/s00425-002-0819-0

Munnik, T., Meijer, H.J.G., Ter Riet, B., Hirt, H., Frank, W., Bartels, D. and Musgrave, A. (2000) Hyperosmotic stress stimulates phospholipase D activity and elevates the levels of phosphatidic acid and diacylglycerol pyrophosphate. *The Plant Journal*, **22**, 147–154. https://doi.org/10.1046/j.1365313x.2000.00725.x

Munnik, T. (2001) Phosphatidic acid: an emerging plant lipid second messenger. *Trends in Plant Science*, **6**, 227–233. https://doi.org/10.1016/S1360-1385(01)01918-5

Nicol, F., His, I., Jauneau, A., Vernhettes, S., Canut, H. and Hofte, H. (1998) A plasma membrane-bound putative endo-1,4-beta-D-glucanase is required for normal wall assembly and cell elongation in *Arabidopsis*. *The EMBO Journal*, **17**, 5563–5576. https://doi.org/10.1093/emboj/17.19.5563

Nielsen, M.E., Feechan, A., Böhlenius, H., Ueda, T., Thordal-Christensen, H. (2012) Arabidopsis ARF-GTP exchange factor, GNOM, mediated transport required for innate immunity and focal accumulation of syntaxin PEN1. *Proceedings of the National Academy of Sciences*, **109**, 1143–1148. https://doi.org/10.1073/pnas.1117596109

Nishitani, K. and Masuda, Y. (1981) Auxin-induced changes in the cell wall structure: Changes in the sugar composition, intrinsic viscosity and molecular weight distributions of matrix polysaccharides. *Physiologia Plantarum*, **52**, 482–494. https://doi.org/10.1111/j.1399–3054.1981.tb02720.x

Nishiyama, Y. (2009) Structure and properties of the cellulose microfibril. *Journal of Wood Science*, **55**, 241–249. https://doi.org/10.1007/s10086-009-1029-1

Ohlrogge, J. and Browse, J. (1995) Lipid biosynthesis. *The Plant Cell*, **7**, 957–970. https://doi.org/10.1105/tpc.7.7.957

Ohmiya, Y., Samejima, M., Shiroishi, M., Amano, Y., Kanda, T., Sakai, F. and Hayashi, T. (2000) Evidence that endo-1,4-ß-glucanases act on cellulose in suspension-cultured poplar cells. *The Plant Journal*, **24**, 147–158. https://doi.org/10.1046/j.1365-313x.2000.00860.x

Oliver, M., Tuba, Z. and Mishler, B. (2000) The evolution of vegetative desiccation tolerance in land plants. *Plant Ecology*, **151**, 85–100. https://doi.org/10.1023/A:1026550808557

O'Neill, M.A., Eberhard, S., Albersheim, P. and Darvill, A.G. (2001) Requirement of borate cross-linking of cell wall rhamnogalacturonan II for *Arabidopsis* growth. *Science*, **294**, 846–849. https://doi.org/10.1126/science.1062319

Orfila, C., Dal Degan, F., Jorgensen, B., Scheller, H.V., Ray, P.M. and Ulvskov, P. (2012) Expression of mung bean pectin methyl esterase in potato tubers: effect on acetylation of cell wall polymers and tuber mechanical properties. *Planta*, **236**, 185–196. https://doi.org/10.1007/s00425-012-1596-z

Oxelman, B., Kornhall, P., Olmstead, R.G. and Bremer, B. (2005) Further disintegration of Scrophulariaceae. *Taxon*, **54**, 411–425.

Park, A.R., Cho, S.K., Yun, U.J., Jin, M.Y., Lee, S.H., Sachetto-Martins, G. and Park, O.K. (2001) Interaction of the *Arabidopsis* receptor protein kinase Wak1 with a glycine-rich protein, AtGRP-3. *The Journal of Biological Chemistry*, **276**, 26688–26693. https://doi.org/10.1074/jbc.M101283200

Park, Y.B. and Cosgrove, D.J. (2012) A revised architecture of primary cell walls based on biomechanical changes induced by substrate-specific endoglucanases. *Plant Physiology*, **158**, 1933–1943. https://doi.org/10.1104/pp.111.192880

Park Y.B. and Cosgrove, D.J. (2015) Xyloglucan and its interactions with other components of the growing cell wall. *Plant Cell Physiology*, **56**, 180–194. https://doi.org/10.1093/pcp/pcu204

Pauly, M. and Keegstra, K. (2016) Biosynthesis of the plant cell wall matrix polysaccharide xyloglucan. *Annual Reviews of Plant Biology*, **67**, 235–298. https://doi.org/10.1146/annurev-arplant-043015-112222

Pedersen, H.L., Fangel, J.U., McCleary, B., Ruzanski, C., Rydahl, M.G., Ralet, M.C., Farkas, V., von Schantz, L., Marcus, S.E., Andersen, M.C.F., Field, R., Ohlin, M., Knox, J.P., Clausen, M.H. and Willats, W.G.T. (2012) Versatile high resolution oligosaccharide microarrays for plant glycobiology and cell wall research. *The Journal of Biological Chemistry*, **287**, 39429–39438. https://doi.org/10.1074/jbc.M112.396598

Pelloux, J., Rusterucci, C. and Mellerowicz, E.J. (2007) New insights into pectin methylesterase structure and function. *Trends in Plant Science*, **12**, 267–277. https://doi.org/10.1016/j.tplants.2007.04.001

Perrot-Rechenmann, C. (2010) Cellular responses to auxin: division versus expansion. *Cold Spring Harbor Perspectives in Biology*, **2**, a001446. https://doi.org/10.1101/cshperspect.a001446

Persson, S., Sorensen, I., Moller, I., Willats, W. and Pauly, M. (2011) Dissection of plant cell walls by high-throughput methods. *Annual Plant Review*, **41**, 43–64. https://doi.org/10.1002/9781119312994.apr0431

Petersen, J., Eriksson, S.K., Harryson, P., Pierog, S., Colby, T., Bartels, D. and Röhrig, H. (2012) The lysine-rich motif of intrinsically disordered stress protein CDeT11-24 from *Craterostigma plantagineum* is responsible for phosphatidic acid binding and protection of enzymes from damaging effects caused by desiccation. *Journal of Experimental Botany*, **63**, 4919–4929. https://doi.org/10.1093/jxb/ers173

Phillips, J.R., Fischer, E., Baron, M., van den Dries, N., Facchinelli, F., Kutzer, M., Rahmanzadeh, R., Remus, D. and Bartels, D. (2008) *Lindernia brevidens*: a novel desiccation-tolerant vascular plant, endemic to ancient tropical rainforests. *The Plant Journal*, **54**, 938–948. https://doi.org/10.1111/j.1365-313X.2008.03478.x

Plazinski, W. (2011) Molecular basis of calcium binding to polyguluronate chains. Revising the egg-box model. *Journal of Computational Chemistry*, **32**, 2988–2995. https://doi.org/10.1002/jcc.21880

Porembski, S. and Barthlott, W. (2000) Granitic and gneissic outcrops (inselbergs) as centers of diversity for desiccation-tolerant vascular plants. *Plant Ecology*, **151**, 19–28. https://doi.org/10.1023/A:1026565817218

Porembski, S. (2011) Evolution, diversity, and habitats of poikilohydrous vascular plants. In: *Plant desiccation tolerance* (Lüttge, U., Beck, E., Bartels, D. eds.) Berlin: Springer, pp. 139–154

Rahmanzadeh, R., Müller, K., Fischer, E., Bartels, D. and Borsch, T. (2005) The Linderniaceae and Gratiolaceae are further lineages distinct from the Scrophulariaceae (Lamiales). *Plant Biology*, **7**, 67–78. https://doi.org/10.1055/s-2004-830444

Rascio, N. and La Rocca, N. (2005) Resurrection plants: the puzzle of surviving extreme vegetative desiccation. *Critical Reviews in Plant Sciences*, **24**, 209–225. https://doi.org/10.1080/07352680591008583

Ringli, C., Hauf, G. and Keller, B. (2001) Hydrophobic interactions of the structural protein GRP1.8 in the cell wall of protoxylem elements. *Plant Physiology*, **125**, 673–682. https://doi.org/10.1104/pp.125.2.673

Rose, J.K., Braam, J., Fry, S.C. and Nishitani, K. (2002) The XTH family of enzymes involved in xyloglucan endotransglucosylation and endohydrolysis: current perspectives and a new unifying nomenclature. *Plant Cell and Physiology*, **43**, 1421–1435. https://doi.org/10.1093/pcp/pcf171

Ruelland, E., Cantrel, C., Gawer, M., Kader, J-C. and Zachowski, A. (2002) Activation of phospholipase C and D is an early response to a cold exposure in Arabidopsis suspension cells. *Plant Physiology*, **130**, 999–1007. https://doi.org/10.1104/pp.006080

Ryden, P., Sugimoto-Shirasu, K., Smith, A.C., Findlay, K., Reiter, W.D. and McCann, M.C. (2003) Tensile properties of Arabidopsis cell walls depends on both a

xyloglucan cross-linked microfibrillar network and rhamnogalacturonan II-borate complexes. *Plant Physiology*, **132**, 1033–1040. https://doi.org/10.1104/pp.103.021873

Ryser, U., Schorderet, M., Guyot, R. and Keller, B. (2004) A new structural element containing glycine-rich proteins and rhamnogalacturonan I in the protoxylem of seed plants. *Journal of Cell Science*, **117**, 1179–1190. https://doi.org/10.1242/jcs.00966

Sachetto-Martins, G., Franco, L.O. and de Oliveira, D.E. (2000) Plant glycine-rich proteins. A family or just proteins with a common motif? *Biochimica et Biophysica Acta*, **1492**, 1–14. https://doi.org/10.1016/S0167-4781(00)00064-6

Sasidharan, R., Voesenk, L.A.C.J. and Pierik, R. (2011) Cell wall modifying proteins mediate plant acclimatization to biotic and abiotic stresses. *Critical Reviews in Plant Sciences*, **30**, 548–562. https://doi.org/10.1080/07352689.2011.615706

Schäferhoff, B., Fleischmann, A., Fischer, E., Albach, D.C., Borsch, T., Heubl, G. and Müller, K.F. (2010) Towards resolving Lamiales relationships: insights from rapidly evolving chloroplast sequences. *BMC Evolutionary Biology*, **10**, 352. https://doi.org/10.1186/1471-2148-10-352

Schägger, H. and von Jagow, G. (1987) Tricine-sodium dodecyl sulfate-polyacrylamide gel electrophoresis for the separation of proteins in the range from 1 to 100 kDa. *Analytical Biochemistry*, **166**, 368–379. https://doi.org/10.1016/0003-2697(87)90587-2

Scheich, C., Kümmel, D., Soumailakakis, D., Heinemann, U. and Büssow, K. (2007) Vectors for co-expression of an unrestricted number of proteins. *Nucleic Acid Research*, **35**, e43. https://doi.org/10.1093/nar/gkm067

Seine, R., Fischer, E. and Barthlott, W. (1995) Notes on the Scrophulariaceae of Zimbabwean inselsbergs, with the description of *Lindernia syncerus* sp. nov. *Feddes Repertorium*, **106**, 7–12. https://doi.org/10.1002/fedr.19951060104

Sherwin, H.W. and Farrant, J.M. (1996) Differences in rehydration of three desiccation tolerant angiosperm species. *Annals of Botany*, **78**, 703–710.

Sherwin, H.W. and Farrant, J.M. (1998) Protection mechanisms against excess light in the resurrection plants *Craterostigma wilmsii* and *Xerophyta viscosa*. *Plant Growth Regulation*, **24**, 203–210. https://doi.org/10.1023/A:1005801610891

Simmons, T.J., Mortimer, J.C., Bernardinelli, O.D., Pöppler, A.C., Brown, S.P., Deazevedo, E.R., Dupree, R. and Dupree, P. (2016) Folding xylan onto cellulose fibrils in the plant cell wall revealed by solid state NMR. *Nature Communications*, **7**, 13902. https://doi.org/10.1038/ncomms13902

Spadoni, S., Zabotina, O., Di Matteo, A., Mikkelsen, J.D., Cervone, F., de Lorenzo, G., Mattei, B. and Bellincampi, D. (2006) Polygalacturonase-inhibiting protein interacts with pectin through a binding site formed by four clustered residues of arginine and lysine. *Plant Physiology*, **141**, 557–564. https://doi.org/10.1104/pp.106.076950

Staehelin, L.A. and Moore, I. (1995) The Plant Golgi Apparatus. Structure, Functional Organization and Trafficking Mechanisms. *Annual Review of Plant Physiology and Plant Molecular Biology*, **46**, 261–288. https://doi.org/10.1146/annurev.pp.46.060195.001401

Sterling, J.D. (2001) The Catalytic Site of the Pectin Biosynthetic Enzyme alpha-1,4-Galacturonosyltransferase Is Located in the Lumen of the Golgi. *Plant Physiology*, **127**, 360–371. https://doi.org/10.1104/pp.127.1.360

Svitkina, T.M., Shevelev, A.A., Bershadsky, A.D. and Gelfand, V.I. (1984) Cytoskeleton of mouse embryo fibroblasts. Electron microscopy of platinum replicas. *European Journal of Cell Biology*, **34**, 64–74. PMID:6539695

Tenhaken, R. (2015) Cell wall remodelling under abiotic stress. *Frontiers in Plant Science*, **5**, 771. https://doi.org/10.3389/fpls.2014.00771

Testerink, C. and Munnik, T. (2011) Molecular, cellular, and physiological responses to phosphatidic acid formation in plants. *Journal of Experimental Botany*, **62**, 2349–2361. https://doi.org/10.1093/jxb/err079

Thomson, W.W. and Platt, K.A. (1997) Conservation of cell order in desiccated mesophyll of *Selaginella lepidophylla* ([Hook and Grev] Spring). *Annals of Botany*, **79**, 439–447.

Towbin, H., Staehelin, T. and Gordon, J. (1979) Electrophoretic transfer of proteins from polyacrylamide gels to nitrocellulose sheets: procedure and some applications. *Proceedings of the National Academy of Sciences of the United States of America*, **76**, 4350–4354. https://doi.org/10.1073/pnas.76.9.4350

Ueki, S. and Citovsky, V. (2002) The systemic movement of a tobamovirus is inhibited by a cadmium-ion-induced glycine-rich protein. *Nature Cell Biology*, **4**, 478–486. https://doi.org/10.1038/ncb806

Ufer, G., Gertzmann, A., Gasulla, F., Röhrig, H. and Bartels, D. (2017) Identification and characterization of the phosphatidic acid-binding *A. thaliana* phosphoprotein PLDrp1 that is regulated by PLDα1 in a stress-dependent manner. *The Plant Journal*, **92**, 276–290. https://doi.org/10.1111/tpj.13651

Uraji, M., Katagiri, T., Okuma, E., Ye, W., Hossain, M.A., Masuda, C., Miura, A., Nakamura, Y., Mori, I.C., Shinozaki, K. and Murata, Y. (2012) Cooperative function of PLDδ and PLDa1 in abscisic acid-induced stomatal closure in Arabidopsis. *Plant Physiology*, **159**, 450–460. https://doi.org/10.1104/pp.112.195578

Urano, K., Maruyama, K., Jikumaru, Y., Kamiya, Y., Yamaguchi-Shinozaki, K. and Shinozaki, K. (2017) Analysis of plant hormone profiles in response to moderate dehydration stress. *The Plant Journal*, **90**, 17–36. https://doi.org/10.1111/tpj.13460

Valenzuela-Avendaño, J.P., Mota, I.A.E., Uc, G.L., Perera, R.S., Valenzuela-Soto E.M. and Aguilar, J.J.Z. (2005). Use of a simple method to isolate intact RNA from partially hydrated *Selaginella lepidophylla* plants. *Plant Molecular Biology Reporter*, **23**, 199–200. https://doi.org/10.1007/BF02772713

VanBuren, R., Wai J., Zhang, Q., Song, X., Edger, P.P., Bryant, D., Michael, T., Mockler, T. and Bartels, D. (2017) Seed desiccation mechanisms co-opted for vegetative desiccation in the resurrection grass *Oropetium thomeaum*. *Plant Cell & Environment*, **40**, 2292–2306. https://doi.org/10.1111/pce.13027

VanBuren, R., Wai, C.M., Pardo, J., Giarola, V., Ambrosini, S., Song, X. and Bartels, D. (2018) Desiccation tolerance evolved through gene duplication and network rewiring in Lindernia. *The Plant Cell,* **30**, 2943–2958. https//doi.org/10.1105/tpc.18.00517

Verhertbruggen, Y., Marcus, S.E., Haeger, A., Ordaz-Ortiz, J.J. and Knox, J.P. (2009) An extended set of monoclonal antibodies to pectic homogalacturonan. *Carbohydrate Research*, **344**, 1858–1862. https://doi.org/10.1016/j.carres.2008.11.010

Verma, C., Singh, R.K., Singh, R.B. and Mishra, S. (2014) Biochemical and In-silico Studies on Pectin Methylesterase from G9 Variety of *Musa acuminata* for Delayed Ripening. *The Open Biochemistry Journal*, **9**, 15–23. https://doi.org/10.2174/1874091X01509010015

Verslues, P.E. and Juenger, T.E. (2011) Drought, Metabolites, and Arabidopsis Natural Variation: A Promising Combination for Understanding Adaptation to Water-Limited Environments. *Current Opinion in Plant Biology*, **14**, 240–245. https://doi.org/10.1016/j.pbi.2011.04.006

Vicré, M., Sherwin, H.W., Driouich, A., Jaffer, M.A. and Farrant, J.M. (1999) Cell wall characteristics and structure of hydrated and dry leaves of the resurrection plant *Craterostigma wilmsii*, a microscopical study. *Journal of Plant Physiology*, **155**, 719–726. https://doi.org/10.1016/S0176-1617(99)80088-1

Vicré, M., Lerouxel, O., Farrant, J.M., Lerouge, P. and Driouich, A. (2004) Composition and desiccation-induced alterations of the cell wall in the resurrection plant *Craterostigma wilmsii*. *Physiologia plantarum*, **120**, 229–239. https://doi.org/10.1111/j.0031-9317.2004.0234.x

Wang, L., Shang, H., Liu, Y., Zheng, M., Wu, R., Phillips, J., Bartels, D. and Deng, X. (2009) A role for a cell wall localized glycine-rich protein in dehydration and rehydration of the resurrection plant *Boea hygrometrica*. *Plant Biology*, **11**, 837–848. https://doi.org/10.1111/j.1438-8677.2008.00187.x

Wang, T., Zabotina, O. and Hong, M. (2012) Pectin-cellulose interactions in the Arabidopsis primary cell wall from two-dimensional magic-angle-spinning solid-state nuclear magnetic resonance. *Biochemistry*, **51**, 9846–9856. https://doi.org/10.1021/bi3015532

Willats, W.G., Marcus, S.E. and Knox, J.P. (1998) Generation of a monoclonal antibody specific to (1-->5)-alpha-L-arabinan. *Carbohydrate Research*, **308**, 149–152. https://doi.org/10.1016/S0008-6215(98)00070-6

Willats, W.G., Orfila, C., Limberg, G., Buchholt, H.C., van Alebeek, G.J., Voragen, A.G., Marcus, S.E., Christensen, T.M., Mikkelsen, J.D., Murray, B.S. and Knox, J.P. (2001) Modulation of the degree and pattern of methyl-esterification

of pectic homogalacturonan in the plant cell walls. *Journal of Biological Chemistry*, **276**, 19404–19413. https://doi.org/10.1074/jbc.M011242200

Winter, K. (2019) Ecophysiology of constitutive and facultative CAM photosynthesis. *Journal of Experimental Botany*, **erz002**, https://doi.org/10.1093/jxb/erz002

Wolf, S. (2017) Plant cell wall signalling and receptor-like kinases. *Biochemical Journal*, **474**, 471–492. https://doi.org/10.1042/BCJ20160238

Wood, A.J. (2005) Eco-physiological adaptations to limited water environments. In: *Plant abiotic stress* (Haegawa PM, Jenks MA eds.). Oxford, UK. Blackwell Press, pp. 1–13

Wood, A.J. and Jenks, M.A. (2007) Plant desiccation tolerance: diversity, distribution, and real-world applications. In: *Plant desiccation tolerance* (Jenks, M.A., Wood, A.J. eds.) Oxford, UK: Blackwell Publishing, pp. 3–10

Wormit, A. and Usadel, B. (2018) The multifaceted role of pectinmethylesterase inhibitors. *International Journal of Molecular Sciences*, **19**, 2878. https://doi.org/10.3390/ijms19102878

Wu, A.M., Rihouey, C., Seveno, M., Hörnblad, E., Singh, S.K., Matsunaga, T., Ishii, T., Lerouge, P. and Marchant, A. (2009) The *Arabidopsis* IRX10 and IRX10-LIKE glycosyltransferases are critical for glucuronoxylan biosynthesis during secondary cell wall formation. *The Plant Journal*, **57**, 718–731. https://doi.org/10.1111/j.1365-313X.2008.03724.x

Wu, H.C., Hsu, S.F., Luo, D.L., Chen, S.J., Huang, W.D., Lur, H.S. and Jinn, T.L. (2010) Recovery of heat shock-triggered released apoplastic Ca^{2+} accompanied by pectin methylesterase activity is required for thermotolerance in soybean seedlings. *Journal of Experimental Botany*, **61**, 2843–2852. https://doi.org/10.1093/jxb/erq121

Wu, H.C. and Jinn, T.L. (2010) Heat shock-triggered Ca^{2+} mobilization accompanied by pectin methylesterase activity and cytosolic Ca^{2+} oscillation are crucial for plant thermotolerance. *Plant Signaling & Behavior*, **5**, 1252–1256. https://doi.org/10.4161/psb.5.10.12607

Wu, H.C., Bulgakov, V.P. and Jinn, T.L. (2018) Pectin methylesterases. Cell wall remodeling proteins are required for plant response to heat stress. *Frontiers in Plant Science*, **9**, 1612. https://doi.org/10.3389/fpls.2018.01612

Yan, J., He, H., Fang, L. and Zhang, A. (2018) Pectin methylesterase31 positively regulates salt stress tolerance in Arabidopsis. *Biochemical and Biophysical Research Communications*, **496**, 497–501. https://doi.org/10.1016/j.bbrc.2018.01.025

Yobi, A., Schlauch, K.A., Tillett; R.L., Yim, W.C., Espinoza, C., Wone, B.W., Cushman, J.C. and Oliver, M.J. (2017) *Sporobolus stapfianus*: Insights into desiccation tolerance in the resurrection grasses from linking transcriptomics to metabolomics. *BMC Plant Biology*, **17**, 67. https://doi.org/10.1186/s12870-017-1013-7

Yokoyama, R. and Nishitani, K. (2006) Identification and characterization of *Arabidopsis thaliana* genes involved in xylem secondary cell walls. *Journal of Plant Research*, **119**, 189–194. https://doi.org/10.1007/s10265-006-0261-7

Yu, L., Nie, J., Cao, C., Jin, Y., Yan, M., Wang, F., Liu, J., Xiao, Y., Liang, Y. and Zhang, W. (2010) Phosphatidic acid mediates salt stress response by regulation of MPK6 in *Arabidopsis thaliana*. *New Phytologist*, **188**, 762–773. https://doi.org/10.1111/j.1469-8137.2010.03422.x

Yuan, S., Yajun, Wu. and Cosgrove, D.J. (2001) A fungal endoglucanase with plant cell wall extension activity. *Plant Physiology*, **127**, 324–333. https://doi.org/10.1104/pp.127.1.324

Zablackis, E., Huang, J., Muller, B., Darvill, A.G. and Albersheim, P. (1995) Characterization of the cell wall polysaccharides or *Arabidopsis thaliana* leaves. *Plant Physiology*, **107**, 1129–1138. https://doi.org/10.1104/pp.107.4.1129

Zhang, G.F. and Staehelin, L.A. (1992) Functional Compartmentation of the Golgi Apparatus of Plant Cells. Immunocytochemical Analysis of High-Pressure Frozen- and Freeze-Substituted Sycamore Maple Suspension Culture Cells. *Plant Physiology*, **99**, 1070–1083. https://doi.org/10.1104/pp.99.3.1070

Zhang, W., Qin, C., Zhao, J. and Wang, X. (2004) Phospholipase D*α*1-derived phosphatidic acid interacts with AB1 phosphatase 2C and regulates abscisic acid signalling. *Proceedings of the National Academy of Sciences of the United States of America*, **101**, 9508–9513. https://doi.org/10.1073/pnas.0402112101

Zhang, Q. and Bartels, D. (2016) Physiological factors determine the accumulation of D-glycero-D-ido-octulose (D-g-D-i-oct) in the desiccation tolerant resurrection plant *Craterostigma plantagineum*. *Functional Plant Biology*, **43**, 684–694. https://doi.org/10.1071/FP15278

Zhang, Q. and Bartels, D. (2018) Molecular responses to dehydration and desiccation in desiccation-tolerant angiosperm plants. *Journal of Experimental Botany*, **69**, 3211–3222. https://doi.org/10.1093/jxb/erx489

Zhao J. (2015) Phospholipase D and phosphatidic acid in plant defence response: from protein-protein and lipid-protein interactions to hormone signalling. *Journal of Experimental Botany*, **66**, 1721–1736. https://doi.org/10.1093/jxb/eru540

Zhou, Y., Kobayashi, M., Awano, T., Matoh, T. and Takabe, K. (2018) A new monoclonal antibody against rhamnogalacturonan II and its application to immunocytochemical detection of rhamnogalacturonan II in *Arabidopsis* roots. *Bioscience, Biotechnology, and Biochemistry*, **82**, 1780–1789. https://doi.org/10.1080/09168451.2018.1485479

Zia, A., Walker, B.J., Oung, H.M., Charuvi, D., Jahns, P., Cousins, A.B., Farrant, J.M., Reich, Z. and Kirchhoff, H. (2016) Protection of the photosynthetic apparatus against dehydration stress in the resurrection plant *Craterostigma pumilum*. *The Plant Journal*, **87**, 664–680. https://doi.org/10.1111/tpj.13227

8. ACCESSION NUMBERS

The Genbank accession numbers used here are KT893871.1 (CpGRP1), KT893872.1 (CpWAK1) and JQ067608.1 (CpLEA-like 11-24).

The UniProtKB accession numbers used here are A0A0S2ZYI4 (CpGRP1), A0A0S2ZYM7 (CpWAK1), Q9LVQ0 (AtPME31), P02769 (BSA) and O23764 (CpLEA-like 11-24).

IV. ACKNOWLEDGMENTS

I thank D. Bartels for giving me the opportunity to do my PhD thesis in her laboratory. Under your supervision I was able to largely improve my scientific skills and it was always a pleasure to work with you.

I would like to thank J.P. Knox for providing the monoclonal antibodies and helping me with many scientific questions.

I am grateful to V. Giarola for supporting me during my whole stay in the laboratory. You helped me with countless problems and questions.

I want to thank all past and current members in the laboratory of D. Bartels. I am very glad to had you all as my colleagues. Thank you for being always helpful and creating a nice working atmosphere.

I want to thank C. Buchholz and T. Dieckmann for providing plant material, C. Marikar and E. Schulz for helping with administrative issues, H-J. Ensikat for help with the scanning electron microscopy, S. Raj, A. Ammar and P. Dörmann for help with lipid binding experiments and M. Kobayashi (Graduate School of Agriculture, Kyoto University, Kyoto) for providing the 42-6 antibody. S. Manduzo and A. Sergeeva helped with providing the expression constructs for the recombinant CpGLP1 and CpWAK1, respectively.

Part of this work was inspired by discussions with J. Renaut and my colleagues within the SMARTWALL project. The work was supported by the DFG (BA712-18-1).

Last but not least I would like to thank Hang for always motivating me. You always believe in me even when I am struggling to have faith in myself.

Thanks to my parents and my grandparents for always supporting me. Without you nothing of this work would have been possible.

V. DECLARATION

I hereby declare that this PhD dissertation is my own work, except where explicitly stated otherwise in the text or in the bibliography.

Bonn, den 04.12.2019

Niklas Udo Jung

VI. LIST OF PUBLICATIONS

This thesis contains parts from:

Jung, N.U., Giarola, V., Chen, P., Knox, J.P. and Bartels D. (2019) *Craterostigma plantagineum* cell wall composition is remodelled during desiccation and the glycine-rich protein CpGRP1 interacts with pectins through clustered arginines. *The Plant Journal*, **100**, 661–676. https://doi.org/10.1111/tpj.14479

in the summary, introduction, materials and methods (except 3.11), results (except 4.3.1, 4.3.2, 4.3.10, 4.4.2, 4.5) and discussion (except 5.4).

Chen, P., Jung, N.U., Giarola, V. and Bartels, D. (2019) The dynamic responses of cell walls in resurrection plants during dehydration and rehydration. *Frontiers in Plant Science*, accepted

in the introduction (2.4) and discussion (5.5).

Other publications:

Giarola, V., Jung, N.U., Singh, A., Satpathy, P. and Bartels, D. (2018) Analysis of *pcC13-62* promoters predicts a link between *cis*-element variations and desiccation tolerance in Linderniaceae. *Journal of Experimental Botany*, **69**, 3773–3784. https://doi.org/10.1093/jxb/ery173

Passon, M., Weber, F., Jung, N. and Bartels, D. (2019) Profiling of phenolic compounds in desiccation-tolerant and non-desiccation-tolerant Linderniaceae. *in preparation*

VII. CONFERENCES

31st Conference: MBP 2018 Molecular Biology of Plants; Dabringhausen, Germany; 20.02.2018-23.02.2018; Poster presentation: Changes in cell wall architecture during dehydration/rehydration in the desiccation-tolerant plant *Craterostigma plantagineum*